uOttawa

L'Université canadienne
Canada's university

FACULTÉ DES ÉTUDES SUPÉRIEURES ET POSTOCTORALES

uOttawa

L'Université canadienne
Canada's university

FACULTY OF GRADUATE AND POSDOCTORAL STUDIES

Marilyne Delorme
AUTEUR DE LA THÈSE / AUTHOR OF THESIS

M.Sc. (Biochemistry)
GRADE / DEGREE

Department of Biochemistry, Microbiology and Immunology
FACULTÉ, ÉCOLE, DÉPARTEMENT / FACULTY, SCHOOL, DEPARTMENT

Downregulation of ATRX Disrupts Cell Proliferation and Cell Cycle Progression

TITRE DE LA THÈSE / TITLE OF THESIS

David Picketts
DIRECTEUR (DIRECTRICE) DE LA THÈSE / THESIS SUPERVISOR

CO-DIRECTEUR (CO-DIRECTRICE) DE LA THÈSE / THESIS CO-SUPERVISOR

EXAMINATEURS (EXAMINATRICES) DE LA THÈSE / THESIS EXAMINERS

John Bell

Bruce McKay

Gary W. Slater
Le Doyen de la Faculté des études supérieures et postdoctorales / Dean of the Faculty of Graduate and Postdoctoral Studies

DOWNREGULATION OF ATRX DISRUPTS CELL PROLIFERATION AND CELL CYCLE PROGRESSION

By

Marilyne Delorme

Thesis submitted in partial fulfillment of the requirements for the degree of
Masters of Science (Biochemistry)

Departement of Biochemistry, Microbiology and Immunology
Faculty of Medecine
University of Ottawa

Your file Votre référence
ISBN: 978-0-494-46472-4
Our file Notre référence
ISBN: 978-0-494-46472-4

Abstract

ATRX is a chromatin remodelling protein of the SNF2 family of chromatin remodelling proteins. Mutations in the *ATRX* gene have been shown to cause the ATR-X syndrome, an X-linked mental retardation disorder. ATRX is part of a chromatin-remodelling complex with Daxx that localizes to PML nuclear bodies or pericentromeric heterochromatin and is thought to regulate gene expression. In mice, Atrx inactivation results in embryonic lethality whereas conditional forebrain specific Atrx ablation showed impaired development and disorganization of the cortex. Furthermore, ATRX phosphorylation was shown to be cell cycle dependant, suggesting an important role for ATRX in cell cycle regulation. In this study we investigated the effects of ATRX downregulation in cell culture models, using siRNA transient transfection, a clone expressing an shRNA targeted to ATRX, and $Atrx^{null}$ MEFs. ATRX downregulated cells showed reduced growth rates and cell cycle defects at the G1 and S phases of the cell cycle. Moreover, ATRX ablation was associated with an altered Rb phosphorylation status and decreased expression of the cyclin A and E2F-1 proteins. Taken together our results suggest that ATRX may play a significant role in cell cycle progression that is pertinent for proper development.

Acknowledgments

During my passage through the Picketts' lab I met many people who helped me in the accomplishment of my Masters' degree. I would like to thank my supervisor David Picketts for giving me the opportunity to work on this project. Dave's patience, support and scientific guidance was much appreciated during the course of my project. I would also like to thank all the present and past member of the Picketts' Lab; Maureen, Emma, Mike, Chantal, Tina, Steve, Matt, Darren, Damiano, Marie and Dahmane. Thank you for sharing your knowledge and good advice with me. I will always remember the good times spent in and out of the lab, I really enjoyed working and partying with all of you. A big thanks to my numerous friends from the 3rd and 4th floor, you made my Masters much more than just a degree. I also wish to thank my thesis advisory committee, Drs. Valerie Wallace and Jim Dimitroulakos, for their scientific guidance.

I would like to acknowledge Dr. Rashmi Kothary for providing the original psiRNA-hH1 neo vector, Dina Shafey who generated the psiRNA LacZ plasmid and Dr. Robin Parks for providing the LacZ and Cre adenovirus. I wish to thank Dr. Bruce Mckay for taking the time to discuss the project with me, the helpful advice and providing the E2F-1 and cyclin A antibodies. Also, thank you to Jeff Hamill, for performing the Cyclin E analysis by flowcytometry and Tina Price-O'Dea for performing the embryo genotyping.

I would like to thank my family, Alain, Lise-Anne and Catherine who support me in all my projects. And finally, Special thanks to Alenko for his support and encouragement during the ups and downs of my Master's degree and manuscript writing.

Table of Contents

List of Abbreviations

ADT: adenosine-5'- diphosphatase
ATMDS: alpha thalassemia myelodysplastic syndrome
ATP: adenosine-5'- triphosphate
ATPase: adenosine-5'- triphosphatase
ATR-X: alpha thalassemia mental retardation syndrome
ATRX: alpha thalassemia mental retardation syndrome (gene or protein)
ATRXt: alpha thalassemia mental retardation syndrome truncated protein isoform
bp: base pair
BrdU: 5-bromo-2-deoxyuridine
BRM: brahma
BRG1: brahma-related gene 1
BSA: bovine serum albumin
Cdk: cyclin dependant kinase
cDNA: complementary deoxyribonucleic acid
CHD: chromodomain and helicase-like domain
CT: computed tomography
DAPI: 4'6-diamino-2-phenylindole
Daxx: death domain-associated
DMEM: Dulbecco's Modified Eagle Medium
DMSO: dimethyl sulfoxide
DNA: deoxyribonucleic acid
DNMT: DNA methyl transferase
dNTP: deoxynucleotide-5'-triphosphate
dsRNA: double stranded RNA
ECL: enhanced chemoluminescence
EDTA: ethylenediaminetetraacetic acid
EZH2: Enhancer of Zeste homolog 2
FBS: fetal bovine serum
G0: gap 0
G1: gap 1
G2: gap 2
H1: histone 1
H2A: histone 2A
H2B: histone 2B
H3: histone 3
H4: histone 4
H5: histone 5
HAT: histone acetyltransferase
HbH: haemoglobin H
HDAC: histone deacetylase
HP1α: heterochromatin protein 1 α
HPLC: high pressure liquid chromatography
HPV: human papilloma virus

HRP: horse radish peroxidase
HU: hydroxyurea
ISWI: imitation switch
JNK: c-Jun-N-terminal kinase
K: lysine
Kb: kilobase
kDa: kiloDalton
L1: larval stage 1
LB: Luria-Bertani
M: mitotic
MEF: mouse embryonic fibroblast
MOI: multiplicity of infection
MR: mental retardation
MRI: magnetic resonance imaging
mRNA: messenger ribonucleic acid
PARP-1: Poly(ADP-ribose) polymerase-1
PBS: phosphate-buffered saline
PCH: pericentromeric heterochromatin
PCR: polymerase chain reaction
PH3: phosphohistone H3
PHD: plant homeodomain
PI: propidium iodide
PML: promyelocytic leukemia
PML-NB: promyelocytic leukemia nuclear body
pRb: hyperphosphorylated Rb
PVDF: polyvinylidene diflouride
Rb: retinoblastoma
RISC: RNA-induced silencing protein complex
RNA: ribonucleic acid
RNAi: ribonucleic acid interference
RPM: rotation per minute
RT: reverse transcriptase or room temperature
SEM: standard error of the mean
SDS: sodium dodecyl sulfate
shRNA: small hairpin RNA
siRNA: small interfering RNA
SNF: sucrose non-fermenting
SWI: mating type switching
TAE: tris-acetate/EDTA buffer
TBST: tris-buffer saline with Tween 20
TF: transcription factor
TUNEL: terminal uridine deoxynucleotidyl transferase dUTP nick end labeling
UV: ultra violet
V: volt
WT: wild type
XLMR: X-linked mental retardation

List of Figures

1 Introduction

1.1 The ATR-X syndrome

1.1.1 Clinical genetics of the ATR-X syndrome

The ATR-X syndrome, X-linked alpha-thalassemia mental retardation syndrome, is caused by mutations in the *ATRX* gene. To date, 168 individuals have been identified with the syndrome and its prevalence is estimated to be less than 1-9 cases in 1,000,000 (Gibbons 2006). The ATR-X syndrome is characterised by a variable degree of mental retardation, facial dysmorphism, genital abnormalities, developmental delay and alpha thalassemia in affected males (Gibbons, Brueton et al. 1995). ATR-X patients can be recognised by distinctive facial features such as a flat nasal bridge, a small triangular up turned nose, midface hypoplasia and an upswept frontal hair line. The mouth is characterized by a ''carp-like'' appearance where the lower lip is inverted and full with excessive drooling (figure 1). Genital abnormalities are also common in these individuals and observed in 80% of cases (Gibbons 2006). The broad spectrum of genital deformity ranges from mild defects such as undescended testes to more severe cases with ambiguous genitalia. Psychomotor developmental milestones are delayed, the affected individual will often start walking late in childhood and some never develop the skill and are wheelchair bound. Hypotonia is also really common in early childhood. Speaking abilities are non-existent in most individuals but some can communicate with a few words and signs (Gibbons and Higgs 2000). The majority of the ATR-X affected individuals are dependant on their care givers for daily routine activities. Severe to profound mental retardation is seen in most of the ATR-X cases but new reports suggest a broader range of MR (mental retardation) severity.

Figure 1. Facial features of the ATR-X patients

Photographs of three ATR-X affected patients. These boys show distinctive facial features of the disease. Note the flat nasal bridge, the small triangular up turned nose, mid-face hypoplasia and an upswept frontal hair line. The mouth is characterized by a full and inverted lower lip and is described as ''carp-like''. Photographs were adapted from Dr. Gibbons studies (Gibbons, Brueton et al. 1995; Gibbons 2006).

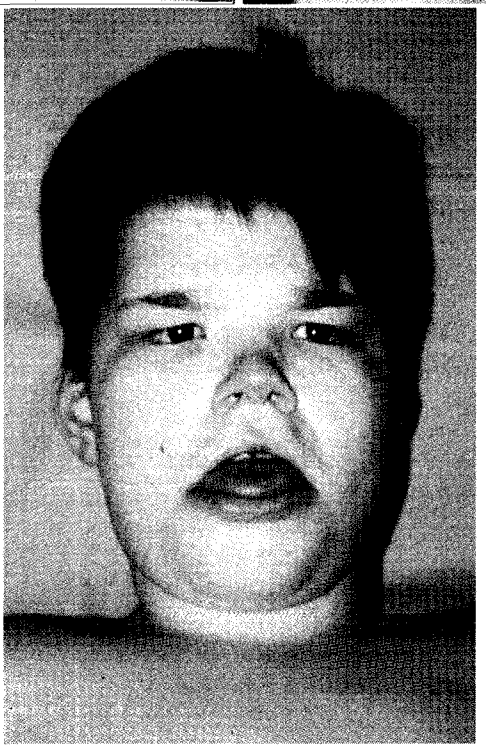

For example, in one family, an *ATRX* mutation gave rise to moderate MR in all affected males (Carpenter, Qu et al. 1999) whereas in another family, all affected males with the same *ATRX* mutation had various degrees of MR from moderate to profound (Guerrini, Shanahan et al. 2000). Seizures take place in 30% of the ATR-X patients and are from clonic/tonic or myoclonic origin. Affected individuals are born with a normal sized head but frequently develop microcephaly after birth and it may be correlated to mild cerebral atrophy seen by computed tomography (CT) and magnetic resonance imaging (MRI) in some individuals (Gibbons 2006).

The presence of alpha thalassemia in ATR-X individuals was found to be one of the key characteristics of the syndrome in its early discovery (Weatherall, Higgs et al. 1981). Now, it is known that not all ATR-X patients have alpha thalassemia. Several families have ATR-X affected members who show no indication of alpha thalassemia (Villard, Lacombe et al. 1996; Villard, Toutain et al. 1996). In general, approximately 90% of ATR-X patients demonstrate some sign of alpha thalassemia (Gibbons 2006). This rare form of anaemia is characterized by a reduction of the α-globin chains in the peripheral blood. It can be detected by the presence of an excess of beta chains forming HbH (haemoglobin H) inclusions in the red blood cells. Those HbH inclusions can be observed by light microscopy in blood samples treated with 1% brilliant cresyl blue. The α-globin chain level should be reduced by 30-40% to be able to see HbH inclusions (Higgs, Vickers et al. 1989). As stated earlier, some patients do not have HbH inclusions (no sign of alpha thalassemia) (Villard, Lacombe et al. 1996; Villard, Toutain et al. 1996) but they may still have down-regulated expression of the α-globin gene which can't be detected with this test. The ATR-X patients with alpha thalassemia are not severely affected by other haematological abnormalities

normally seen in individuals affected by the classic form of alpha thalassemia (mutation in the α-globin complex). The different haematological abnormalities between ATR-X syndrome and the classic alpha thalassemia are most likely due the different mutated gene causing the disease.

ATR-X syndrome is an X-linked recessive disease. Females carrying *ATRX* mutations develop normally and show no sign of MR; they do not have the ATR-X syndrome because of a "skewed" or "non- random" X chromosome inactivation. Generally, the mutant *ATRX* allele is preferentially inactivated in most unaffected female carriers (Gibbons, Suthers et al. 1992). Nevertheless, there are some exceptions: two carrier females, one with normal intelligence and the other with mild MR were shown to both have a random X inactivation (Gibbons, Suthers et al. 1992; Wada, Sugie et al. 2005). Therefore skewed X inactivation may not be the preferential test to determine female carriers. Similarly, a low level of HbH inclusion is present in only 25% of the carrier females (Gibbons, Brueton et al. 1995). The most effective method to determine if a female carries the diseased allele is to identify the mutation in the *ATRX* gene. There is a 50% chance for the carrier female to give the diseased allele to a child but since only males are affected there is a 25% chance of having an ATR-X child per pregnancy. Genetic counselling and prenatal diagnosis is available for ATR-X carrier females. It has been reported that the ATR-X syndrome can also arise from germline mosaicism (Bachoo and Gibbons 1999). Furthermore, a non-carrier female with an affected child may be at risk to have additional affected children (Bachoo and Gibbons 1999).

1.1.2 Molecular genetics of the ATR-X syndrome

The locus responsible for the ATR-X syndrome was found to localise between Xq12-q21.31 by linkage analysis in 1992 (Gibbons, Suthers et al. 1992). The ATRX protein was then identified as a novel member of the SNF2 superfamily of proteins (Gibbons, Picketts et al. 1995; Picketts, Higgs et al. 1996). The *ATRX* gene is specifically located at Xq13.3 and spans about 300 kb of genomic DNA, contains 36 exons and encodes the full-length ATRX protein (~280 kDa) (Picketts, Higgs et al. 1996). A truncated isoform called ATRXt (~180 kDa) can arise from a failure of intron 11 to be spliced which contains an alternative intronic poly(A) signal (figure 2); this isoform is conserved between human and mouse (Garrick, Samara et al. 2004). The ATRX protein was found to contain two important regions which are characteristic of the SWI/SNF chromatin remodelling protein family: a plant homeodomain (PHD)-like zinc-finger domain located in the N-terminus (Gibbons, Bachoo et al. 1997; Villard, Lossi et al. 1997) and a C-terminal putative helicase/ATPase domain of the SNF2 family (figure 2) (Gibbons, Picketts et al. 1995; Picketts, Higgs et al. 1996). Conversely, the ATRXt isoform only contains the PHD-like domain and not the ATPase/helicase domain (Garrick, Samara et al. 2004). Both of these domains are highly conserved between the human and the mouse ATRX homologue, suggesting a functional importance of these regions (Picketts, Tastan et al. 1998). In addition, the majority of the *ATRX* mutations found in ATR-X syndrome patients are single base missense mutations which occur mainly in the PHD zinc-finger (65%) and helicase/ATPase domain (25%) (Berube, Smeenk et al. 2000; Gibbons 2006) (figure 2). Mutations in *ATRX* result in decreased levels of the ATRX protein or its activity in affected individuals (Picketts, Higgs et al. 1996). It was found that mutations resulting in the truncation of the last 100 amino

Figure 2. Schematic diagram of the ATRX gene and protein products

The top part of the figure illustrates the *ATRX* gene; the 35 exons are represented by the boxes and separated by the introns (the thin horizontal line, not to scale). The gene is flanked by the 3' and 5' UTR (untranslated regions). The circles identify the type and position of different *ATRX* mutations found in ATR-X syndrome patients (above the gene) and in ATMDS (alpha thalassemia myelodysplastic syndrome) (below the gene). The filled circles represent mutations that would cause protein truncation (nonsense or leading to a frame shift). The open circles represent missense mutations and small deletions that maintain the reading frame; deletions are indicated by horizontal lines. Recurrent mutations are represented by larger circles, and the number of the independent families in which it was found. The lower part of the figure illustrates the two ATRX protein isoforms ATRX (full length) and ATRXt (truncated). Both proteins contain the zinc finger domain (ADD) but the ATPase/helicase domain is only found in the full length ATRX. The (P) and (Q) represent the P box and a glutamine rich region respectively. Figure was adapted from Gibbons et al. 2008 (Gibbons, Wada et al. 2008).

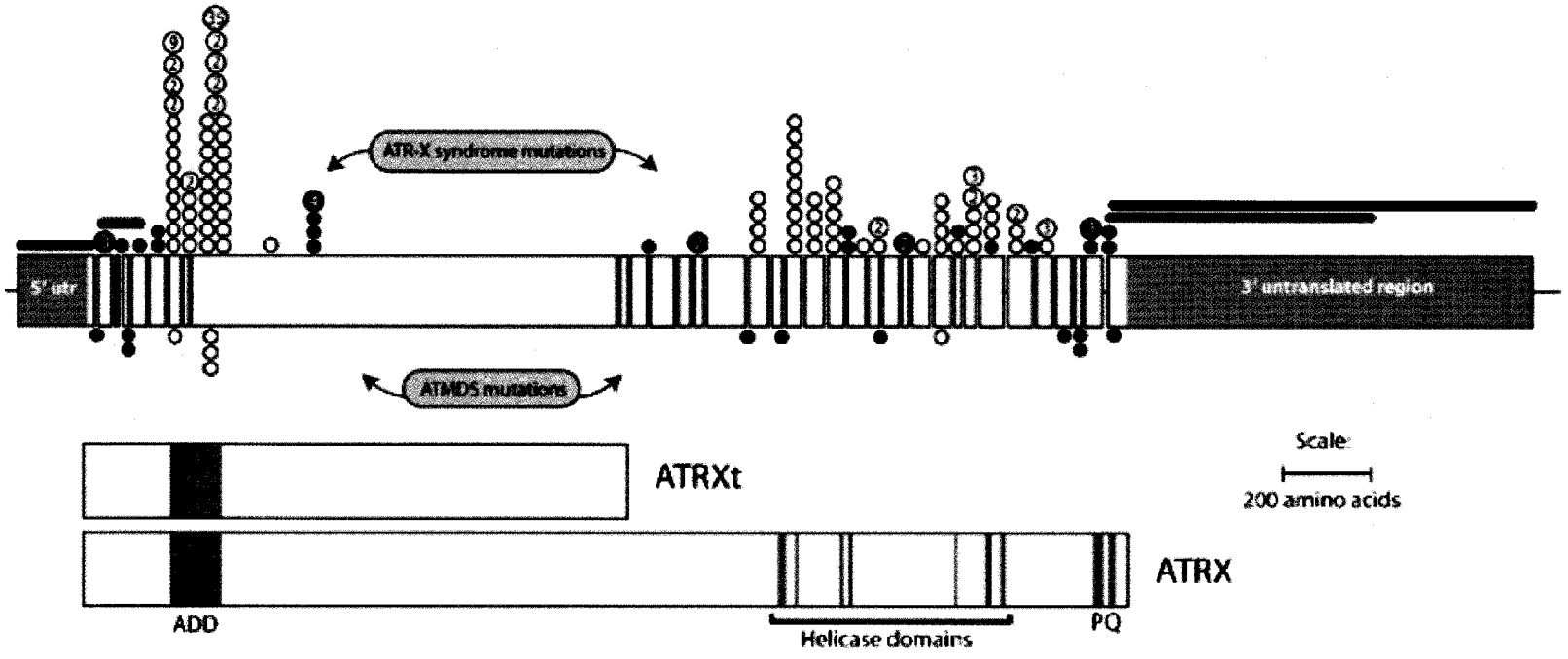
ATR-X syndrome mutations
5' utr
3' untranslated region
ATMD5 mutations
ATRXt
Scale:
200 amino acids
ATRX
ADD
Helicase domains
PQ

acids gave rise to individuals with severe genital abnormalities, therefore linking the C-terminal region of ATRX to genital development (Picketts, Higgs et al. 1996). No other prevailing genotype-phenotype correlation or links between the severity of the MR and mutations have been established yet. Furthermore, the severity of the alpha thalassemia is also very variable within individuals carrying the same mutation suggesting that other genetic factors may modulate α-globin expression (Gibbons, Bachoo et al. 1997).

Mutations in the *ATRX* gene have also been identified in other X-linked MR disorders including Carpenter-Waziri syndrome, Juberg-Marsidi syndrome, Smith-Fineman-Myers syndrome and X-linked MR (XLMR) with spastic paraplegia although none of these diseases show signs of alpha thalassemia (Villard, Gecz et al. 1996; Abidi, Schwartz et al. 1999; Lossi, Millan et al. 1999; Villard, Fontes et al. 2000). Given that *ATRX* encodes a protein that modulates chromatine structure I will now review the structure and the dynamic properties of chromatin in the following section.

1.2 Chromatin structure

Each cell in our body contains 2 meters of DNA which needs to be compacted in an organised way to fit into the cell nucleus. The packaging of DNA into chromatin plays a critical role in regulating processes such as replication, recombination and gene transcription. The basic unit of the eukaryotic chromatin packaging is the nucleosome which is also referred to as the "beads on the string" (figure 3) (Alberts 1999). The nucleosome "bead" is a histone octamer core of 11 nm composed of two molecules of histones H2A, H2B, H3 and

Figure 3. Chromatin structure and packaging

Illustration of the ordered chromatin compaction levels involved in mitotic chromosome formation. Figure obtained from *Molecular biology of the cell* (Alberts 1999).

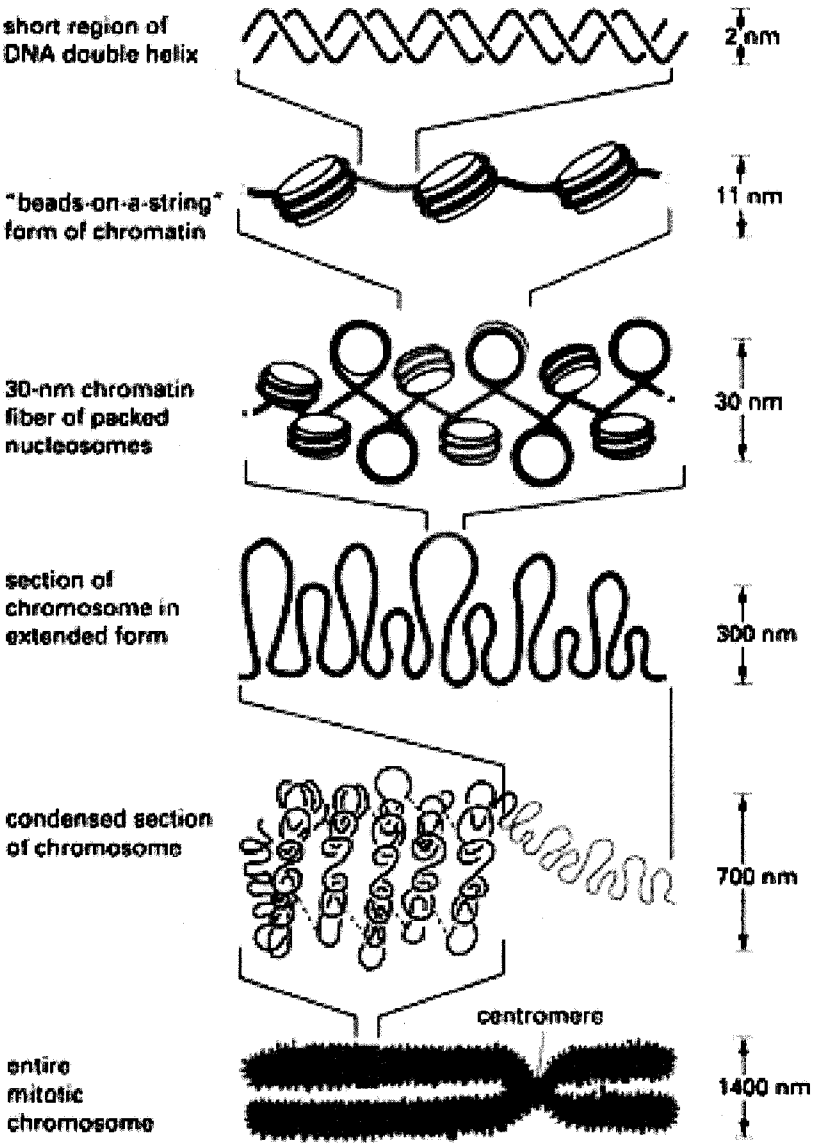

NET RESULT: EACH DNA MOLECULE HAS BEEN PACKAGED INTO A MITOTIC CHROMOSOME THAT IS 10,000-FOLD SHORTER THAN ITS EXTENDED LENGTH

H4. Each nucleosome spans approximately 200 bp of DNA where 146 bp are wrapped around the histone octamer core and 50 bp of free DNA represents the "string" separating each nucleosome (Luger, Mader et al. 1997; Alberts 1999). The "beads on the string" structure is further compacted into a 30 nm thick chromatin fibre which is thought to depend on interactions with the "linker" histones H1 and H5. The chromatin is additionally compacted to form the chromosomes through chromatin loops and other structures that remain poorly understood (Alberts 1999). Even though chromatin packaging is extensive its structure is really dynamic to facilitate cellular processes such as transcription.

The DNA can be further organised into two types of chromatin states: heterochromatin, which is more compact and associated with gene repression and euchromatin which is less compacted and correlates with transcriptional activation. Humans have 20% of their genome packaged into heterochromatin; it is found in the centromeric and telomeric regions of the chromosomes and contains a low amount of single copy genes but high amounts of repetitive DNA (Dimitri, Corradini et al. 2005). The heterochromatin replicates in late S phase and is transcriptionally repressed (Westphal and Reuter 2002). Conversely, the euchromatin is located between the centromere and the telomere and contains most of the single-copy genes (Dimitri, Corradini et al. 2005).

Nucleosomes associated with heterochromatin are usually hypoacetylated and methylated at lysine 9 of histone H3 (H3K9me) and lysine 20 of histone H4 (H4K20me); these features usually correspond to gene silencing. However, transcriptionally active euchromatin is associated with acetylation of H3 and H4 N-terminal tails and methylation of H3K4 (Strahl and Allis 2000). Histone modification is one of the methods used by the cell

to remodel chromatin. In addition, several other proteins and complexes act directly on chromatin structure to regulate DNA accessibility and transcription.

There are two main mechanisms that increase accessibility of the genome to DNA binding proteins: chromatin modifying activities, which introduce covalent modifications on histone tails or the histone core; and chromatin remodelling activities, which alter the DNA–histone interaction non-covalently. The histone tails extend from the lateral surface of the histone octamer. The flexible tails are highly basic and are the substrates for numerous enzymes that introduce a variety of post-translational modifications including acetylation, methylation, phosphorylation, ADP-ribosylation and ubiquitination. These histone modifications dictate interactions of the histones with other proteins which sequentially regulate chromatin structure (Wu and Grunstein 2000). On the other hand, chromatin remodelling proteins, like SWI/SNF family members, use energy from ATP-hydrolysis to typically modify nucleosomal positioning thereby regulating gene expression (Schulze and Wallrath 2007). Both mechanisms of covalent and non-covalent histone modification seem to be equally important and can act in concert for transcriptional regulation.

1.3 SWI/SNF protein family

SWI/SNF chromatin remodelling ATPases are found in multi-protein complexes where the energy derived from ATP hydrolysis is used to induce changes in the histone octamer–DNA interaction. These changes include nucleosome sliding on the genomic DNA, conformational changes in histone–DNA interactions, and histone loss or nucleosome disassembly giving access to target genes (Mohrmann and Verrijzer 2005; Saha, Wittmeyer

et al. 2006). The catalytic subunits of chromatin remodelling complexes are members of the SNF2 family of DNA-dependent ATPases. This large family of ATPases can be grouped into multiple subfamilies that have conserved structure and function (Flaus, Martin et al. 2006). Three of the most highly characterized subfamilies are: (1) the SWI/SNF ATPases, named after the yeast phenotype in which they were first discovered (mating type switching (SWI) and sucrose non fermenting (SNF)) (Carlson and Laurent 1994), (2) the imitation switch (ISWI) ATPases and (3) the chromodomain and helicase-like domain (CHD) ATPases (Neely and Workman 2002).

Chromatin remodelling complexes of the SWI/SNF subfamily contain from 9-15 subunits, including a conserved core and other non-conserved components (Martens and Winston 2003). Unique complexes are thought to regulate differential subsets of genes (Mohrmann, Langenberg et al. 2004). Indeed, studies have shown that a given SWI/SNF ATPase can control expression of diverse target genes in different cell types or under different conditions (Krebs, Fry et al. 2000; Bezhani, Winter et al. 2007). SWI/SNF chromatin remodelling complexes modulate gene expression through recruitment to target gene promoters by specific transcription factors (TF) (Simone 2006). With its ATPase activity the SWI/SNF complex can disrupt DNA-histone interactions resulting in chromatin remodelling that promotes DNA accessibility or inaccessibility (Mohrmann and Verrijzer 2005; Saha, Wittmeyer et al. 2006). Chromatin remodelling ATPases also cooperate with histone modifying enzymes such as histone acetyltransferases (HATs) and deacetylases. HATs add acetyl groups to lysines at the amino termini of the core histones allowing activation of gene expression whereas, histone deacetylases induce gene repression by removing the acetyl groups attached to the histone tails (Brown, Lechner et al. 2000).

SWI/SNF chromatin complexes are thought to act as transcriptional activators but other studies have shown a role in transcriptional repression (Sudarsanam and Winston 2000; Narlikar, Fan et al. 2002). Other cellular roles including sister chromatid cohesion and proper chromosome segregation during mitosis have also been shown to require SWI/SNF ATPase complexes (Huang, Hsu et al. 2004).

1.4 ATRX: potential roles

Members of the SNF2 family of proteins, which includes ATRX, were shown to be involved in a variety of cellular functions such as replication, DNA repair, transcriptional regulation, and recombination (Carlson and Laurent 1994; Matson, Bean et al. 1994). DNA repair does not seem to be a potential ATRX function since there is no ultraviolet sensitivity or higher risk of malignancy reported in ATR-X syndrome patients (Gibbons, Picketts et al. 1995). The specific function of ATRX is still unknown but it has been suggested to be implicated in transcriptional regulation. As stated previously, the α-globin expression is down-regulated in ATR-X patients although, the closely related β-globin gene expression is unaffected. These two related genes may be regulated differently because of their chromatin interactions since they are in distinct chromosomal environments. This reinforces the role of ATRX as a chromatin remodelling protein, like the other SNF2-like proteins (Gibbons, Picketts et al. 1995). Additionally, many studies have demonstrated a potential role for ATRX via chromatin interaction and modification.

ATRX structurally resembles other chromatin remodelling proteins because it contains PHD-like zinc-finger and ATPase/helicase domains. It was also shown that ATRX

is part of a multi-protein complex similar in size to other SWI/SNF complexes (Berube, Jagla et al. 2002). In a separate study, ATRX was shown to be part of a complex with the Daxx (death domain-associated) protein, a transcriptional co-repressor. Moreover, this complex displays chromatin remodelling activity *in vitro* (Xue, Gibbons et al. 2003; Tang, Wu et al. 2004). There are a collection of other studies that will be summarized in the following sentences that provide further circumstantial evidence that ATRX regulates chromatin structure and function. HP1α (heterochromatin protein 1α), a protein which regulates epigenetic gene silencing by promoting and maintaining chromatin condensation, was shown to interact with ATRX by a yeast two-hybrid assay (Le Douarin, Nielsen et al. 1996). That same interaction was confirmed in HeLa cell mitotic extracts by co-immunoprecipitation (Berube, Smeenk et al. 2000). ATRX was found to bind the chromatin associated protein EZH2 (Enhancer of Zeste homolog 2) through its SET domain. The region of ATRX interacting with HP1α and the EZH2 protein was proposed to be located between the PHD and the ATPase/helicase domains (Le Douarin, Nielsen et al. 1996; Cardoso, Timsit et al. 1998), a region which is not well conserved between mouse and human (Picketts, Tastan et al. 1998).

Lymphoblast cell lines derived from ATR-X patients were found to have modified methylation patterns of highly repetitive DNA sequence in the genome (Gibbons, McDowell et al. 2000). Although ATRX does not have a DNA methyltransferase (DNMT) motif, the PHD-like domain of ATRX is closely related to the one found in the human DNMT3 family of *de novo* methyltransferases (Okano, Bell et al. 1999; Xie, Wang et al. 1999). The PHD-like domain of ATRX also resembles the cysteine-rich regions required for interactions with histone deacetylases (HDACs) (Zhang, Ng et al. 1999). Taken together these studies provide

potential evidence that ATRX may interact with the methylation machinery and histone acetylation complexes to modulate DNA accessibility (Gibbons, McDowell et al. 2000). Therefore, mutations in *ATRX* could alter gene expression through modification of methylation and acetylation patterns in the genome. Moreover, ATRX localisation and its multiple interacting proteins further suggest it has a role in chromatin remodelling.

ATRX is localized to pericentromeric heterochromatin (PCH) during interphase and mitosis (McDowell, Gibbons et al. 1999). Further analysis showed that ATRX has a nuclear speckled staining pattern and associates with the nuclear matrix at interphase (Berube, Smeenk et al. 2000). At the onset of M phase, ATRX is phosphorylated and associates mainly to condensed chromosomes and with the HP1α protein (Berube, Smeenk et al. 2000). ATRX was also found to co-localise with other protein such as Daxx and the PML (promyelocytic leukemia) protein in the PML nuclear bodies (Xue, Gibbons et al. 2003). The transcriptional regulator Daxx associates with ATRX and both proteins are part of the same chromatin remodelling complex (Tang, Wu et al. 2004). The Daxx and ATRX protein-protein interaction is thought to be mediated by the N-terminal paired amphipathic alpha helices domain of Daxx (Ishov, Vladimirova et al. 2004). Moreover, this association was restricted to the full length protein and not observed for ATRXt (Garrick, Samara et al. 2004).

The PML protein is concentrated in nuclear structures called PML-nuclear bodies (PML-NB), which are thought to play a role in transcriptional activation, DNA replication, apoptosis and viral infection (Regad and Chelbi-Alix 2001; Borden 2002). Although ATRX and Daxx associate with PML-NBs, their sub-cellular localisation changes to be associated with the heterochromatin in a cell cycle dependent manner (Ishov, Vladimirova et al. 2004).

One group suggested that Daxx interacts with PML by its C-terminal end (Ishov, Sotnikov et al. 1999) and recruits ATRX to the PML-NB by its N-terminal tail in a cell cycle dependent fashion. In the same way, phosphorylated ATRX can recruit Daxx to the heterochromatin at late S phase. This cell cycle dependant association suggests the formation of a Daxx-ATRX complex at PCH immediately after DNA replication possibly to re-establish the epigenetic state of silent heterochromatin (Ishov, Vladimirova et al. 2004). Another study suggested that at G2 phase, PML-NBs are organised spherical structures where ordered layers of HP1α, ATRX, Daxx and PML protein surround a satellite DNA core, like layers in a "Jawbreaker" candy. The formation of this PML-NB is again thought to be involved in the quick recovery of condensed heterochromatin on satellite DNA before mitosis. (Luciani, Depetris et al. 2006). ATRX association to the PCH, its protein-protein interactions, its cell cycle dependent localisation and phosphorylation further suggest a role for ATRX chromatin remodelling in the regulation of the cell cycle.

Work previously done in our laboratory using an Atrx forebrain KO mouse model demonstrated a decrease in Daxx protein expression and an increase in PARP-1 (Poly(ADP-ribose) polymerase-1) gene expression and poly(ADP-ribosyl)ation (unpublished data). One of the roles of the PARP-1 protein is to survey and maintain genome integrity (de Murcia, Niedergang et al. 1997; Wang, Stingl et al. 1997). PARP-1 recognises and binds to DNA breaks, whereupon PARP-1 then becomes activated by auto poly(ADP-ribosyl)ation and subsequently adds ADP-ribose to other chromatin associated proteins like histones. These protein modifications mediate chromatin structure giving access to the break area for DNA repair (Poirier, de Murcia et al. 1982; Realini and Althaus 1992). PARP proteins were also found to modulate chromatin structure, regulate gene transcription and cell division by

interfering with transcription factor and cofactor binding in the absence of DNA breaks (Kraus and Lis 2003). The increased PARP-1 activation observed in the Atrx KO mice may be due to an increase in DNA strand breaks or a compensatory transcriptional effect due to the lack of Atrx.

The importance of ATRX in development is evident by the severe developmental delay described in the ATR-X patient. An important role for ATRX during development was confirmed by investigation of an $Atrx^{null}$ mouse which resulted in embryonic lethality at E9.5 (Garrick, Sharpe et al. 2006). In the absence of Atrx, E7.5 embryos were dramatically smaller and developmentally retarded suggesting a proliferation defect (Garrick, Sharpe et al. 2006). Moreover, conditional forebrain specific Atrx KO mice have a smaller cortex due to enhanced neuronal loss by apoptosis (Berube, Mangelsdorf et al. 2005). Similarly, Atrx overexpression was associated with abnormal growth of neuroprogenitors and disorganization of the cortex suggesting the importance of Atrx dosage for proper development (Berube, Jagla et al. 2002). Another study on *xnp-1*, the *ATRX* homologue in *C. elegans*, demonstrated that this gene is also essential in worm embryogenesis and gonadogenesis (Cardoso, Couillault et al. 2005). All together, the developmental and proliferation defects in these models propose a potential role for ATRX in cell cycle control.

Recent work published during the course of our experiments further demonstrated the importance of ATRX in cell cycle progression. A study showed that the depletion of ATRX in HeLa cells affects the M phase progression more specifically, a prolonged pro-metaphase to metaphase transition. The phase transition prolongation corresponded to defects in chromosome cohesion, congression and segregation in ATRX depleted cells *in vitro* and *in*

vivo (Ritchie, Seah et al. 2008). Similarly, other studies showed that disruption of ATRX binding to centromeres resulted in abnormal chromosome alignment at metaphase II in mouse oocytes (De La Fuente, Viveiros et al. 2004). These results suggest a requirement for ATRX during mitosis. Atrx was also found to be involve in cell proliferation, the Garrick group showed that cultured $Atrx^{null}$ ES cells have perturbed growth although the cause remains undefined (Garrick, Sharpe et al. 2006). Taken together, these studies highlight the importance of ATRX activity and expression level for proper cell cycle progression.

Work in *C.elegans* has shown that *xnp-1* (ATRX homolog) and *lin-35* (Rb homologue) genetically interact during *C. elegans* larval development. *C. elegans lin-35* mutants usually have normal vulval development, yet depletion by RNAi of *xnp-1* in these mutants resulted in a larval growth arrest at the first larval stage (L1). Similarly, *xnp-1* ablation in hpl-2 (HP1α homologue) mutants also arrested larval development at L1. Additionally, *C. elegans xnp-1* mutants have severe gonadogenesis defects (Cardoso, Couillault et al. 2005). These findings suggest that ATRX, Rb and HP1α may function together to maintain cell growth. In addition, unpublished data from the same authors found that ATRX and Rb interact in human lymphoblastoid cells by co-immunoprecipitation (Cardoso, Couillault et al. 2005).

Other SWI/SNF proteins are also involved in cell cycle progression. BRM and BRG1, two SWI/SNF chromatin remodelling proteins have been shown to interact with Rb (Dunaief, Strober et al. 1994; Dyson 1998). A recent study suggested that Rb can recruit HDAC and SWI/SNF together into a single complex. They also found that these complexes act as repressors to regulate the gene transcription of cyclins and cdks during the cell cycle

(Zhang, Gavin et al. 2000). The implication that the SWI/SNF family members BRG1 and BRM function in cell cycle progression further support a role for other chromatin remodelling proteins like ATRX to be important for this process too. Therefore, a role for ATRX during cell cycle progression should be further investigated. As a prelude I will provide an overview of the cell cycle with particular emphasis on the Rb/E2F checkpoint that occurs in the G1 phase.

1.5 An overview of the cell cycle and the role of Rb and E2F at G1 phase

The cell cycle is an intricate process that involves various regulatory proteins that direct the cell through a precise sequence of events culminating in mitosis and the production of two daughter cells. The cell cycle is divided into the interphase and the M (mitotic) phase. The M phase includes prophase, metaphase, anaphase and telophase. The interphase contains the G1, S and G2 phase. In the G1 phase (gap 1) the cells are preparing for DNA synthesis, in S phase the DNA is replicated and in the G2 phase (gap 2) the cells are preparing for mitosis which will occur in the following M phase. The G0 (gap 0) phase is between the M and G1 phase, it contains cells that are not actively cycling and terminally differentiated cells. The progression through the different cell cycle stages is regulated by the cdks (cyclin dependant kinases) and the cyclin proteins (Alberts 1999). The different cyclins bind precise cdks to regulate their activity and to target them to the nucleus. The cyclins are responsible for the activation of the kinase activity of the cdk at specific cell cycle check points, therefore, tight regulation of the expression of the cyclins is essential (figure 4 A, B). The cyclic expression of the cyclins is due to degradation of these proteins by ubiquitination at specific times during cell cycle progression (Darzynkiewicz, Gong et al. 1996; Rechsteiner

and Rogers 1996). As illustraded in figure 4 A and B, I will describe the different cyclins and cdks involved in the cell cycle progression. Starting at the the G1 phase, Cyclin D is expressed and formes a complex with cdks4/6 which becomes activated. Cyclin D protein is required for G1 progression and is degraded by ubiquitination at the end of the G1 phase when cyclin E starts to be expressed. Cyclin E expression promotes S phase entry and is degraded in mid S phase. Cyclin A starts to be expressed at S phase as cyclin E is degraded. Cyclin A is important for S phase progression it is expressed through the S phase and is degraded at the G2 to M phase transition. Both cyclins E and A associate with cdk2 to form an active cyclin-cdks complex. During the G2 phase as the cell prepares for mitosis, cyclin B starts to be expressed and associated with cdk1. Cyclin B-cdk1 is important G2/M transition, it is expressed until the end of mitosis where its expression abruptly stops. Then the cycle continues as the two daughter cells then re-enter G1 or stop dividing by entering G0 (figure 4 A, B).

Phosphorylation state for protein activation/inactivation is another important regulation mechanism of the cell cycle. The cdks are serine/threonine kinases that phosphorylate a variety of substrates at specific phases to control cell cycle progression. For example, at G1 phase the cyclinD-cdk4/6 complex inactivates Rb by phosphorylating it on multiple residues (figure 4 C). The active hypophosphorylated Rb binds the E2F transcription factors and prevents E2F target genes from being transcriptionally activated. When Rb is hyperphosphorylated E2F is released and activates the transcription of genes necessary for cell cycle progression (Arroyo and Raychaudhuri 1992; Mudrak, Ogris et al. 1994) (figure 4 C). Rb remains in a hyperphosphorylated state until the end of mitosis (Weinberg 1995). Similarly, at the S, G2 and M phases the other cyclin-cdk complexes

Figure 4. Cyclin involvement and expression during cell cycle progression and Rb pathway

(A) Illustration of the cell cycle with its important phases. The various cyclin-cdk complexes essential for progression through the cell cycle are indicated. (B) Schematic drawing of cell cycle-dependent levels of cyclins. Thickness of hashed bars indicates relative intracellular cyclin concentration. (C) Schematic drawing of activation of E2F by the cyclinD-cdk4,6 complex. Cyclin D associates with cdk4 or cdk6 to phosphorylate Rb, which releases E2F to activate transcription of genes necessary for cell cycle progression. Illustrations adapted from Schafer et al. 1998 (Schafer 1998).

A

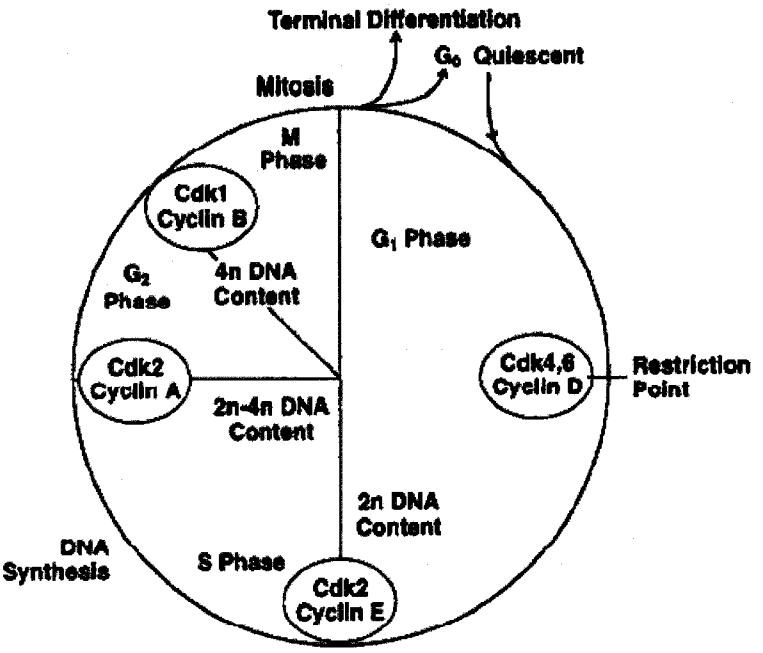
Terminal Differentiation
G_0 Quiescent
Mitosis
M Phase
Cdk1 Cyclin B
G_1 Phase
G_2 Phase
4n DNA Content
Cdk2 Cyclin A
Cdk4,6 Cyclin D
Restriction Point
2n-4n DNA Content
2n DNA Content
DNA Synthesis
S Phase
Cdk2 Cyclin E

B

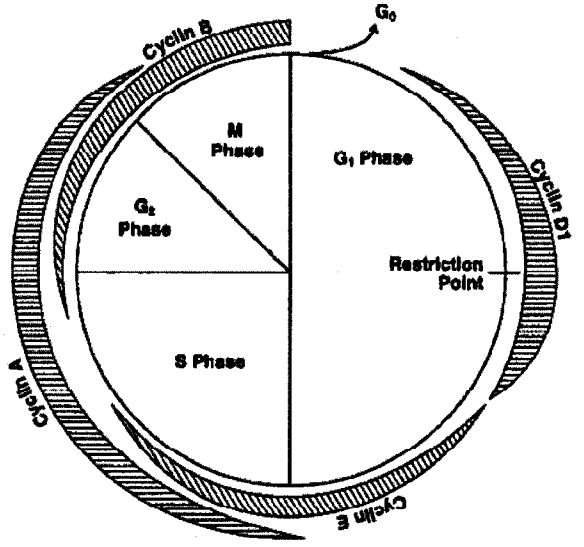
Cyclin B
G_0
M Phase
G_1 Phase
Cyclin D1
G_2 Phase
Restriction Point
S Phase
Cyclin A
Cyclin E

C

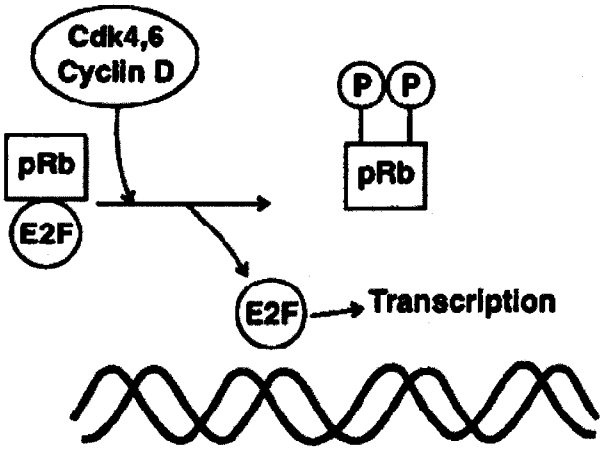
Cdk4,6 Cyclin D
P P
pRb
pRb
E2F
E2F
Transcription

described earlier (figure 4 A) phosphorylate and activate/inactivate cell cycle regulatory proteins.

1.6 Generation of models with reduced ATRX expression levels

1.6.1 siRNA and shRNA

The use of RNAi (RNA interference) based down regulation of gene expression is a widely exploited tool in molecular biology. The mechanism of gene silencing by RNAi is well characterized and results in target mRNA degradation (Novina and Sharp 2004). It is also a naturally occurring process in eukaryotes thought to defend against invading nucleic acids such as viruses and transposons (Vance and Vaucheret 2001; Plasterk 2002). The RNAi pathway (figure 5) commences in the cytoplasm when long dsRNA (double stranded RNA) molecules are recognized by Dicer. The RNase III enzyme Dicer processes the dsRNA into smaller 21-25 nucleotide duplexes called siRNA (small interfering RNA). The siRNA associates with RISC (RNA-induced silencing protein complex) which becomes activated and separates the siRNA duplex. One strand of the siRNA duplex remains associated with RISC and targets the homologous sequence specific mRNA. The target mRNA is cleaved by RISC which is then released and the mRNA further degraded by exonucleases. The degradation of the target mRNA will result in decreased synthesis of the protein encoded by the mRNA and finally a loss of protein function which can by referred to as a protein "knockdown" (reviewed in Rutz and Scheffold 2004).

Figure 5. The RNA interference pathway

The dsRNA and shRNA are processed by Dicer into smaller 21-25 nucleotide duplexes called siRNA. The siRNA associates with RISC and this complex targets specific mRNA sequences for cleavage and degradation. Illustration obtained from Rutz et al. 2004 (Rutz and Scheffold 2004).

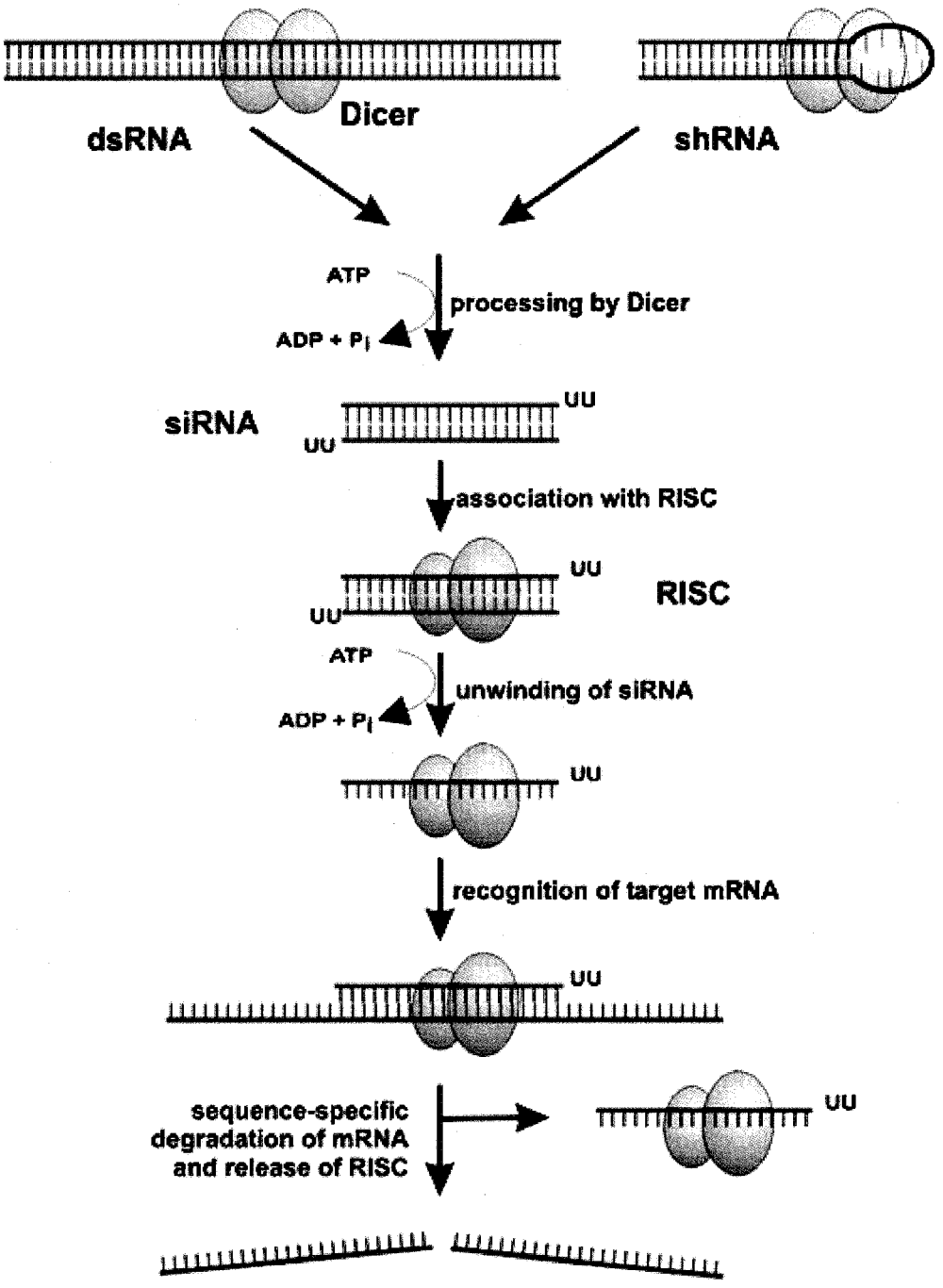
dsRNA
Dicer
shRNA
ATP
ADP + Pi
processing by Dicer
siRNA
UU
UU
association with RISC
UU
UU
RISC
ATP
ADP + Pi
unwinding of siRNA
UU
recognition of target mRNA
UU
sequence-specific
degradation of mRNA
and release of RISC
UU

In this study, siRNA and shRNA (small hairpin RNA) oligonucleotides were utilized for ATRX down regulation in a HeLa cell culture system. For transient transfection experiments the siRNAs were transfected into the cell to generate transient ATRX knockdown effective for ~96 hours. For long term gene silencing, we transfected cells with a shRNA expressing plasmid and stable clones were selected. The expression plasmid produces a transcript of the sense and antisense target linked by a spacer sequence. This transcript can form a stem-loop or hairpin structure which is recognised and cleaved by Dicer to generate the siRNA molecule. The subsequent mechanism involved in shRNA knockdown is identical to that described for siRNA (figure 5).

1.6.2 Atrx KO MEFs

The third method of Atrx knockdown used in this study takes advantage of the existing *Atrx*$^{flox/flox}$ mouse line. These mice have the exon 18 of the *Atrx* gene flanked by *loxP* recognition sites for the CRE recombinase and a *loxP* flanked MC1-neo^{r} cassette in intron 17 (figure 6) (Garrick, Sharpe et al. 2006). The *Atrx*$^{flox/flox}$ mice were used in multiple studies to create Atrx KO mouse models. When mated with mice expressing Cre, the F1 generation will contain mice with an inactive Atrx protein lacking exon 18. Atrx total KO mice were generated that way and proved to be embryonic lethal (Garrick, Sharpe et al. 2006). Atrx can also be conditionally ablated in specific tissues by having the Cre expression driven by tissue specific promoters. Atrx was conditionally inactivated in the forebrain by driving Cre expression under the control of the Forkhead box transcription

Figure 6. Schematic representation of the *Atrx*^{flox} gene and recombination products

The *Atrx*$^{flox/flox}$ mice have the exon 18 of the *Atrx* gene flanked by *loxP* recognition sites for the CRE recombinase and a *loxP* flanked MC1-neo^{r} cassette in intron 17 (top of the figure). After Cre expression, three possible recombination events can be mediated by the Cre recombinase (labelled A, B, and C). The recombined *Atrx* gene is lacking the exon 18 which encodes the first motif in the ATPase/helicase domain essential for Atrx function (lower section of the figure). Diagram adapted from Garrick et al. 2006 (Garrick, Sharpe et al. 2006).

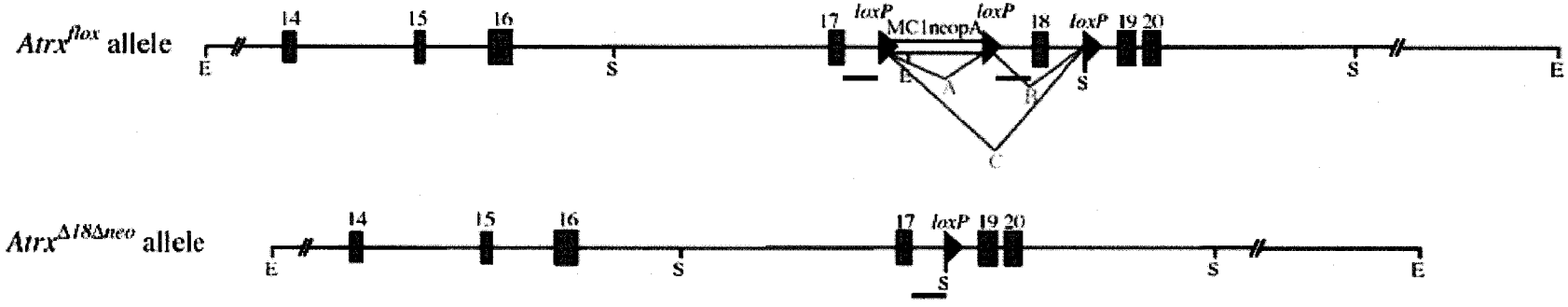
Atrx^flox allele
14
15
16
17
loxP
MC1neopA
loxP
18
loxP
19
20
E
S
E
A
B
S
S
E
C
Atrx^Δ18Δneo allele
14
15
16
17
loxP
19
20
E
S
S
S
E

factor, *Foxg 1* and *Nestin* (neuronal intermediate filament protein) promoters (Berube, Mangelsdorf et al. 2005) which are respectively a forkhead box G1 transcription factor and a type VI intermediate filament expressed in neurones. While exon 18 deletion by Cre recombination inactivates Atrx function by removing the ATPase/helicase binding domain, it was also observed that the full-length protein is unstable and degraded while the truncated isoform remains unaffected (Berube, Mangelsdorf et al. 2005; Garrick, Sharpe et al. 2006). Primary cell culture lines in which Atrx is inactivated can also be created in a similar way. $Atrx^{null}$ ES cells were generated from $Atrx^{flox}$ ES cells transfected with a Cre-recombinase expression plasmid (Garrick, Sharpe et al. 2006). In my study, I took advantage of the $Atrx^{flox}$ mouse line to generate $Atrx^{null}$ mouse embryonic fibroblasts (MEFs) from $Atrx^{flox}$ MEFs infected with a Cre recombinase expressing adenovirus.

1.7 Rationale, hypothesis, and research objectives

Mutations in the *ATRX* gene give rise to developmental delay, physical abnormalities and mental retardation in ATR-X patients. Although, the precise role of ATRX is still unknown it functions as part of a chromatin remodelling complex, involved in gene regulation and normal brain development. Recent studies have also uncovered a potential function for ATRX in chromosomal segregation at mitosis and for cell proliferation. Additionally, the role of the SWI/SNF family members BRG1 and BRM in cell cycle progression further suggests that other chromatin remodelling proteins like ATRX may similarly regulate this process. In this regard, we hypothesise that ATRX is an important regulator of proliferation and cell cycle progression. To explore this hypothesis the following objectives were set:

1. Establish stable ATRX knockdown cell lines for study
2. Characterize the growth, death and cell cycle progression in the absence of ATRX in these cell lines
3. Identify potential cell cycle genes and check points controlled by ATRX
4. Corroborate our findings in a primary cell line model

Taken together, this study will define the role for ATRX in cell cycle progression thereby providing potential insight into the pathogenesis of the ATR-X syndrome.

2 Materials and methods

2.1 General Materials

General chemicals such as TRIS, NaCl, KCl, Na_2PO_4, KH_2PO_4, Glycine, SDS (sodium dodecyl sulfate), EDTA (ethylenediaminetetraacetic acid) used for buffer preparation were obtained from Fisher Scientific (Ottawa, ON), Sigma-Aldrich (Oakville, ON), and Invitrogen (Burlington, ON). Other reagents including agarose, ethidium bromide, Triton-X-100 and Tween 20 were obtained from Invitrogen (Burlington, ON) and Fisher Scientific (Ottawa, ON). Ethanol, methanol and sterile HPLC water were obtained from Fisher Scientific (Ottawa, ON). The bacterial culture materials: Bacto-Yeast, Bacto-Tryptone, Bacto-Agar were obtained from VWR International (Mississauga, ON). All the plasticware used for cell culture and general lab purposes including T75, T25, 10 cm, and 6 cm culture dishes; 96, 12 and 6 wells plates; 50 ml and 15 ml tubes and microcentrifuge tubes were obtained from Fisher Scientific (Ottawa, ON). The provenance of the other materials used is stated throughout the methods section as they are used.

2.2 Methods

2.2.1 Maintenance of cell lines

HeLa and HeLa Tet-ON cells (ATCC, Manassas, Virginia) were maintained in culture in T75 cell culture flasks in DMEM (Dulbecco's Modified Eagle Medium) (Invitrogen, Burlington, ON) supplemented with 10% FBS (fetal bovine serum) (HyClone, Logan, UT) and 1% penicillin/streptomycin (Invitrogen, Burlington, ON). The stable

psiRNA ATRX3 C5 cell line was cultured in the same media but supplemented with 800 μg/ml G418 (Invitrogen, Burlington, ON) during clone selection or with 400 μg/ml G418 for regular culture and maintenance of the cells. HeLa cells were split 1:5 to 1:10 every 2-3 days or when 80% confluent. Basically, the cells were washed 2 times with PBS (phosphate-buffered saline; 8g NaCl, 0.2g KCl, 1.44g Na_2PO_4, 0.24g KH_2PO_4 in 1L of H_2O), removed from the plate by incubating the cells with 1ml of 1X Trypsin-EDTA for 3-5 min, then re-suspended in complete media and reseeded into clean culture dishes.

MEFs extracted from the *Atrx*$^{flox/Y}$ and *Atrx*$^{flox/flox}$ mice were cultured in DMEM supplemented with 10% FBS, 1% penicillin/streptomycin. MEF cultures were split 1:3 every 2-3 days or when 80% confluent as described above with the exception that only 1ml of 0.5X Trypsin-EDTA was used to remove the cells from the plate.

To freeze and preserve cells, they were first washed in PBS, then trypsinized and washed in complete media, before pelleting the cells for 5 min at 1,000 rpm (rotations per minute). Cell pellets were resuspended in freezing media (complete DMEM media + 10% DMSO (dimethyl sulfoxide, Sigma, Oakville, ON)) with one third of the HeLa cells from an 80% confluent T75 flask frozen added to one cryo-vial with 1.5 ml of freezing media. The frozen cells are preserved at -80°C or in liquid nitrogen until needed. To cryopreserve MEFs, one confluent 10cm dish was resuspended in 1ml of freezing media (FBS + 10% DMSO) and frozen down at -80°C in a cryo-vial. When required, cryopreserved cells were thawed in a 37 °C water bath, washed in complete media, precipitated for 5 min at 1,000 rpm and resuspended in 5 ml of complete media for seeding in a T25 flask.

2.2.2 Generation of the ATRX shRNA expression plasmid

The expression vector psiRNA-hH1 neo (figure 7) (InvivoGen, San Diego, CA) (Elbashir, Harborth et al. 2001; Elbashir, Lendeckel et al. 2001; Brummelkamp, Bernards et al. 2002) was used to express an shRNA targeted for silencing the *ATRX* gene. The siRNA sequences were designed to target exon 1 of the *ATRX* gene. The siRNA oligonucleotides contained a 5' overhang compatible with the *BbsI* restriction sites on the psiRNA-hH1neo plasmid and a 5-9 base pair spacer region to allow for the formation of a hairpin structure. The sequences of the oligonucleotides designed are presented in the appendix (Appendix A). To clone the ATRX siRNA insert in the psiRNA-hH1 neo plasmid the vector was initially digested with the restriction enzyme *BbsI* (New England Biolabs, Ipswich, MA) to generate 2 fragments of 339 and 2640 base pairs. The fragments were separated on a 1% agarose gel supplemented with 50 ng/ml of EtBr in 1XTAE (40mM Tris-acetate, 1mM EDTA) in the Bio-Rad Mini Sub-Cell GT apparatus (Bio-Rad, Mississauga, ON) with a current of 100V. The 2640 bp band was cut out of the gel using a razor blade under UV (ultra violet) light and extracted from the gel using the DNA and Gel Band Purification Kit (Amersham Bioscience, Piscataway, NJ) following the manufacturer's instructions. The sense and antisense siRNA oligonucleotides (Appendix A) were annealed to form the siRNA insert. Basically, 2 ul each of the sense and antisense oligonucleotide (25 μM) was mixed with 6 ul of 0.5 M NaCl and 20 μl of water, and then incubated at 80°C for 2 minutes. The heating block was then removed and allowed to cool to 35°C before removing the sample. The siRNA inserts were then ligated to the *BbsI* digested psiRNA-hH1neo vector. The ligation was performed by incubating for 2 hours at 27 °C, 100 ng of the *BbsI* digested psiRNA-hH1neo plasmid fragment, 1 μl of the annealed siRNA insert, 1 μl of T4 DNA ligase (New England Biolabs,

Figure 7. The psiRNA-hH1 neo plasmid

The psiRNA-hH1 neo vector was used to express an shRNA targeted for *ATRX* in HeLa cells. The shRNA oligonucleotide was cloned in the vector between the BbsI restriction sites. The vector contains an H1 promoter to drive the shRNA expression. It also contains the Neo gene which confers resistance to the antibiotics kanamycin in bacteria and G418 in mammalian cells. Map obtained from psiRNA-hH1 neo plasmid product information sheet (InvivoGen, www.invivogen.com).

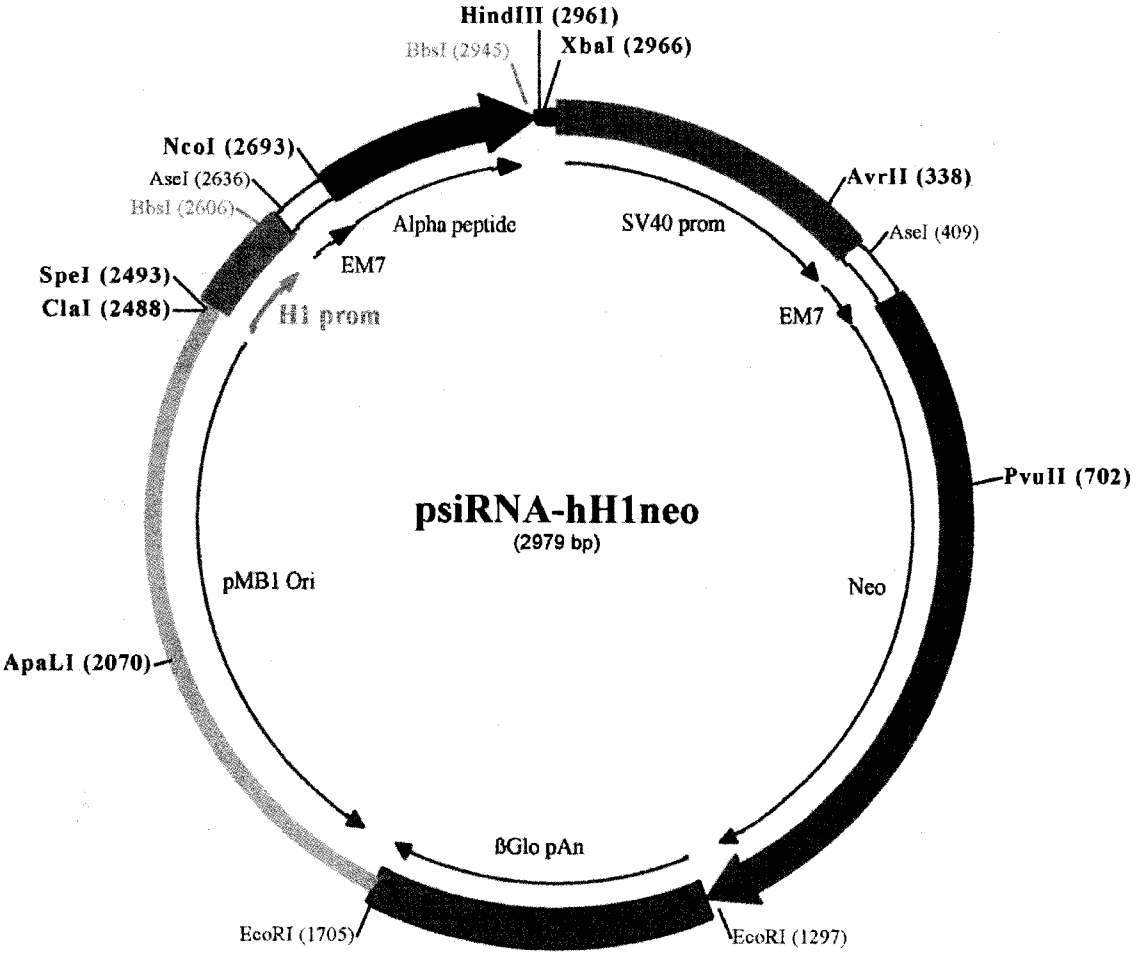
HindIII (2961)
BbsI (2945)
XbaI (2966)
NcoI (2693)
AseI (2636)
BbsI (2606)
AvrII (338)
AseI (409)
Alpha peptide
SV40 prom
EM7
SpeI (2493)
ClaI (2488)
H1 prom
EM7
PvuII (702)
psiRNA-hH1neo
(2979 bp)
pMB1 Ori
Neo
ApaLI (2070)
ßGlo pAn
EcoRI (1705)
EcoRI (1297)

Ipswich, MA), 2 µl of 10X ligation buffer and 14 µl of water.The ligation products were transformed into competent stable 2 cells (Invitrogen, Burlington, ON) using a heat shock method as follows: in a 15 ml bacterial culture tube, 150 µl of competent cells and 10 µl of the ligation product were mixed and incubated on ice for 20 minutes then heat shocked at 42°C for 45 sec and placed back on ice for 2 minutes. Next, 1 ml of LB (Luria-Bertani) broth (1% Bacto-Tryptone, 0.5% Bacto-Yeast, 171.1 mM NaCl) was added and incubated at 37°C with agitation for 1 hour. After the incubation, 150 µl of transformed cells were plated in bacterial culture dishes containing agar (1.5% Bacto-Agar in LB broth) supplemented with 30ug/ml kanamycin (Invitrogen, Burlington, ON). The bacterial plates were incubated overnight at 37°C. The next day, the selected colonies were picked with a sterile toothpick and placed in a 15ml culture tube containing 3 ml of LB broth supplemented with 30ug/ml of kanamycin and incubated overnight with shaking at 37°C. The following day, the plasmids were extracted by boiling lysis, described in the following sentences. Briefly, 1 ml of bacterial culture is precipitated at 13,000 rpm for 2 minutes and re-suspended in 350 µl of STET buffer (0.1 M NaCl, 0.01 M Tris-HCl pH8, 0.001 M EDTA pH8, 5% Triton-X-100). Then, 25 µl of prepared lysozyme (10 mg in 0.01 M Tris-HCl pH8; Sigma, Oakville, ON) was added and the mix was incubated at 100°C for 40 sec. After the incubation, the bacterial cell lysate was centrifuged for 10 min at 12,000 rpm at room temperature, the supernatant removed to a new tube and 40 µl of 2.5 M NaOAc pH5.2 and 420 µl of 100% isopropanol were added to it. The mixture was vortexed and incubated 5 minutes at room temperature. The solution was then centrifuged at 12,000 rpm for 5 minutes at 4°C, the supernatant discarded, the pellet washed with 1 ml of 70% Ethanol and centrifuged again at 12,000 rpm for 2 minutes. The supernatant was removed and the DNA pellet allowed to air dry before

dissolving in 30 µl of water. The plasmid DNA concentration was quantified at 260nm using a DU® 640 spectrophotometer (Beckman Coulter, Mississauga, ON)

We confirmed the presence of the shRNA insert with an *AseI* digestion. A parental plasmid generates 2 fragments, while a recombinant plasmid is linearized since one of the two *AseI* sites is lost during the initial preparation of the vector with the *BbsI* digestion. For the digestion: 500 ng of plasmid (1 µl) was cut with 1 µl of *AseI* (New England Biolabs, Ipswich, MA), 2 µl of NEB3 buffer (New England Biolabs, Ipswich, MA) and 16µl of water to make a final volume of 20 µl. The *AseI* digest was incubated for 1 hour at 37°C, then 10 µl of the digested products were electrophoresed on a 1% agarose gel made in 1X TAE (4.84 g Tris, 1.14 ml acetic acid, 2 ml 0.5M EDTA pH8, adjust to 1 L with water) supplemented with ethidium bromide (Ausubel 2001). The samples were mixed in 10X agarose gel sample buffer (250 mg bromophenol blue, 33 ml of 150 mM Tris pH7.6, 60 ml glycerol, 7 ml water) and run at 100V side by side with 10 µl of a 1 Kb+ ladder (Invitrogen, Burlington, ON). Following the identification of positive clones containing the siRNA insert, a new plasmid extraction was performed from 1 ml of the bacterial cultures using the Qiaprep spin Miniprep kit (Qiagen, Mississauga, ON). The plasmid extraction kit yields cleaner DNA and is more suitable for subsequent sequencing of the plasmid DNA. The DNA was quantified and sent for sequencing with the primer OL381 (reverse primer, Invitrogen, Burlington, ON) and the primer psiRNA-hH1neo fwd (forward primer, Cortec, Kingston, ON) (see sequence in Appendix B) at the StemCore Laboratories DNA sequencing facility (Ottawa, ON). After obtaining and analyzing the sequencing results, a clone was chosen for large scale plasmid preparation. In this regard, 200 µl of bacterial culture was grown overnight at 37°C in 200 ml of LB broth supplemented with 30 µg of kanamycin. The next day, the plasmids were

isolated from the bacterial culture using a Qiagen Maxiprep kit (Qiagen, Mississauga, ON). The plasmid preparation was quantified with the DU® 640 spectrophotometer at 260nm. Then, 500 ng of plasmid was digested with *AseI* to re-confirm that the shRNA insert was present prior to dividing it into aliquots for storage at -20°C for future use.

2.2.3 Generation and selection of stable cell lines expressing shRNA against LacZ and ATRX.

To begin selection of stable clones, $7X10^5$ HeLa cells were plated on a 10 cm plastic culture dish and incubated overnight to adhere onto the plates. On day 2, the cells were transfected following the guidelines stipulated in the Invitrogen Lipofectamine protocol. Plasmid DNA (8 ug) in 800 µl of serum free DMEM (Solution A) was mixed with 740 µl of serum free DMEM containing 60 µl of Lipofectamine (Invitrogen, Burlington, ON) (Solution B) and allowed to incubate at room temperature for 30 minutes. The plated cells were washed with 5 ml of PBS, then 4.8 ml of serum free DMEM was added to the A/B solution and put on the washed cells to incubate for 4 hour at 37°C. After incubation, the media was changed for complete DMEM (10% FBS, 1% penicillin/streptomycin) and the cells were incubated again for 48h. Finally, the media was changed to complete DMEM supplemented with 800 µg/ml G418, Geneticin, (Invitrogen, Burlington, ON) for clone selection. The selection media was changed every 3 days for a period of 2 weeks, until colonies emerged. Individual colonies were taken from the plate with a pipette tip and resuspended in 0.5 ml of complete DMEM supplemented with 800 µg/ml of G418 into individual wells of a 24 well plate (figure 8). A total of 20 psiRNA-hH1neo ATRX-3

Figure 8. Schematic diagram of the strategy used to generate the psiRNA ATRX clones

The psiRNA-hH1 neo vector that contains the shRNA oligonucleotide is transfected in the HeLa cells. The cells are then selected in G418 containing media. The colonies formed after selection are picked and expanded individually to generate the clones for further analysis of ATRX knockdown by immunoblot.

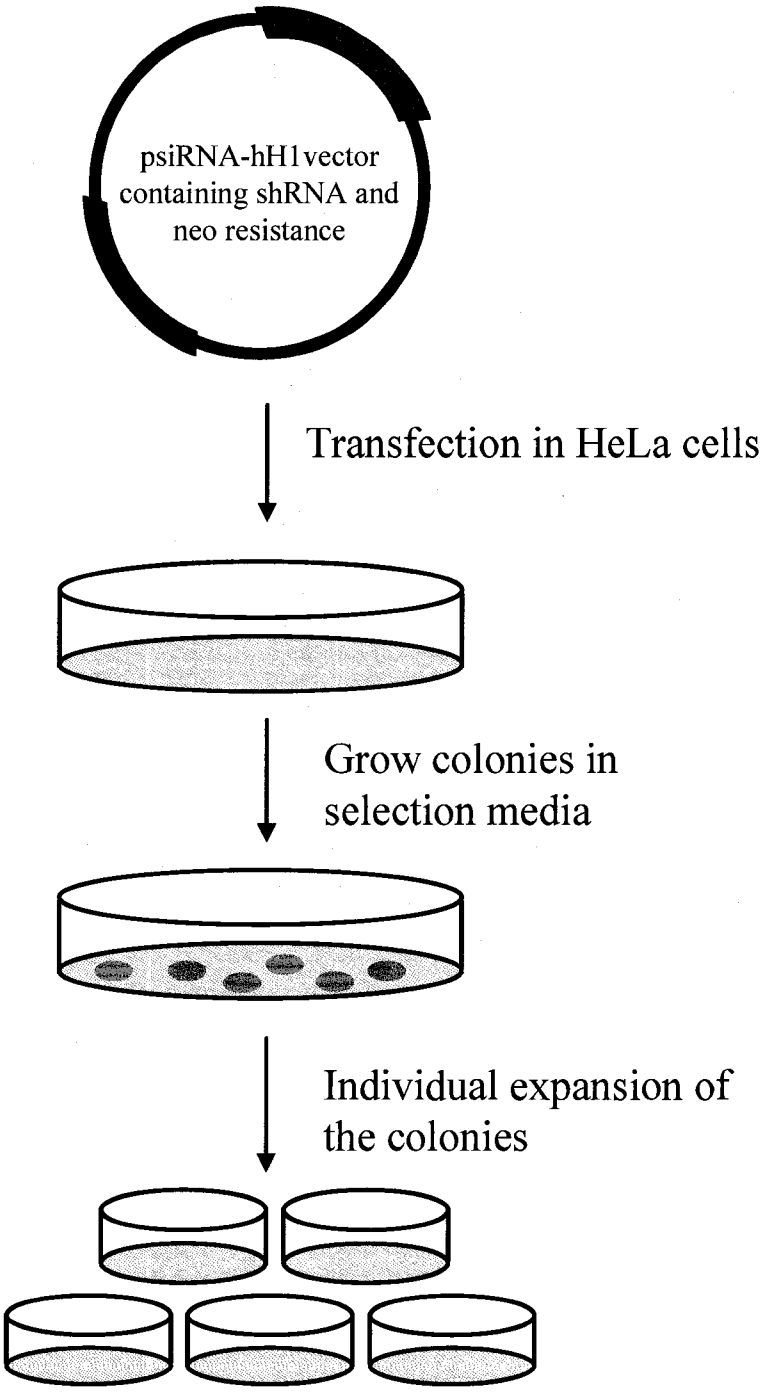
psiRNA-hH1vector containing shRNA and neo resistance
Transfection in HeLa cells
Grow colonies in selection media
Individual expansion of the colonies

colonies were expanded and frozen down for further study. The name of the clones corresponds to the vector name + the shRNA insert and its position on the 24 well plate.

2.2.4 Transient transfection of ATRX siRNA in HeLa cells

HeLa cells were seeded in the wells of a 6 well culture dish at $0.5X10^6$ cells per well and incubated overnight to adhere to the dish. For each transfection reaction the following solutions were prepared: (A) 300µl of 100nM siRNA solution in OPTIMEM media (Invitrogen, Burlington, ON); and solution (B) 30µl of a 1:2 mixture of lipofectanime 2000 reagent (Invitrogen, Burlington, ON) and OPTIMEM media. Solution B was incubated for 15 minutes at room temperature then solutions A and B were mixed and brought to a volume of 600µl with OPTIMEM and incubated for 30 minutes at room temperature (Dalby, Cates et al. 2004). A volume of 1.4 ml of OPTIMEM was added to each transfection reaction after the incubation to obtain a final volume of 2ml. The plated cells were washed with OPTIMEM and covered with the transfection solution and incubated for 6hrs at 37°C/5% CO_2. The cells were then trypsinised and split in a 1:3 dilution in new 6 well culture plates and incubated until the desired time point.

2.2.5 Generation of MEFs (mouse embryonic fibroblast) from *Atrx*^{floxed} mice

The mice used in this study were *Atrx* $^{flox/flox}$ maintained on a C57 BL6 background. The *Atrx* floxed mice have been described previously (Berube, Mangelsdorf et al. 2005). To obtain the embryos used for generating primary mouse embryonic fibroblast cultures an *Atrx* $^{flox/flox}$ female and an *Atrx* $^{flox/Y}$ male were time-mated.

The pregnant females were sacrificed at E13.5, both arms of the uterus were removed from the mouse and set in a 10cm cell culture dish with sterile PBS. Each embryo was removed from the uterus and the yolk sac was excised prior to placing the embryos into a clean culture dish containing PBS. The embryos were decapitated and the head kept in individual 1.5ml tubes for genotyping by PCR. The organs were eviscerated and discarded. Each embryo body was put in a clean 10cm cell culture dish with 5ml of 1X trypsin-EDTA, cut into small pieces using two scalpel knives and then incubated at 37°C for 15 minutes. After the incubation, the embryonic tissue was further broken down by trituration in the trypsin using a serological pipette followed by the addition of 5ml of complete DMEM (10% FBS, 1% penicillin/streptomycin) to neutralize the trypsin solution. The embryonic cells were placed in a 15ml falcon tube and centrifuged at 12,000 rpm for 5 minutes. The media was then aspirated and the cell pellet was resuspended in 9 ml of complete DMEM, and aliquoted (3ml) into three 10cm cell culture dishes containing 5ml of complete DMEM (A 2007). The MEF cultures were incubated at 37°C/5%CO_2 and grown until confluency at which time the MEFs were either used for experiments or cryopreserved for future use.

Tina Price-O'Dea kindly performed the genotyping for my study. The DNA from the head of each embryo used for the extraction of MEFs was isolated by "hotshot" alkaline lysis DNA extraction (Truett, Heeger et al. 2000). A piece of the embryo's head was incubated at 95°C for 30 min in 75 µl of alkaline lysis reagent (25 mM NaOH + 0.2 mM disodium EDTA, pH 12) then cooled to 4°C. The lysate was then neutralized with 75 µl of neutralizing reagent (40 mM Tris-HCl). PCR genotyping for sex determination was performed on the cell lysate using the following primers: Sry-F, Sry-R, Fabp1-F and Fabp1-R (sequences listed in Appendix B). The PCR mix contained 5 µl of 10X PCR buffer , 1 µl of 10 mM

dNTPs, 1.5 µl of 50 mM $MgCl_2$, 0.25 µl of each primer (4), 0.3 µl of Taq polymerase (Invitrogen, Burlington ON) and 40.2 µl of water. Reactions were incubated at 95°C for 20 sec, 57°C for 20 sec, and 72°C for 40 sec for a total of 35 cycles. PCR results were examined on a 1% agarose gel/1X TAE as previously described (section 2.2.2).

2.2.6 Adenovirus treatment of MEFs

2.2.6.1 Infection

The two adenoviruses used in this study express either LacZ or CRE recombinase and both were kindly provided by Dr. Robin Parks (OHRI, Ottawa, ON) (Ng, Parks et al. 2002).

Cells ($1.2X10^6$) were seeded in 10 cm cell culture dishes and incubated at 37°C/5%CO_2 for a minimum of 4 hours to allow the cells to adhere to the dish. The amount of virus needed for the infection was optimized using a MOI (multiplicity of infection) ranging from 10-500, with an MOI of 250 found to be optimal for exon 18 excision. The appropriate volume of virus for an MOI of 250 was mixed in sterile PBS to reach a final volume of 1.5ml. Once adherent, the cells were washed with PBS and the virus solution was deposited on the cells for incubation at 37°C/5%CO_2 for 1 hour. The culture plates were rocked every 15 minutes to ensure equal distribution of the virus throughout the dish. Following this initial infection period, 8 ml of complete DMEM was added to the dish and the incubation continued at 37°C/5%CO_2 until the designated time point.

2.2.6.2 *Verification of the Cre recombinase induced excision of the floxed exon 18 in the Atrx floxed MEF cultures.*

Atrx floxed MEFs were seeded in 10 cm culture dishes ($1.2X10^6$ cells/dish) and infected the next day with a gradient of MOI (from 10 to 500). Then, 48h post-infection the MEFs from the 10cm dishes were scraped off and collected in a 1.5 ml tube. An RNA extraction was performed using the RNeasy plus mini RNA extraction kit (Qiagen, Mississauga, ON) following the manufacturer's protocol and then the RNA was reverse transcribed (RT) to generate cDNA. To perform the RT reaction the following ingredients were mixed, incubated at 65°C for 5 min and then put on ice: 1ul of RNA (0.5-1 μg), 1 μl of random primers, 1 μl of 10mM dNTPs and 10 μl of water. Then, 4μl of 5X first strand buffer and 2 μl of 0.1 M DTT were added and the mixture was incubated for 1 min at 42°C. Next, 1 μl of SuperScript II RT was added and the incubation was continued for 1 hour at 42°C. All RT-PCR reagents were obtained from Invitrogen (Burlington, ON). The region spanning the floxed sequence was amplified by PCR using the primers Seq 36.2 and pps1.15 (sequences listed in Appendix B). β-actin amplification was used as a control (primer sequence shown in Appendix B). The PCR mix for exon 18 excision verification contained 1 μl of cDNA, 5 μl of 10X PCR buffer , 1 μl of 10 mM dNTPs, 1.5 μl of 50 mM $MgCl_2$, 1 μl of each primer , 0.5 μl of Taq polymerase (Invitrogen, Burlington ON) and 39 μl of water. The PCR mix was incubated at 96°C for 30 sec, 60°C for 30 sec and 72°C for 30 sec and repeated for 35 cycles. Afterwards 10 μl of the PCR reaction mix was electrophoresed on a 1% agarose gel as previously described (section 2.2.2) and photographed under UV light. The resulting bands at 648 bp and 520 bp are representative of the cDNA fragment with exon 18 present or excised, respectively.

2.2.7 TUNEL assay

Cells were plated in 6 well plates containing cover slips ($2.5X10^5$ cells/well) or in 4 well chamber slides (40 000 cells/well) depending on the experiment and incubated at $37^oC/5\%CO_2$ overnight to let the cells adhere to the slide/dish. Cells were fixed with 4% PFA for 5 minutes at room temperature and rinsed twice with PBS. A positive control slide was created by digesting the DNA with DNAseI. To achieve this, the slide was incubated in a DNAseI solution (50mM Tris-HCl pH7.5, 1mg/ml BSA, DNAseI 15U/ml; Sigma, Oakville, ON) at room temperature for 10min and rinsed twice with PBS. The cells were permeabilised in 0.1% Triton-X/0.1% sodium citrate for 2 minutes on ice. The TUNEL labeling (terminal uridine deoxynucleotidyl transferase dUTP nick end labeling) was performed using the *In Situ* Cell Death Detection Kit (Roche Applied Science, Laval, QC) according to the manufacturer's instructions included with the kit (Negoescu, Guillermet et al. 1998). After TUNEL labeling the cells were DAPI stained for 2min in 1μg/ml DAPI solution and washed in PBS for 10 minutes before being mounted with a drop of fluorescent mounting medium (DakoCytomation, Carpinteria, CA).

2.2.8 Immunoblotting

2.2.8.1 RIPA protein extraction

Cell pellets were re-suspended in 75-150 μl of RIPA buffer (50 mM Tris pH 7.4, 150 mM NaCl, 0.2% SDS, 1% NP-40, protease inhibitor CompleteMini EDTA-free; Boehringher Mannheim, Laval, QC) according to the pellet size. The lysate was incubated on ice for 30 min then the DNA was digested by adding 10 μl of DNAseI 10U/μl (Sigma, Oakville, ON)

and incubated for 5 min at 37°C. The DNAse I treatment should significantly reduce the viscosity of the sample and the digestion was repeated, if necessary. Following DNAse I treatment the mixture was centrifuged for 15 min at 13,000 rpm at 4°C and the supernatant was recovered. The protein concentration of the sample was quantified by a Bradford assay (Bradford 1976) using the Bio-Rad Protein Assay reagent (Bio-Rad, Mississauga, ON) following the manufacturer's protocol.

2.2.8.2 Protein gel and Western transfer

For each protein sample 30 μg of protein was loaded onto a NuPAGE® Novex® 3-8% Tris-Acetate gel (Invitrogen, Burlington, ON). The gel was electrophoresed at 150 volts for 1 hour and 15 min using the XCell *SureLock*™ Mini-Cell with 1X NuPAGE® Tris-Acetate SDS Running Buffer (Invitrogen, Burlington, ON). The proteins on the gel were transferred onto a PVDF Immobilon–P Transfer Membrane (Millipore, Billerica, MA) using a TRANS-BLOT® SD SEMI-DRY TRANSFER CELL (Bio-Rad, Mississauga, ON) in 1X transfer buffer (50mM Tris base, 40mM Glycine, 10% SDS, 20% MeOH). Proteins were transferred to the membrane for 3 hours at 50 mAmp.

2.2.8.3 Western blotting

After transfer, the Western membrane was soaked in blocking buffer (5% milk/TBST) overnight or for a minimum of 1 hour (Ausubel 2001). The membrane was incubated with the primary antibody diluted in 5% milk/TBST in a plastic bag on a shaking platform for 1 hour (or as indicated) then washed 3 times in TBST for 10 minutes. The membrane was

incubated with a secondary antibody diluted in 5% milk/TBST conjugated to HRP (horseradish peroxidase) for 1 hour, washed 3 times in TBST for 10 minutes and rinsed twice in PBS. The ECL Plus Western Blotting Detection System (GE Healthcare, Buckinghamshire UK) was used for detection following the manufacturer's protocol. The membrane was exposed to CL-XPosure film (Thermo scientific, Rockford, IL) in an exposition cassette and developed in the Kodak M35A X-OMAT film processor.

2.2.8.4 Antibodies used for immunoblotting

Primary Antibodies:

- Anti-ATRX 39F mouse monoclonal raised against a GST fusion protein of ATRX amino acids 85-319, dilution 1:5 (gift from Dr Douglas Higgs, Institute of Medecine Oxford, UK (McDowell, Gibbons et al. 1999))
- Anti-ATRX H-300 rabbit polyclonal, dilution 1:500 (Santa Cruz Biotechnology, Santa Cruz, CA)
- Anti-DAXX M-112 rabbit polyclonal, dilution 1:500 (incubated overnight) (Santa Cruz Biotechnology, Santa Cruz, CA)
- Anti-PAR (Poly ADP-ribose) mouse monoclonal, dilution 1:1000 (incubated overnight) (Trevigen, Gaithersburg, MD)
- Anti-β-Actin mouse monoclonal, dilution 1:15000 (Sigma, Oakville, ON)
- Anti-Human Retinoblastoma mouse monoclonal, dilution 1:250 (overnight incubation) (BD Pharmingen, Mississauga, ON)
- Anti-Cyclin A (H-432) rabbit polyclonal, dilution 1:1000 (Santa Cruz Biotechnology, Santa Cruz, CA)

- Anti-E2F-1 (C-20) rabbit polyclonal, dilution 1:1000 (Santa Cruz Biotechnology, Santa Cruz, CA)
- Anti-SNF2H sheep polyclonal antibody raised against a fusion protein of the NH_2-terminus of human SNF2H, dilution 1:2000 (incubated for 3 hours) (Affinity Biologicals Inc., Ancaster, ON)
- Anti-Laminin A/C (346) mouse monoclonal, dilution 1:500 (incubated overnight) (Santa Cruz Biotechnology, Santa Cruz, CA)

Secondary Antibodies:

- Sheep α mouse HRP conjugated, dilution 1:2500 (Sigma, Oakville, ON)
- Goat α rabbit HRP conjugated, dilution 1:2500 (Sigma, Oakville, ON)
- Goat α sheep HRP conjugated, dilution 1:2500 (Sigma, Oakville, ON)

2.2.9 Immunofluorescence

2.2.9.1 ATRX, Daxx, HP1α and PH3 staining cell staining

Cells were plated on cover slips in a 6 well plate or in 4 well chamber slides and fixed with an ethanol: methanol (3:1) solution (-20°C) for 5 minutes at 4°C then washed 4 times in PBS. The cells were permeabilised for 5min at room temperature with 0.2% Triton-X in PBS and washed for 5 minutes in PBS before blocking with 2% BSA/PBS for 1hour. The fixed cells were incubated with the primary antibody diluted in 2% BSA/PBS for one hour then washed with PBS, 3 times for 10 minutes each (Ausubel 2001). After incubation with the secondary antibody for one hour, the cells were washed with PBS, 3 times for 10 minutes each wash. The cells were counterstained with DAPI (1 μg/ml solution) for 2 min

and washed in PBS for 10 minutes. The cover slips were mounted on a glass slide with a drop of fluorescent mounting medium (DakoCytomation, Carpinteria, CA) and sealed with nail polish. In some instances, cells were synchronized at the G1/S phase with 200 mM HU (hydroxyurea) for 16 hrs before performing the staining procedure. Slides were viewed using a Zeiss AXIO Images.M1 fluorescent microscope (Carl Zeiss Canada Ltd., Toronto ON).

For immunofluorescence, the primary antibodies described above (Section 2.2.8.4) were used at different dilutions as outlined here: anti-ATRX H-300 rabbit polyclonal, dilution 1:100; anti-ATRX 23C mouse monoclonal, dilution 1:20; anti-Daxx M-112 rabbit polyclonal, dilution 1:50. In addition, we used an anti-HP1α mouse monoclonal, 1:100 (Upstate, Lake Placid, NY) and Anti-phospho-Histone H3 (Ser10) rabbit polyclonal antibody (1:100; Upstate, Lake Placid, NY) as a primary and the following secondary antibodies: Alexa Fluor 594 goat anti-rabbit IgG, 1:1500 (Molecular Probes, Eugene, OR); Alexa Fluor 488 goat anti-rabbit IgG, 1:1500 (Molecular Probes, Eugene, OR).

2.2.9.2 BrdU staining

Cells cultured on glass cover slips were pulse-labeled with the addition of BrdU (5-bromo-2-deoxyuridine) (50μM) to the media for 1hour. After incubation, cells are washed with PBS and fixed in 4% PFA (paraformaldehyde) for 5 minutes at RT (room temperature). The antigen retrieval and BrdU staining procedure was performed according to the methodology described in (Berube, Mangelsdorf et al. 2005).

2.2.9.3 BrdU /PH3 double labeling

Cells were pulsed for 1 hour as described in section 2.2.9.2. Cells were subsequently fixed, prepared and stained for phosopho-histone H3 like previously described (section 2.2.9.1). After the phospho-histone H3 staining the cells are re-fixed in 4% PFA for 5 minutes before performing the BrdU and DAPI staining as described (Berube, Mangelsdorf et al. 2005).

2.2.10 Cell growth competition assay

HeLa psiRNA LacZ and psiRNA ATRX3 C5 were mixed in equal proportions with HeLa Tet-ON cells and $0.5X10^6$ cells of each mixed population were seeded in 10 cm plastic culture dishes. Cells were incubated at $37^{\circ}C/5\%CO_2$ and split 1:3 and/or harvested on day 0, 2, 4, 6, 8 and 10. At each time point cells were harvested and washed in 2% BSA/PBS then frozen until DNA extraction.

DNA from all the samples was extracted in parallel using lysis buffer (50 mM Tris pH 8.0, 100mM EDTA, 1% SDS, 100 mM NaCl). The cell pellets were re-suspended in 500 µl of lysis buffer plus 50 µl of proteinase K (20 mg/ml) and 25 µl of RNAse A (1 µg/µl) then incubated at $56^{\circ}C$ for 2-3 hours. After the incubation, 500 µl of phenol was added to the samples, mixed and then centrifuged at 13,000 rpm for 5 min. The aqueous top layer containing the DNA was removed and transferred to a new tube, then similarly extracted with 500 µl of chloroform. The aqueous layer was removed to a new tube and the DNA was precipitated by the addition of 600 µl of 100% EtOH and centrifugation at 13,000 rpm for 15 min. The pellets were washed with 70% EtOH and the DNA re-suspended in 100 µl of

sterile water. The DNA concentration was quantified using the BioPhotometer (Eppendorf, Mississauga, ON).

The presence of each cell line at each time point was determined using PCR amplification of the specific plasmid carried by the cell line. The psiRNA hH1-neo plasmid was amplified using the primers OL381 and psiRNA-hH1neo fwd (all primer sequences can be found in Appendix B). The integrated pTet-ON plasmid present in the HeLa Tet-ON cell was amplified using the primers pTet-on rtTA fwd #2 and pTet-on rtTA rev. β-actin was used as a control for amplification. The PCR mix contained 2 µl of DNA, 5 µl of 10X PCR buffer, 1 µl of 10 mM dNTPs, 1.5 µl of 50 mM $MgCl_2$, 0.5 µl of each primer, 0.5 µl of Taq polymerase and 39 µl of water. The PCR mix was incubated at 96°C for 30 sec, 60°C for 30 sec, and 72°C for 30 sec, for 30 cycles to amplify the plasmids or for 25 cycles to amplify β-actin. Following amplification, 10 µl of the PCR reaction was run on a 1% agarose gel as described in section 2.2.2. The psiRNA-hH1 neo and pTet-ON give rise to a 512 and a 333 bp band, respectively.

2.2.11 Growth assay

To determine the growth of cells in culture we utilized both a WST-1 assay and a serum starvation growth assay which are described seaparately below.

WST-1 growth assay: *Atrx* $^{flox/Y}$ MEFs were seeded in 96 well plates with 3000 cells per well and allowed to adhere to the plate overnight. The next morning the MEFs were infected with 30 µl (MOI 250) of adenovirus as previously described (section 2.2.6.1). After

the infection the cells were incubated at 37°C/5%CO_2 until the set time points (day 0 at infection until day 4 post-infection). Cell proliferation was measured by WST-1 assay (Cook and Mitchell 1989) using the manufacturer's instructions (Roche, Missisauga, ON). Briefly, point 10 µl of WST-1 reagent was added to each well and the plate incubated for 1hr at 37°C/5%CO_2. The plates were read at 450 nm and 690nm on a SpectraMAX 190 spectrophotometer (Molecular Devices, Sunnyvale CA).

Serum starvation growth assay: HeLa cells, psiRNA LacZ and psiRNA ATRX3 C5 cell lines were seeded in 6 well plates in triplicate (15,000 cells per well). The cells were incubated for 6 hours at 37°C/5%CO_2 to adhere to the wells. The cells were synchronized in serum deprived media (DMEM, 0.2% FBS, 1% penicillin/streptomycin) for 72h. The cells were released from the block by replacing the serum deprived media with complete media and the growth was monitored by counting cells at day 0 through day 4. The cells were harvested and then re-suspended in 850 µl of complete media. The cells in suspension were counted using the Vi-Cell XR cell counter (Beckman Coulter, Mississauga, ON). Similar growth assays were performed on unsynchronized cells using the same method.

2.2.12 Flowcytometry

2.2.12.1 BrdU/PI cell staining

The cells to be analyzed were BrdU pulsed with 30 µM BrdU media (section 2.2.9.2). The pulsed cells were rinsed in PBS, trypsinized and counted (Stubbert, Hamill et al. 2007). For each sample $1X10^6$ cells were precipitated (7min at 1,200 rpm), rinsed twice in PBS, and

fixed with 1 ml of 70% ethanol at -20°C overnight. The fixed cells were washed twice in PBS again and incubated in 1 ml of PBS + RNAse A (0.5mg/ml) at 37°C for 30 min. Following the incubation, the cells were washed with 1 ml of PBS and precipitated at 1,200 rpm for 7 min. The cells were then resuspended in 1 ml of 0.1N HCL + 0.7% Triton-X and incubated on ice for 15 min, followed by a wash with 1 ml of PBS. The cells were resuspended in 1 ml of sterile water and the samples incubated for 15 min at 97°C. After the incubation, cells were put on ice again for 15 min, washed with 1ml of PBS/0.5% Tween 20 and precipitated (7 min at 1,200 rpm). Next, the cells were incubated with 100 µl of HBT (PBS, 0.05% FBS, 0.005% Tween 20) containing 1:100 dilution the primary antibody anti-BrdU (BD Biosciences, Mississauga, ON) for 30 min at RT, then washed with 1ml of HBT and precipitated for 7 min at 1500 rpm. Then cells were incubated with 150 µl of the FITC conjugated secondary antibody anti-mouse diluted 1:20 in HBT for 30 min in the dark and precipitated for 7 min at 1,500 rpm. Finally, each cell sample was resuspended in 400-800 µl of PI (propidium idodine) solution with RNAse A (50 µg/ml PI, 40µg/ml RNase A) and incubated for at least 30 min before flowcytometry analysis on Beckman Coulter FACS station. Cell cycle distribution of the cell population was analyzed with the FCS Express 2 software (DeNovo Software, Thornhill, ON).

2.2.12.2 Time couse BrdU/PI

HeLa cells, psiRNA LacZ and psiRNA ATRX3 C5 clones were seeded in 10 cm dishes in triplicate for each time point (0, 6, 12, 16, 20, 24 and 28hrs). Cells were BrdU pulse labeled as described above and chased for the indicated times with fresh complete media. At the designated time points, the cells were prepared for BrdU and PI staining and

analyzed as described above. The cell cycle profile of each time point was analyzed with the ModFit software (Verity Software House, Topsham, ME) Note that the BrdU+ cell number at time 0 hr was designated 100% in S phase for the purpose of analysis.

2.2.12.3 CyclinE/PI staining

Cells were trypsinized, fixed and washed in PBS as described above (section 2.2.12.1). The fixed cells were resuspended in 0.25% Triton X-100 in PBS and incubated on ice for 15 min then, 1 ml of PBS was added and the cells were precipitated for 7 min at 1,200 rpm. The cells were then washed with 0.5% Tween in PBS and spin down for 7 min at 1,200 rpm. After, the cells were resuspended in 1% BSA in PBS with 0.75 μg of anti-Cyclin E primary antibody (Santa Cruz Biotechnology, Santa Cruz, CA) and incubated at room temperature for 2-3 hours. The antibody was washed with 1 ml of 1% BSA. The cells were then resuspended with 100 μl of 1% BSA in PBS containing a 1:30 dilution of the secondary antibody, Alexa 488 goat anti-rabbit IgG (Molecular Probes, Eugene, OR) and incubated for 30 min at RT. Then the cells were washed with 1 ml of 1% BSA in PBS. Finally, the cells were resuspended in PI and analysed as described in section 2.2.12.1. The cell staining was kindly performed by Jeff Hamill from Dr. Bruce McKay's laboratory.

3 Results

3.1 Transient knockout of ATRX in HeLa cells by siRNA

In our study we used multiple methods to reduce the level of ATRX in cells, one of them being transient transfection of siRNA oligonucleotides. SiRNA oligonucleotides were designed and transfected into HeLa cells to target *ATRX* mRNA for degradation. The level of ATRX protein was shown to be greatly reduced 48h post-transfection (figure 9 A, B). We observed a similar reduction in ATRX protein with both siRNA oligonucleotides, siATRX3 designed in our laboratory and the siATRX pool (a smartpool of 4 siRNA oligonucleotides with proprietary rights from Dharmacon). The protein reduction induced by the siRNA treatment was observed as early as 24 hr by immunoblot (data not shown). In addition, both the full length and truncated ATRX isoforms are reduced by the siRNA treatment (figure 9). The siATRX3 oligonucleotide targets exon 1 therefore we expected to see downregulation of both isoforms. The siATRX pool must also contain one or more oligonucleotides that target the first 11 exons since both isoforms are downregulated.

Previous work from our group has shown that in Atrx KO mouse forebrain there was reduced DAXX and increased PARP-1 protein levels (unpublished data Mangelsdorf and Picketts). In our ATRX siRNA transiently transfected HeLa cells, the level of Daxx and PARP are slightly reduced but controls are similarly affected (figure 9 A and B) suggesting that they did not change in this system. Since the Daxx and PARP protein levels are slightly down in the mock and siControl transfections, the translation of these proteins may

Figure 9. ATRX expression is downregulated in HeLa cells transiently transfected with ATRX siRNA

HeLa cells were transiently transfected with siRNA solutions (100 nM) and incubated for 48 hours prior to analysis. (A) Immunohistochemistry staining for ATRX (red) and Daxx (green) was performed on fixed cells with a DAPI counterstain. We observed strong staining for ATRX in the control samples (Normal, Mock transfected, and siControl) but reduced labelling in the siRNA treated panels. Daxx staining is slightly reduced in the siRNA treatment and in the controls. (B) A western blot analysis of siRNA and control treated samples (30ug of a RIPA protein extract) were probed with antibodies for ATRX, Laminin A/C, Daxx, PARP and β-actin. We observed that ATRX and ATRXt protein expression is almost completely eliminated compared to the transfection controls. However, Daxx and PARP protein levels are similarly downregulated in the siRNA treated cells and controls. Laminin A/C and β-actin were used as loading controls.

A

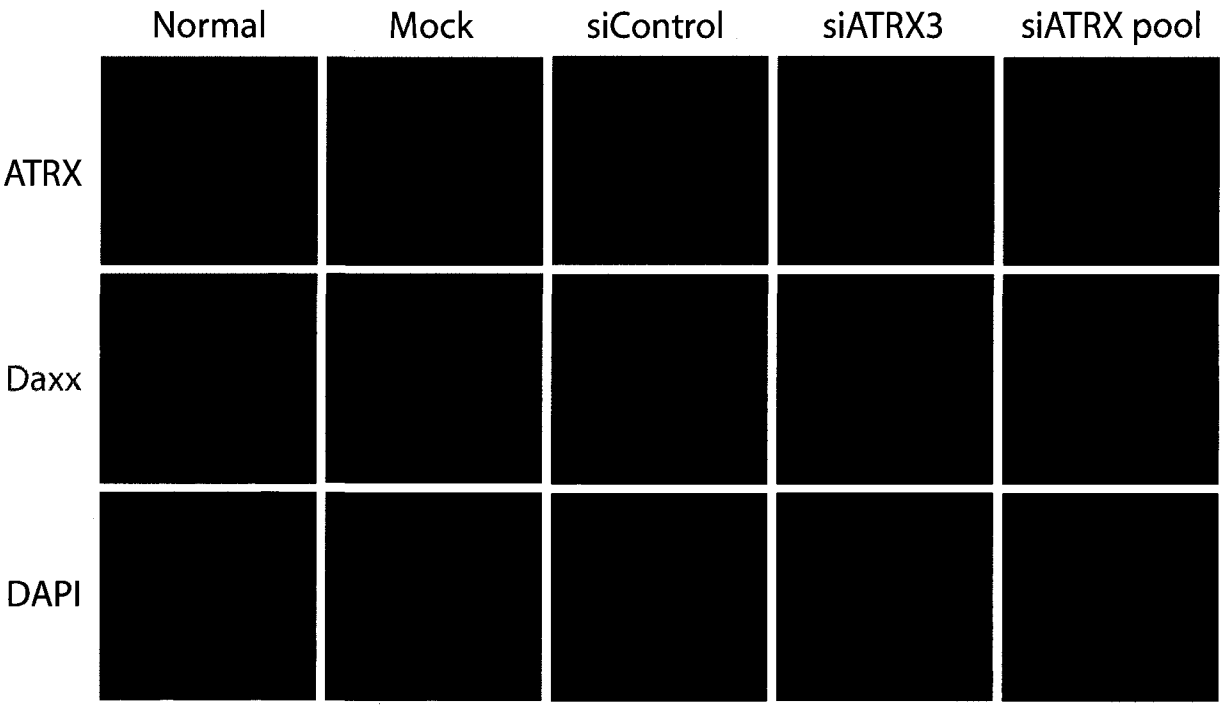
Normal
Mock
siControl
siATRX3
siATRX pool
ATRX
Daxx
DAPI

B

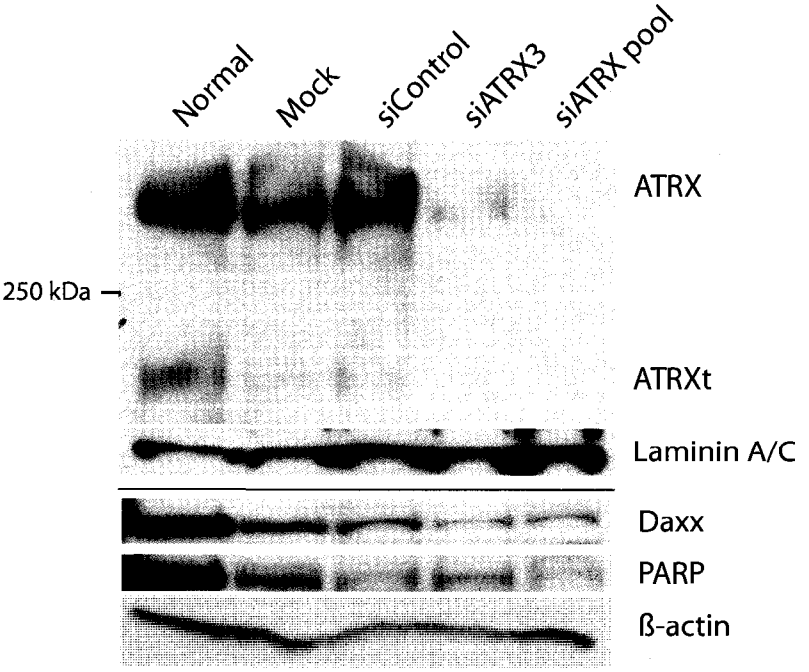
Normal
Mock
siControl
siATRX3
siATRX pool
ATRX
250 kDa
ATRXt
Laminin A/C
Daxx
PARP
ß-actin

possibly be attenuated by the transfection process (Novina and Sharp 2004). On the other hand, since ATRX protein levels in the control samples were not affected, the ATRX reduction obtained from the siRNA was specific and suggests that the same siRNA sequences can be used to generate shRNA expressing stable clones (see Section 3.3).

3.2 The death rate increases in the absence of ATRX in siRNA transfected cells

Death is a natural consequence in cells undergoing stressful treatments such as a transfection. Cell death was noticed in HeLa cell cultures 24 hrs after ATRX siRNA transfection. After cell death quantification by TUNEL staining, the cell loss in the ATRX siRNA transfected cell was significantly increased compared to the siControl transfection and the non-transfected cells (figure 10 B; n=3, siATRX3 $p<0.01$, siATRX pool $p<0.03$). The apoptosis level was measured 24 hrs post-transfection. Although ATRX is downregulated by 24hrs, at such an early time point after transfection a lot of cell death appears in the controls. Therefore, the transfection contributes to the elevated death in the ATRX siRNA treatment. Nonetheless, these results suggest that ATRX downregulation impairs cell survival. Cell replication was also measured to determine if ATRX downregulation had any effect on the S phase population. The ability of the cells to incorporate BrdU seemed to be comparable between control and siRNA treated cells (figure 10 A). Again, the chosen time of 24 hrs post-transfection was not optimal since an effect on cell cycle may not be immediate after the protein downregulation by siRNA treatment. A later time point such as 72 or 96 hrs post-infection might have revealed a BrdU incorporation

Figure 10. The apoptotic and replication status in the transiently transfected HeLa cells

HeLa cells were transiently transfected with 100 nM siRNA solutions and incubated for 24 hours. (A) The percentage of replicating cells was determined as the number of BrdU positive cells over the total cell population (DAPI positive). Three sections were counted from 3 slides for the calculation (n=3). We observed no significant difference in the number of BrdU positive cells in the siRNA treated cells compared to the controls. The error bars represent the SEM. (B) The percentage of cell death was calculated as the number of TUNEL positive cells over the total number of cells (DAPI positive). Three sections from three slide were counted for the calculations (n=3). We observed a significant increase in TUNEL positive cells (designated by *) in the siATRX3 and siATRX pool treated cells when compared to the untreated cells, the mock and the siControl treatments. The student T-test p-values for these comparisons were found to be $p<0.01$ (siATRX3) and $p<0.03$ (siATRX pool). The error bars represent the SEM.

A

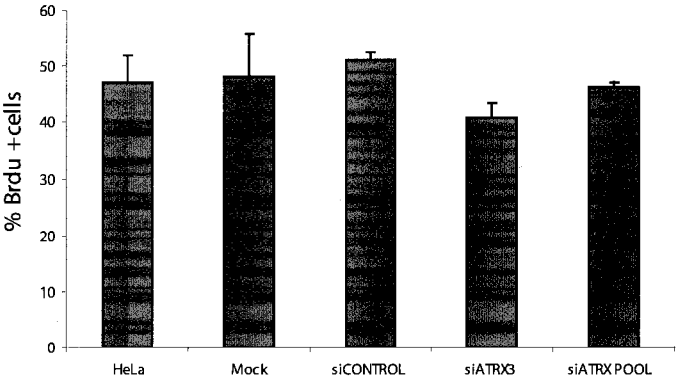
% Brdu +cells
60
50
40
30
20
10
0
HeLa
Mock
siCONTROL
siATRX3
siATRX POOL

B

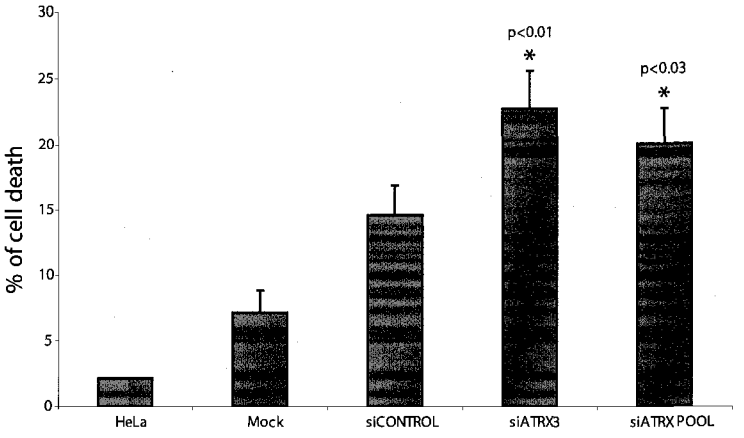
% of cell death
30
25
20
15
10
5
0
p<0.01
*
p<0.03
*
HeLa
Mock
siCONTROL
siATRX3
siATRX POOL

change because other study showed that slower cell growth has been observed in $Atrx^{null}$ ES cells (Garrick, Sharpe et al. 2006).

3.3 Generation of stable cell lines expressing ATRX shRNA

The generation of stable clones expressing ATRX shRNA can permit the study of long term effects of ATRX down regulation on cells. The ATRX shRNA oligonucleotides were cloned in the expression vector psiRNA-hH1 neo G1. The shRNA containing vector was then transfected into HeLa cells and the cells selected with antibiotic (G418) to create the stable cell lines. The three shRNA oligos designed for this study all targeted exon 1 and therefore, should result in the reduced expression of both ATRX isoforms.

The proper ligation of the shRNA oligo in the psiRNA-hH1 neo vector was verified by *AseI* enzymatic digestion. During the cloning procedure the vector was initially digested with *BbsI* to remove a plasmid fragment where the shRNA oligo was inserted during ligation. Positive clones were identified by *AseI* enzymatic digestion. Clones containing the insert will generate a 2686 bp fragment while the negative clones produce 2 fragments of 2227 and 752 bp. Cloning the ATRX oligonucleotides into psiRNA-hH1 neo vector was successful for only one of the three shRNA sequences (Figure 11 A, B). Numerous attempts at cloning the ATRX1 and ATRX2 shRNA oligo in psiRNA-hH1 neo were unsuccessful and eventually abandoned (figure 11 A). Over 250 transformed colonies were screened from multiple ligation reactions, very few were positive and all contained sequence errors. In contrast, the ATRX3 shRNA successfully ligated and transformed without any sequence errors on the first attempt. The integrity of the shRNA construct is important for proper

Figure 11. Cloning the ATRX shRNA in the psiRNA-hH1 neo vector

The ligation of the shRNA oligonucleotide in the psiRNA-hH1 neo vector was verified by *AseI* restriction enzymatic digestion. The digestion products were separated by electrophoresis on a 1% agarose gel and viewed under UV light. The clones containing the insert generated a 2686 bp fragment while the negative clones produced 2 fragments of 2227 and 752 bp. Uncut and *AseI* digested psiRNA-hH1 neo vector was included was a comparative controls. (A) Multiple colonies from insert ATRX1, ATRX2 and ATRX3 were screened; only the ATRX3 colonies contain the shRNA insert. (B) Re-verification of the ATRX3 insert in the bacterial culture used for large scale plasmid preparation.

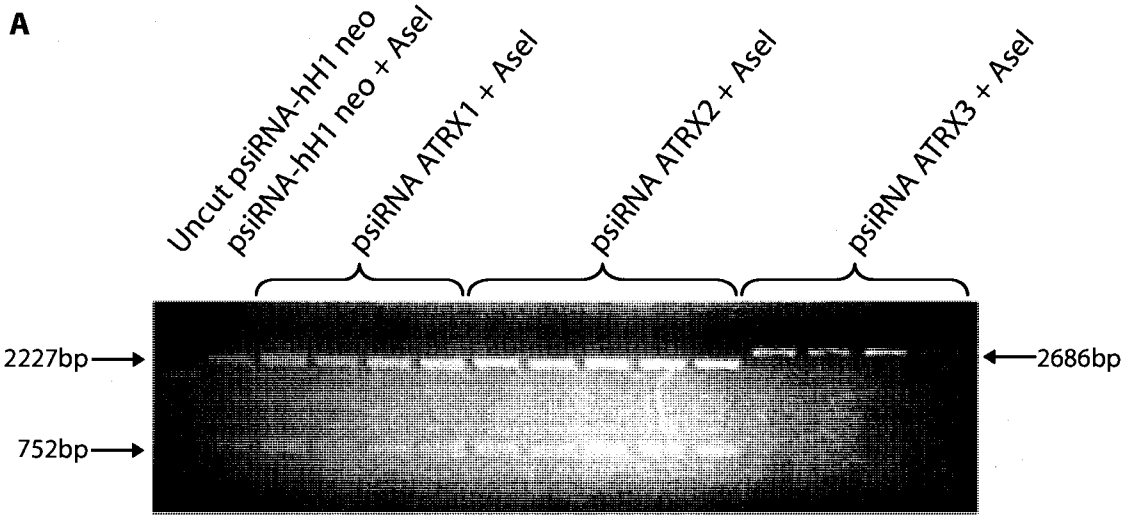
A
Uncut psiRNA-hH1 neo
psiRNA-hH1 neo + AseI
psiRNA ATRX1 + AseI
psiRNA ATRX2 + AseI
psiRNA ATRX3 + AseI
2227bp
752bp
2686bp

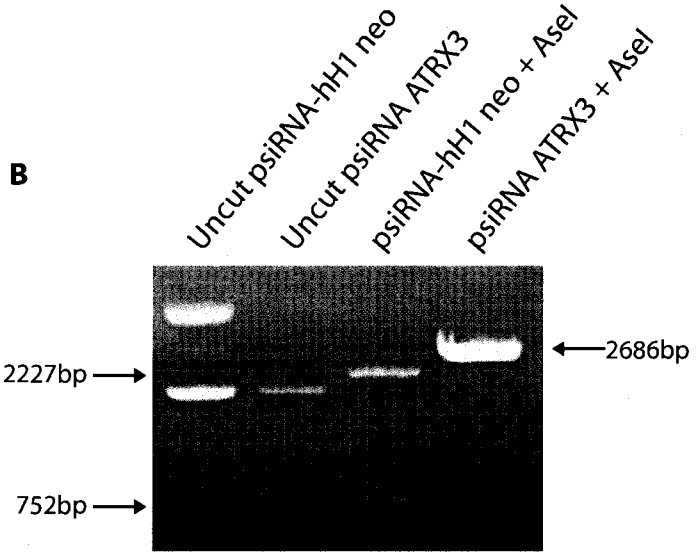
B
Uncut psiRNA-hH1 neo
Uncut psiRNA ATRX3
psiRNA-hH1 neo + AseI
psiRNA ATRX3 + AseI
2227bp
752bp
2686bp

silencing, as a 1-2 basepair mismatch was shown in multiple studies to be non-functional (Rutz and Scheffold 2004). As such, the ATRX3 shRNA containing construct was the only one used for clone generation.

A total of 20 psiRNA ATRX3 colonies were picked to generate clones. Of these, 11 cell lines were able to grow proficiently in culture. Most of the generated clones (8 clones) showed variable degrees of ATRX protein down regulation during the selection process. Surprisingly, as the clone was expanded over time the level of ATRX started to fluctuate. For instance, clones B1, B5 and B6 initially showed a significant reduction in ATRX protein levels but subsequently regained their ATRX expression with time, even if maintained in selection media (figure 12). The resumption of ATRX expression by multiple clones suggests that the promoter driving the shRNA expression was silenced and no shRNA was produced. The single clone with consistent ATRX down regulation over time was the clone C5 (figure 12). Consequently, the psiRNA ATRX3 C5 clone was used for further study. It is important to note that we observed that some aliquots of clone C5 also recovered ATRX expression after a long time in culture (data not shown) therefore, early passage clones were consistently used.

ATRX has a punctuate nuclear staining pattern that co-localizes with both PML nuclear bodies and pericentromeric heterochromatin (McDowell, Gibbons et al. 1999; Berube, Smeenk et al. 2000; Ishov, Vladimirova et al. 2004). As expected, we did not observe the typical ATRX staining patterns in cells analyzed from the psiRNA ATRX3 C5 clone thereby confirming that ATRX was downregulated (figure 13 A). Similarly, immunoblot analysis showed reduced levels of both the full length and truncated isoform of

Figure 12. The downregulated expression of ATRX protein reverted in multiple psiRNA ATRX3 clones

Western blot analysis of the psiRNA ATRX3 clones B1, B5, B6 and C5 (30 μg of RIPA cell extract) during clone culture expanssion. The blots were probed with the ATRX antibody. The western blots were from protein extracts from March (#1), July (#2) and August (#3) 2005, respectively. We observed that ATRX expression in the clone B1, B5 and B6 fluctuates with time. The clone C5 is the only one with a consistient ATRX downregulation in all the western blots when compared to the Hela wt control. The loading controls (SNF2H and β-actin) showed equal amount of protein on each western blot with the exeption of sample B5 in western #1.

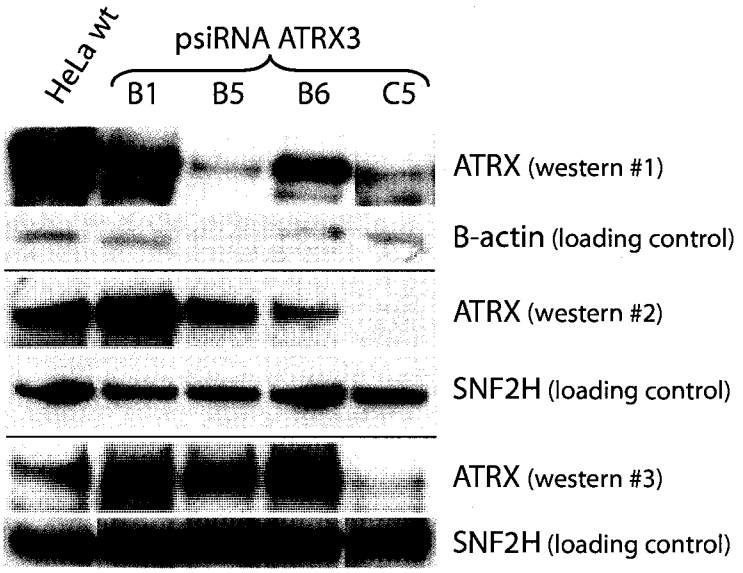
HeLa wt
psiRNA ATRX3
B1
B5
B6
C5
ATRX (western #1)
B-actin (loading control)
ATRX (western #2)
SNF2H (loading control)
ATRX (western #3)
SNF2H (loading control)

Figure 13. ATRX expression is downregulated in psiRNA ATRX3 C5 clone

(A) Normal HeLa cells, psiRNA LacZ and psiRNA ATRX3 C5 clone were fixed and stained by immunohistochemistry for ATRX (red), Daxx (green) and DAPI counterstained (blue). We did observe the typical ATRX speckled staining pattern in the HeLa cells and the psiRNA LacZ clone. The ATRX speckled stining pattern is absent in the psiRNA ATRX3 C5 clone. In addition, Daxx staining is reduced in the psiRNA ATRX3 C5 clone compared to the controls. (B) A western blot from 30ug of a RIPA protein extract was probed for ATRX, Daxx, PARP-1 and β-actin. We observed that ATRX and ATRXt protein expression is almost completely eliminated in the psiRNA ATRX3 C5 clone. Daxx and PARP-1 protein levels in the psiRNA ATRX3 C5 clone and controls are equivalent. The β-actin loading control is even for all the samples.

A

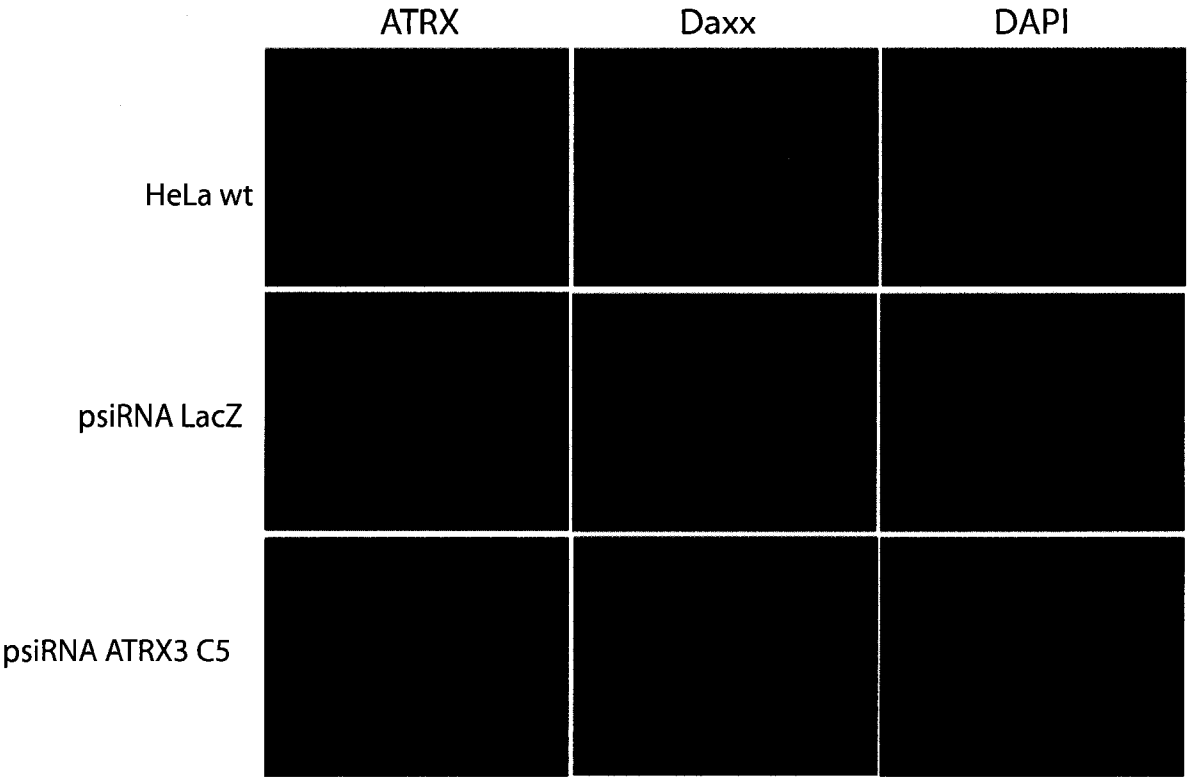
ATRX
Daxx
DAPI
HeLa wt
psiRNA LacZ
psiRNA ATRX3 C5

B

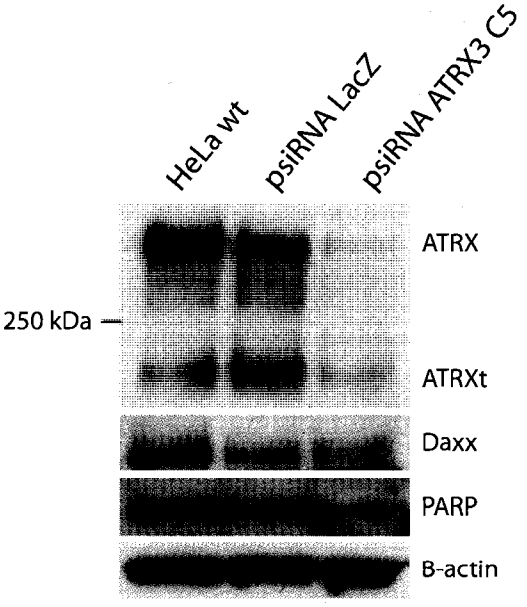
HeLa wt
psiRNA LacZ
psiRNA ATRX3 C5
250 kDa
ATRX
ATRXt
Daxx
PARP
B-actin

ATRX (figure 13 B). Moreover, the Daxx protein level appeared down regulated by IHC which supports previous unpublished observations from our group describing a Daxx reduction in the Atrx forebrain KO mouse (unpublished data). However, Daxx protein levels analyzed by Western blot analysis did notshow a significant change compared to the psiRNA LacZ control (figure 13 B). While PARP-1 protein levels showed increased expression in the Atrx forebrain KO mouse we did not make similar observations with the clone C5.

3.4 Clones lacking ATRX have a slower growth rate

Throughout our analysis of the psiRNA ATRX3 C5 cell line, it was noticed that these cells took longer to become confluent and required less passaging than the control cultures. To further analyse this observation, the growth rate of the C5 clone was quantified. To perform this experiment we first synchronized the cells by serum starvation to block cells in the G1 phase. Subsequently, the cell lines were re-stimulated to grow with the addition of serum. By day 4 and 5 a significant decrease in cell number was observed in the psiRNA ATRX3 C5 clones (figure 14 B; $n=3$, $p<0.05$). These results confirm and quantify the slower growth previously detected by us and other groups (Berube, Mangelsdorf et al. 2005; Garrick, Sharpe et al. 2006). In the experiment performed by Garrick and Sharpe, $Atrx^{null}$ ES cells were rapidly outgrown by the $Atrx^{WT}$ ES cells when equally mixed and cultured together. From these observations, it was suggested that the absence of Atrx has a negative impact on the normal growth of ES cells (Garrick, Sharpe et al. 2006). To confirm our results we performed a similar study to the ES cell experiment. HeLa wild type cell lines stably transfected with the pTet-On vector were mixed equally with the psiRNA LacZ

Figure 14. The psiRNA ATRX3 C5 clone has a slower growth rate

(A) Equivalent numbers of HeLa psiRNA LacZ or psiRNA ATRX3 C5 cells were mixed with HeLa Tet-ON cells and cultured together. After the 0, 2, 4, 6, 8 and 10 days of co-culture, DNA was extracted and the psiRNA-hH1 neo and pTet-ON plasmid were PCR amplified. The PCR products were separated on a 1% agarose gel by electrophoresis. The top three panels represent PCR amplification of the HeLa Tet-ON and psiRNA ATRX3 C5 mix whereas the bottom three panels represent PCR amplification from DNA isolated from the HeLa Tet-ON and HeLa psiRNA LacZ mix. Notice that the psiRNA-hH1 neo plasmid is detected throughout the time course for the HeLa Tet-ON and HeLa psiRNA LacZ mix (bottom panel) but is undetecteable by Day 8 in the HeLa Tet-ON and psiRNA ATRX3 C5 mix (top panel). (B) G1 synchronized cells were released at day 0 and the number of cells in culture was counted from day 0 to day 5. Each time point represents 3 replicates (n=3) and the error bars are the SEM (standard error of the mean). We observed a significant decrease in the growth rate at day 4 and 5 in the psiRNA ATRX3 C5 clone (green) compared to the HeLa wt (blue) and the psiRNA LacZ (red). Statistical difference (indicated by *) between the psiRNA ATRX3 and the 2 controls was calculated using the Student's T-test, $p<0.05$.

A

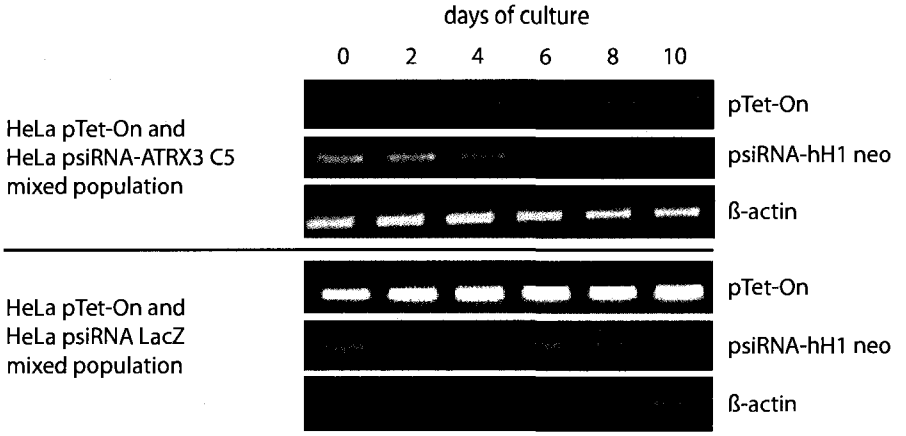
days of culture
0
2
4
6
8
10
HeLa pTet-On and
HeLa psiRNA-ATRX3 C5
mixed population
pTet-On
psiRNA-hH1 neo
ß-actin
HeLa pTet-On and
HeLa psiRNA LacZ
mixed population
pTet-On
psiRNA-hH1 neo
ß-actin

B

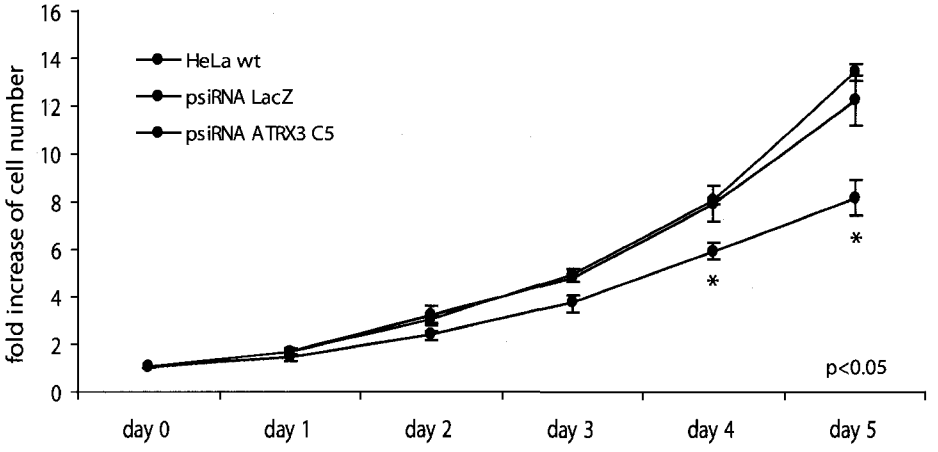
fold increase of cell number
16
14
12
10
8
6
4
2
0
HeLa wt
psiRNA LacZ
psiRNA ATRX3 C5
*
*
p<0.05
day 0
day 1
day 2
day 3
day 4
day 5

containing cells and the psiRNA ATRX3 C5 cell line and allowed to proliferate. Samples were taken at each day of co-culture and the presence of each plasmid in the culture was followed by PCR amplification. After 4 days of co-culturing the psiRNA ATRX3 C5 clone with the HeLa pTet-On cells we observed a decrease in the abundance of the psiRNA-hH1 neo plasmid which was undetectable by day 8 (figure 14 A). Similarly to the $Atrx^{null}$ ES cells, the psiRNA ATRX3 C5 clone population was overgrown by the wild type cells in co-culture. As a control we mixed, HeLa psiRNA LacZ and HeLa pTet-On cells observing that both cell types were maintained under co-culture conditions for the course of the study (figure 14 A). These results further suggest that the normal cell cycle progression or cellular proliferation is impaired when the ATRX protein level is downregulated.

The growth disadvantage characterised in the psiRNA ATRX3 C5 clones can be caused by many factors, one of them being increased apoptosis. The level of apoptosis in C5 cells was quantified by terminal uridine deoxynucleotidyl transferase dUTP nick end labeling (TUNEL) (figure 15 A). About 5.5% of the psiRNA ATRX3 C5 cell population was TUNEL positive, which corresponds to a 2.9 fold increase in cell death in the clone compared to the controls (figure 15 B; $n=3$, $p<0.0005$). Taken together, our results suggest that the increased apoptosis contributes to the slow growth phenotype of the ATRX knockdown clone although it may not be the only factor involved.

3.5 Abnormal G1 and S phase profiles in the C5 clone

Observations from multiple studies have provided evidence that ATRX may play a role in cell cycle progression. One study showed that ATRX associates with the nuclear

Figure 15. The psiRNA ATRX3 C5 clone has an increased level of cell death

(A) HeLa cells, psiRNA LacZ and psiRNA ATRX3 C5 clones were fixed and analysed by TUNEL assay and DAPI counterstained (blue) before microscope visualisation. The staining show an increase number of TUNEL positive cells (red) in the psiRNA ATRX3 C5 clone. (B) The percentage of cell death was calculated as the number of TUNEL positive cells over the total number of cells (DAPI positive). Three sections from three slide were counted for the calculations (n=3). The error bars represent the SEM. We observed a significant increase in TUNEL positive cells (designated by *) in the psiRNA ATRX3 C5 clone when compared to the HeLa cells and the psiRNA LacZ clone. The p-values (from Student's T-test) for this comparison was found to be $p<0.0005$.

A

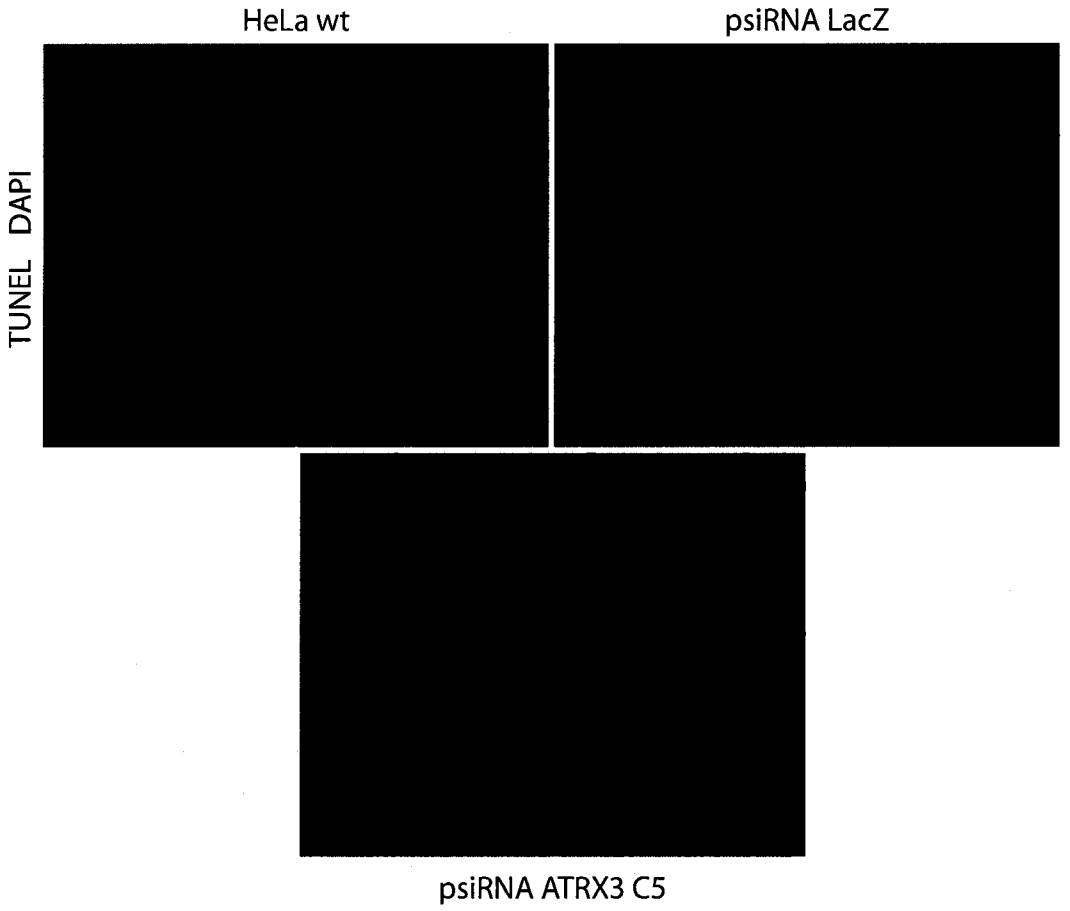
HeLa wt
psiRNA LacZ
TUNEL DAPI
psiRNA ATRX3 C5

B

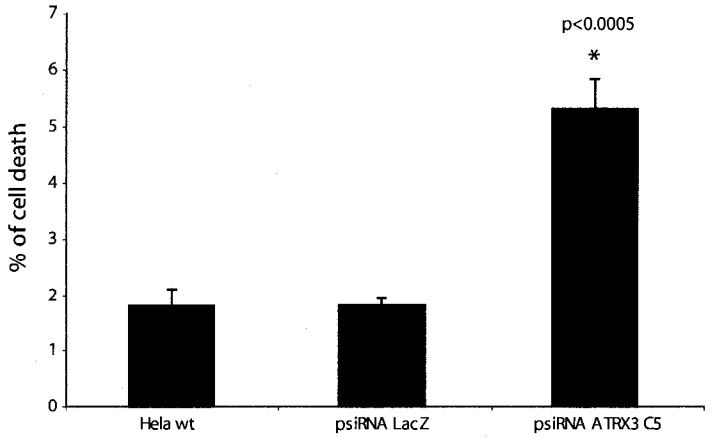
% of cell death
0
1
2
3
4
5
6
7
p<0.0005
*
Hela wt
psiRNA LacZ
psiRNA ATRX3 C5

matrix during interphase, is phosphorylated at the onset of mitosis and also associates with condensed chromatin (Berube, Smeenk et al. 2000). These cell-cycle dependent changes in ATRX nuclear localisation and phosphorylation status further suggest its involvement in cell cycle progression and control (Berube, Smeenk et al. 2000; Ishov, Vladimirova et al. 2004). In addition, ATRX loss was also found to impair chromosomal dynamics at mitosis and meiosis (De La Fuente, Viveiros et al. 2004; Ritchie, Seah et al. 2008). Similarly, ATRX interactions with Daxx are thought to regulate S to G2 phase transition (Ishov, Sotnikov et al. 1999). Furthermore, ATRX interactions with HP1α and PML-NB may regulate heterochromatin re-condensation at late S phase (Luciani, Depetris et al. 2006). Taken together, these findings suggest that ablation of ATRX could have important consequences for progression of the cell through the S to G2 phase of the cell cycle. Consequently, the progression of the cells through the S phase was investigated to see whether altered S phase dynamics is responsible for the slower growth phenotype in the psiRNA ATRX3 C5 clone.

We initially confirmed that ATRX co-localises with replicating chromatin and HP1α during S phase progression of HeLa wt cells by indirect immunofluorescence (figure 16). During a time course where blocked cells were release in S phase, ATRX was found to co-localize with the replicating DNA 6 hrs after cell release (figure 16, top panel). In addition, HP1α did also co-localize with ATRX in the nuclear speckles arrows indicate foci where co-localisation occurs (figure 16, top bottom).

Cell cycle profile analysis was performed by flowcytometry and revealed an increased number of cells in the G1 phase and a decrease in S phase cell number in the

Figure 16. ATRX co-localizes with the replicating heterochromatin and the HP1α protein during S phase

HeLa cells were synchronised at the G1/S phase with 200 mM HU containing media for 16 hours, cells were released, BrdU pulsed and fixed at 0, 2, 6 and 10 hour after the pulse. Immunohistochemistry for ATRX (red) with BrdU (green) is on the top panel whereas ATRX (red) with HP1α (green) staining is on the bottom panel. DAPI counterstain (blue) was performes on all samples. On the merge image, we observed a co-localisation of ATRX with BrdU at 6 hrs post release when the DNA is replicating. Similarly, HP1α was found to co-localise with the ATRX speckles through out S phase in the merge images. White arrows indicate some cells where co-localisation of ATRX-BrdU and ATRX- HP1α can be seen.

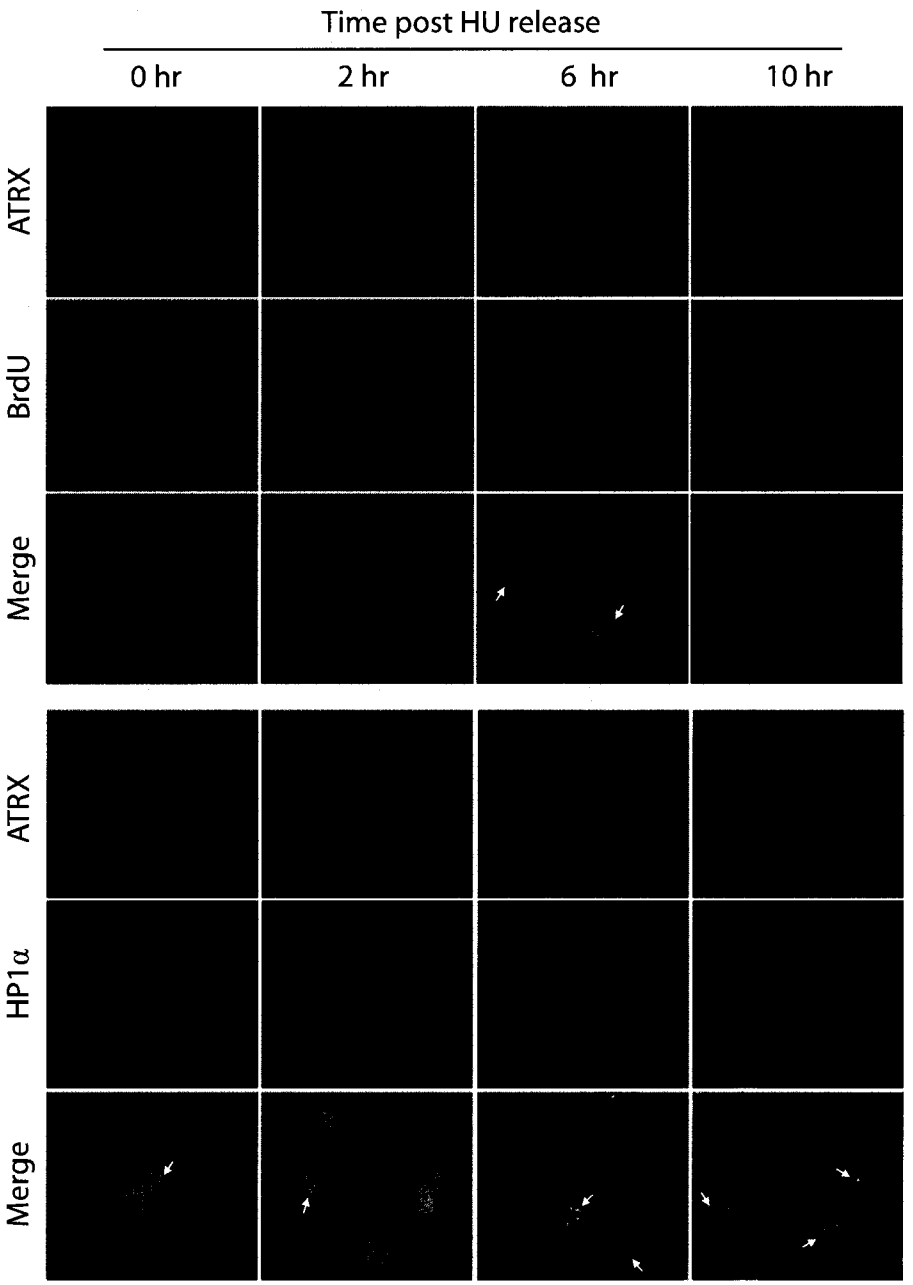
Time post HU release
0 hr
2 hr
6 hr
10 hr
ATRX
BrdU
Merge
ATRX
HP1α
Merge

psiRNA ATRX3 C5 clone compared to the control cell lines. The control cell lines have 55% of cells in S phase and 35% in the G1 phase whereas the C5 clone has 35% of cells in S phase and 55% in the G1 phase (figure 17). Therefore, there is a significant decrease (20%) in the number of cells in S phase and a significant increase (20%) in the number of cells in the G1 phase (figure 17; n=3, G1 phase $p<0.003$ and S phase $p<0.03$). These results suggest that the G1 phase is prolonged and that S phase is shortened and may suggest a defect at the G1-S phase transition. For this reason, a BrdU pulse chase experiment was used to follow cells through their cell cycle progression by flowcytometry to further investigate the nature of the defect. The BrdU+ and BrdU- cells were both followed and indicated a general cell cycle delay (figure 18, 19). This general cell cycle delay is noticeable throughout the time course in the dot plot graph where the BrdU staining intensity was plotted against the DNA content of each cells. The two panels of dot plot representing the normal and the psiRNA LacZ cells are very similar in their cell distribution whereas the psiRNA-ATRX3 C5 clone shows a different cell distribution at corresponding time points (figure 18 A). This difference can particularly be seen in the BrdU+ population (top portion of the dot plot). For example, at the 20 hr time point, the cells are transiting between G1 to G2-M (cluster moving toward the right) in the controls. At that same time point in the clones this transition is not yet happening, the cells are still forming two distinct G1 and G2-M cell clusters (figure 18 A, 20 hr). However, by 24 hr the clones are transitioning from G1 phase to G2-M as the controls did at 20 hr (figure 18 A) suggesting a cell cycle delay of about 4 hours in the psiRNA ATRX3 C5 clones. Conversely, at the 20 hr time point the BrdU- population shows two distinct G1 and G2-M cell clusters in the control but the psiRNA ATRX3 C5 clone still contains cells transitioning from G1 to G2-M confirming the delay seen in the BrdU+ cells.

Figure 17. The cell cycle profile of the psiRNA ATRX3 C5 clone

Asynchronus populations of HeLa cells, psiRNA LacZ and psiRNA ATRX3 C5 clones were BrdU pulsed and fixed. The cells were then immunostained for BrdU and counterstained with PI. Triplicat of each sample were analysed by flowcytometry for BrdU incorporation and DNA content. Cell cycle distribution of the cell population was quantified with the FCS Express 2 software. The graphs represent the percentage of cell found in S phase (blue), G1 phase (green) and G2-M phase (red). The psiRNA ATRX3 C5 clone showed an increase number of cells in the G1 phase ($p<0.003$) and a decrease number of cells in S phase ($p<0.03$) when compareted to the number of cell in thoses phases found in the HeLa and psiRNA LacZ. The error bars represent the SEM. Statistical difference (indicated by *) between the psiRNA ATRX3 and the 2 controls for each phase was calculated using the Student's T-test.

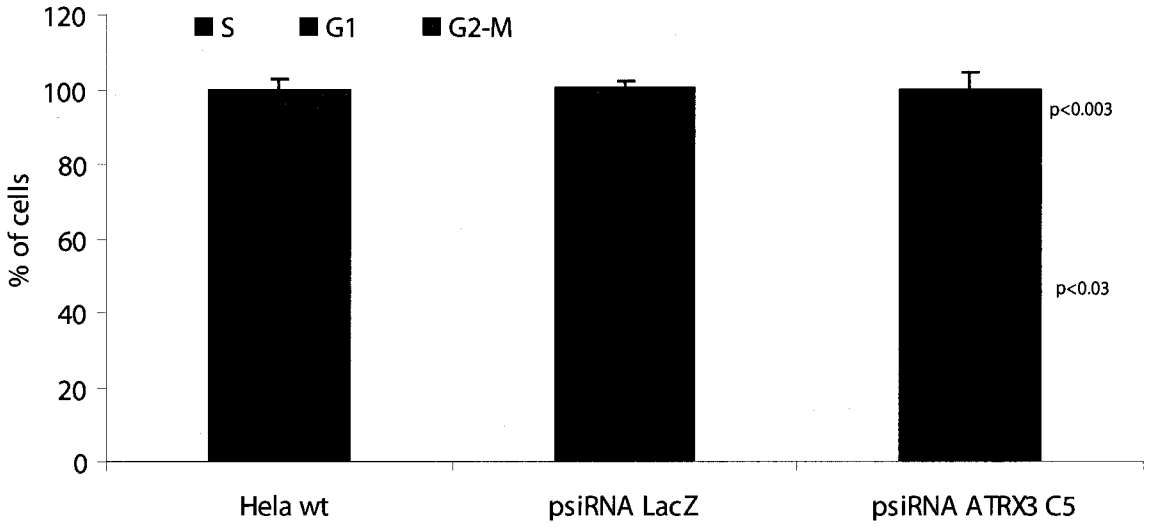
120
100
80
60
40
20
0
% of cells
S
G1
G2-M
p<0.003
p<0.03
Hela wt
psiRNA LacZ
psiRNA ATRX3 C5

Figure 18. Cell cycle progression of the psiRNA ATRX3 C5 clone

The HeLa cells, psiRNA LacZ and psiRNA ATRX3 C5 clones were BrdU pulsed and then chased until the indicated time points. The fixed cells were immunostained for BrdU and counterstained with PI. (A) Cell cycle distribution of the cell population was analyzed and dot plot graphs were generated with the FCS Express 2 software. Dot plots were generated at 0, 6, 12, 16, 20, 24 and 28 hours after the BrdU pulse. The X-axis represents DNA content whereas the Y-axis represents the BrdU staining. The graph areas where the cells in G1, S and G2-M phase are found are indicated on the 0 hr HeLa cell dot plot. Similarly, the areas where the BdrU+ (top portion) and BrdU- (bottom portion) cells are found are indicated. We observed in the psiRNA ATRX3 C5 clone that the cell cycle progression is delayed. (B) The data from the dot plots is shown in tabular form and delineated into the distinct phases of the cell cycle. The table represent the percentage of the BrdU+ cells in each phase through the cell cycle time course, these numbers were calculated from triplicate after analysis with the ModFit software. These numbers are also represented in a graph format in figure 19 A, B and C. The number of BrdU+ cells in S phase at time 0hrs was designated 100% for this analysis.

A

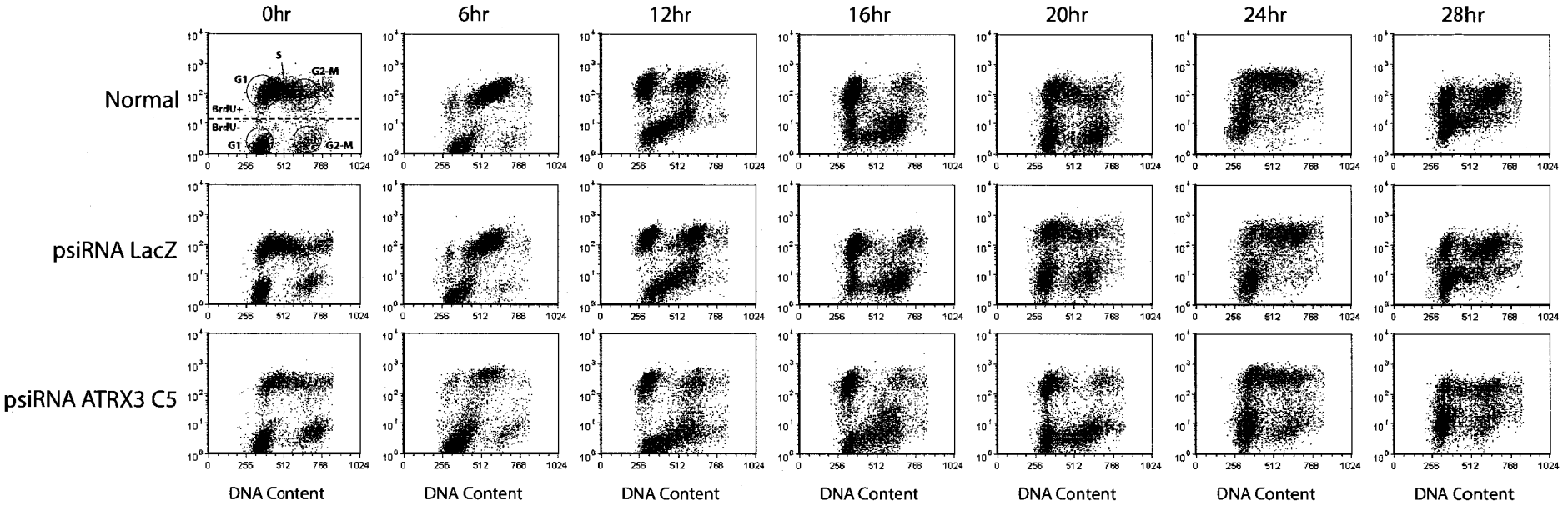

B

		0hr	6hr	12hr	16hr	20hr	24hr	28hr
HeLa WT	G1	0.00	0.00	49.51	72.55	41.85	4.28	25.25
	S	100.00	98.01	8.59	12.51	53.25	95.10	23.65
	G2-M	0.00	1.99	41.89	14.94	4.90	0.61	51.10
psiRNA LacZ	G1	00.00	0.00	51.33	71.70	36.86	1.37	25.89
	S	100.00	98.56	6.79	15.53	58.55	98.18	25.35
	G2-M	0.00	1.44	41.88	12.56	4.59	0.46	48.76
psiRNA ATRX -3 C5	G1	0.00	0.94	62.47	67.60	65.78	23.87	18.81
	S	100.00	95.89	7.48	16.17	19.58	70.09	60.66
	G2-M	0.00	3.18	30.06	16.23	14.64	6.04	20.53

Figure 19. Phase distribution of the psiRNA ATRX3 C5 clone through the cell cycle progression

The HeLa cells, psiRNA LacZ and psiRNA ATRX3 C5 clones were BrdU pulsed and then chased until the indicated time points. The fixed cells were immunostained for BrdU and counterstained with PI. The percentage of cells in each phase through the cell cycle time course was calculated from triplicate (n=3) after analysis with the ModFit software. Each graph represents the percentage of cell in the differents phase, G1 phase (A and D), S phase (B and E) and G2-M phase (C and F) through time for the HeLa cells (blue), psiRNA LacZ (pink) and psiRNA ATRX3 C5 clone (orange). The BrdU+ (A, B and C) and BrdU- (D, E and F) cells populations were also ploted independently. The error bars represent the SEM. Statistical difference (indicated by *) between the psiRNA ATRX3 and the 2 controls for each phase was calculated using the Student's T-test, all p-values were all found to be under 0.05 ($p<0.05$). The number of BrdU+ cell in S phase at time 0hrs was designated 100% for this analysis.

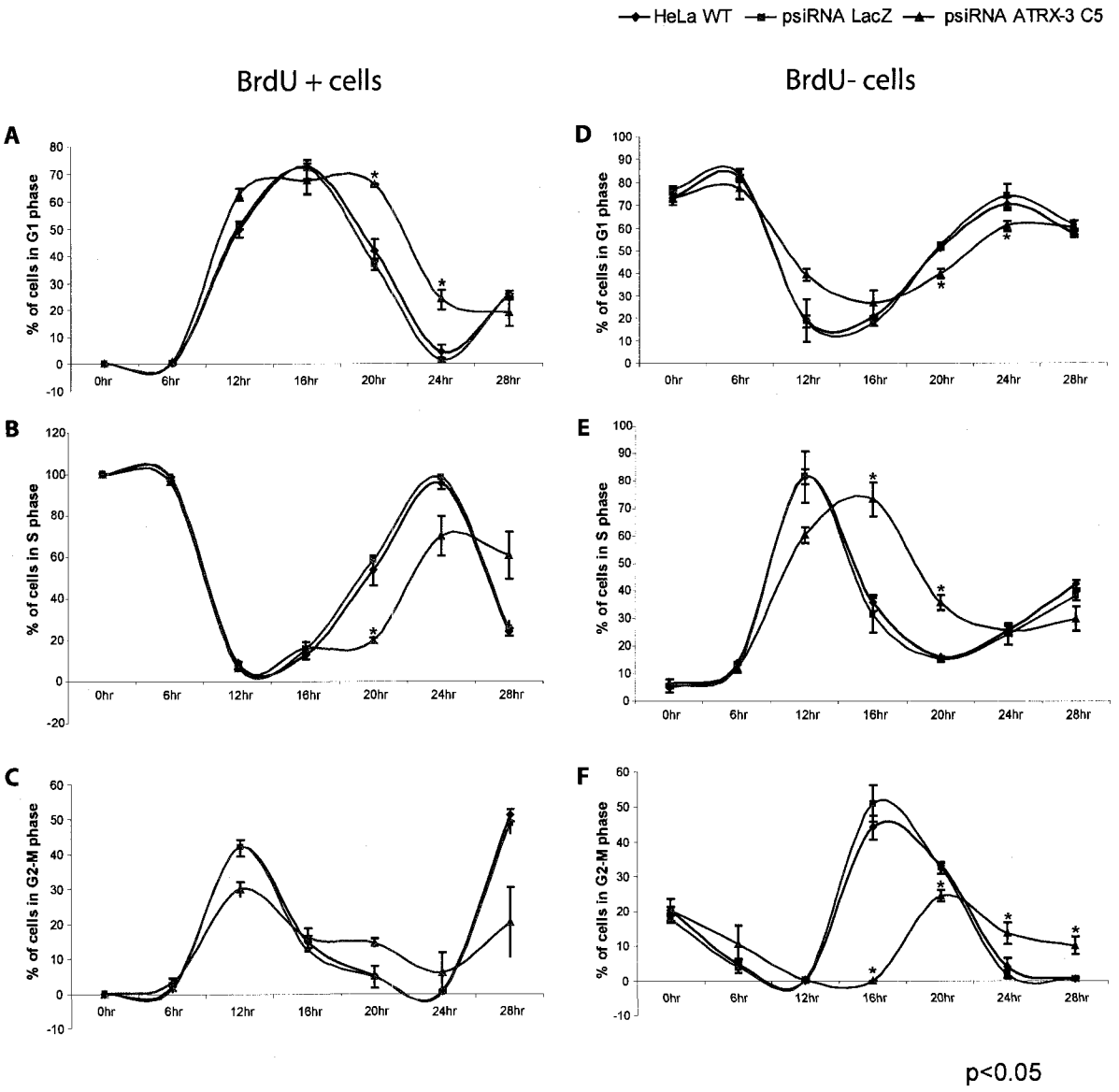
HeLa WT
psiRNA LacZ
psiRNA ATRX-3 C5
BrdU + cells
BrdU- cells
A
B
C
D
E
F
% of cells in G1 phase
% of cells in S phase
% of cells in G2-M phase
0hr
6hr
12hr
16hr
20hr
24hr
28hr
p<0.05

Quantification and analysis of the cell cycle profile at each time point and in both the BrdU+ and BrdU- populations indicated a prolonged and/or a delayed exit of the G1 phase for the psiRNA ATRX3 C5 clone (figure 19 A and D). This delay in exit from the G1 phase results in a delayed entry into the following S and G2-M phases in the BrdU+ and BrdU- cells (figure 19 B, C, E, F). Our initial flowcytometry analysis indicated that the C5 clone had a shorter S phase (figure 17). While this was not clearly observed in this experiment it was suspected given the time points chosen for analysis (figure 19). At 6 hrs and 12 hrs in the BrdU+ cells we see a similar percentage of cells exiting S phase in all cell lines (figure 19 B). However, a time point at 9hrs may reveal a faster exit from S phase in the psiRNA ATRX3 C5 clone. The BrdU+ C5 clone has fewer cells in G2 at 12hrs than the control (figure 19 C) but they are not lagging in S phase as all the cells are already out of S phase (figure 19 B). As such, it demonstrates that a larger proportion of the cells from the C5 clone have progressed further through the cell cycle (ie. they are into G2) and is suggestive of a shorter S phase that was not observed based on the time points examined. In support of this interpretation we observed an overall faster transition from S phase to the next G1 phase at 12hrs in the BrdU+ of the dot plot graphs (figure 18 A, 12 hr). No apparent change in the G2 phase was detected other than a short lag in G2 phase exit from 0 to 12hrs in the BrdU- cells (figure 19 F). This phenomenon probably corresponds to the small percentage of dying cells that occur at mitosis. Taken together, the downregulation of ATRX in HeLa cells causes the cells to cycle faster from S to the subsequent G1 phase most likely from an accelerated S phase with no apparent change in the G2 phase. However, the cell cycle shows a general delay because there is a significantly prolonged G1 phase.

3.6 The expression of Rb, E2F-1 and Cyclin A are downregulated in the psiRNA ATRX3 C5 clone

ATRX downregulation in cells has proven to have a negative impact on cell proliferation but the cause remains undetermined (De La Fuente, Viveiros et al. 2004; Garrick, Sharpe et al. 2006; Ritchie, Seah et al. 2008). The prolonged G1 phase and faster S phase in our model is a novel observation. In this section we examined the expression of multiple proteins involved in cell cycle regulation and check points during the G1 phase. The CyclinD/cdk4/6 complex, Rb (retinoblastoma) and the E2F family members are all involved at the G1 check point necessary for cell cycle progression (Schafer 1998). Interestingly, in a separate study Rb was found to associate with the *C. elegans* ATRX homologue (xnp-1) *in vivo* (Cardoso, Couillault et al. 2005). Moreover, it is has been demonstrated that Rb hypophosphorylation arrests cells in G1 (Weinberg 1995) and is more abundant in quiescent or differentiated cells (Chen, Scully et al. 1989). There is also a precedence for chromatin remodelling in the regulation of this stage of the cell cycle, specifically, that BRM and Brg1 were found to interact with Rb and HDAC to control progression at the G1-S phase transition (Zhang, Gavin et al. 2000). Given this information we examined Rb in our psiRNA ATRX3 C5 clone. We observed that Rb protein levels were altered and that the ratio of hyperphosphorylated to hypophosphorylated protein levels were also different. More precisely, the overall Rb expression level was greatly reduced and the hyperphosphorylated Rb expression level was decreased whereas the hypophosphorylated Rb expression was increased (figure 20). Since it is well documented that Rb represses transcription by binding to the E2F transcription factor family (Chellappan, Hiebert et al. 1991; Dyson 1998; Nevins 1998) we examined E2F-1 levels. The expression of the E2F-1

Figure 20. The protein expression of Rb, E2F-1 and Cyclin A in the psiRNA ATRX3 C5 clone

A western blot from 30ug of a RIPA protein extract from HeLa cells, psiRNA LacZ and psiRNA ATRX3 C5 clone was probed for ATRX, Rb, E2F-1, Cyclin A and β-actin. We observed that ATRX and ATRXt protein expression is completely eliminated in the psiRNA ATRX3 C5 clone. We observed in the psiRNA ATRX3 C5 clone a downregulated expression of the hyperphosphorylated Rb protein (top arrow) whereas the hypophosphorylated Rb (lower arrow) protein level was increased compared to the controls. The protein expression of Cyclin A and E2F-1 was also downregulated in the psiRNA ATRX3 C5 clone. The β-actin loading controls were even for all the samples.

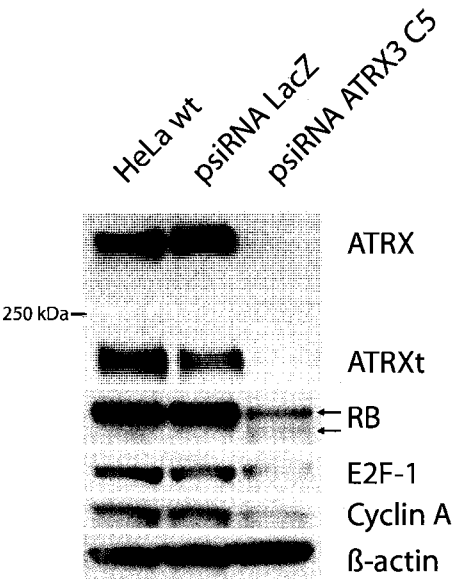
HeLa wt
psiRNA LacZ
psiRNA ATRX3 C5
250 kDa
ATRX
ATRXt
RB
E2F-1
Cyclin A
ß-actin

protein was also found to be decreased in the C5 clone (figure 20). Cyclin A, a protein required for S phase entry (Lavia and Jansen-Durr 1999) and a target gene of the E2F transcription factor family (Schulze, Zerfass et al. 1995), was also reduced in our C5 clone. However, cyclin E, which is expressed during the G1/S transition, showed unchanged protein levels by flowcytometry analysis. Collectively, the changes in Rb phosphorylation status and overall level, and the reduction in E2F-1 and Cyclin A expression levels correlates with the cells being stalled in the G1 phase and suggest a function for ATRX in Rb activation, G1 checkpoint and cell cycle progression.

3.7 Generation of a primary cell culture model lacking Atrx

To confirm our results with the C5 cell line we also generated an Atrx knockout model in primary cells for study. Primary cell models represent more physiologic models to study the cell cycle than the transformed HeLa stable cell line model. In this regard, we chose to generate mouse embryonic fibroblasts from mice conditionally ablated for Atrx. Mice with exon 18 flanked by *loxP* sites were used to generate the MEFs (figure 6). Exon 18 encodes a part of the ATPase/helicase domain and its deletion abolishes remodelling activity and generates an unstable full-length Atrx transcript and protein while the truncated isoform is unaffected by the deletion (Berube, Mangelsdorf et al. 2005; Garrick, Sharpe et al. 2006). Isolated MEF cultures from $Atrx^{flox/Y}$ or $Atrx^{flox/flox}$ animals were infected with a CRE recombinase expressing adenovirus (ad-CRE) to excise the floxed exon 18 and generate Atrx null cultures. Our first experiment was to optimize the infection time and MOI to be used for subsequent experiments. Analysis of MEFs from $Atrx^{flox/Y}$ male or $Atrx^{flox/flox}$ female mice

treated with ad-Cre by PCR amplification of the region bordering the floxed exon 18 confirmed full excision 48 hrs post ad-CRE infection with a MOI of 250 (figure 21 A). Even though no difference was found in the excision efficiency between MEFs extracted from *Atrx*$^{flox/Y}$ male or *Atrx*$^{flox/flox}$ female (data not shown) all the results presented in this section are from experiments performed in MEFs from *Atrx*$^{flox/Y}$ male embryos.

Similar to HeLa cells, we observed that Atrx is located in the nucleus and distributed in a speckled pattern in the MEFs (figure 21 B and figure 13 A). The dark Atrx speckles co-localise with the DAPI bright spots which correspond to pericentromeric heterochromatin. Atrx protein expression is eliminated 48h post ad-CRE infection, while its expression remains in the ad-LacZ control infection (figure 21 A, B). As expected, the truncated Atrx isoform is unaffected by the ad-CRE infection (data not shown). To further characterize this model we examined Daxx and PARP-1 protein levels. No changes in Daxx or PARP protein expression were observed. The ad-Cre infected MEFs show complete Atrx downregulation and can be designated as Atrx^{null} MEFs and used as a primary cell model to verify our previous findings made with the C5 HeLa clone.

3.8 Atrx^{null} MEFs have a reduced growth rate and increased level of cell death

As a result of the previous growth defects observed in the psiRNA ATRX3 C5 clone, the proliferation and death of the ad-CRE infected MEFs were also analysed. Similarly to the C5 clone, a small but significant increase in death was observed in the ad-CRE infected MEFs (figure 22 B; n=3, $p<0.005$). It was also shown that their growth rate is significantly

Figure 21. Atrx is ablated in the Cre infected *Atrx* flox MEF culture

Atrx$^{flox/Y}$ MEFs were infected with ad-LacZ and ad-Cre and incubated for 48 hours. (A) The MOI was optimized for total excision of the exon 18 by the Cre recombinase. RNA extracted from infected MEFs was reversed transcribed and the Atrx region spanning the floxed sequence was amplified by PCR. The PCR products separated by electrophoresis showed a 648 bp and 520 bp bands which represent cDNA fragments with exon 18 present or excised, respectively. An MOI of 250 is required for total exon 18 excision. (B) MEFs treated with ad-LacZ or ad-Cre were fixed and analyzed by immunohistochemistry for Atrx (first column), DAPI counterstain (second column) or the merged image (third column). Note that the speckled pattern of Atrx staining is lost in the MEFs treated with ad-Cre. (C) Similarly, Western blot analysis using 30ug of a RIPA protein extract from ad-LacZ or ad-Cre treated MEFs demonstrated a complete loss of Atrx in the ad-Cre treated cells but no change in Daxx or PARP-1 levels. β-actin was used as a protein loading control.

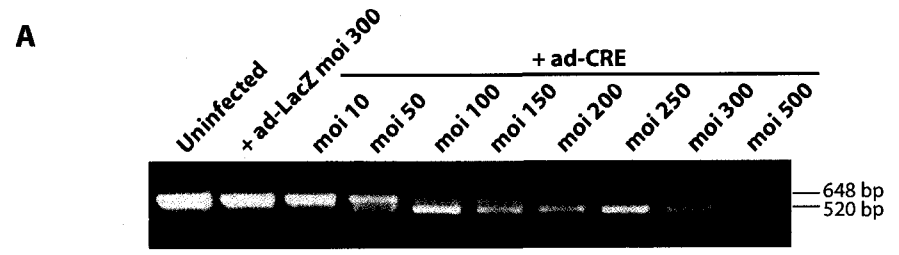
A
Uninfected
+ ad-LacZ moi 300
+ ad-CRE
moi 10
moi 50
moi 100
moi 150
moi 200
moi 250
moi 300
moi 500
648 bp
520 bp

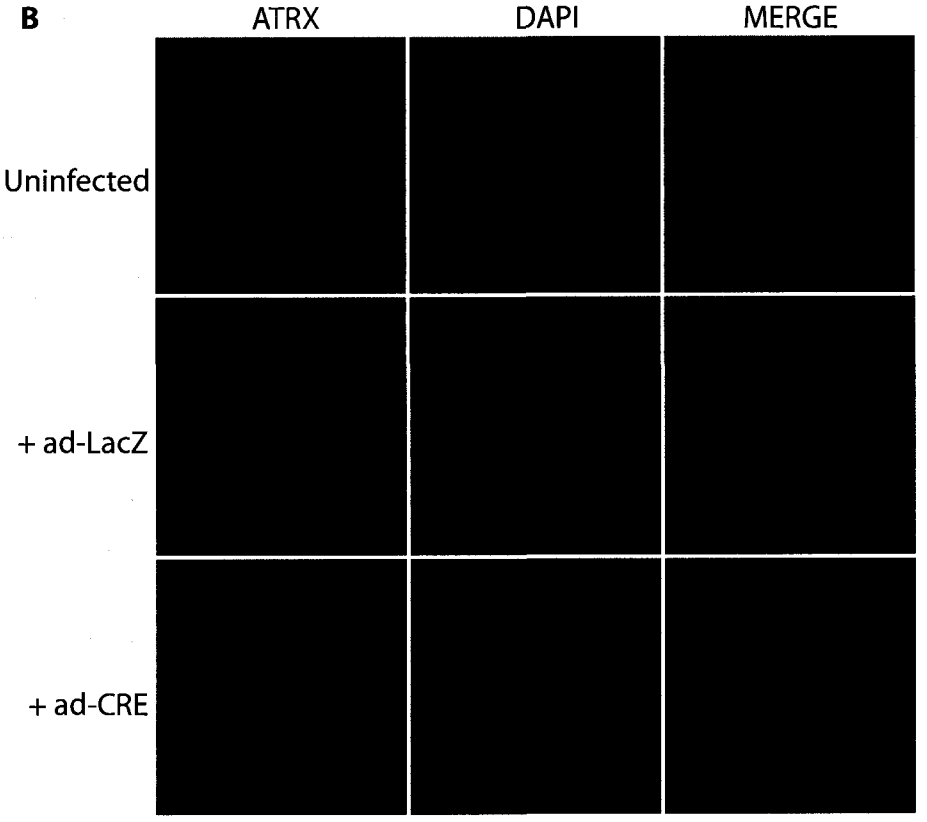
B
ATRX
DAPI
MERGE
Uninfected
+ ad-LacZ
+ ad-CRE

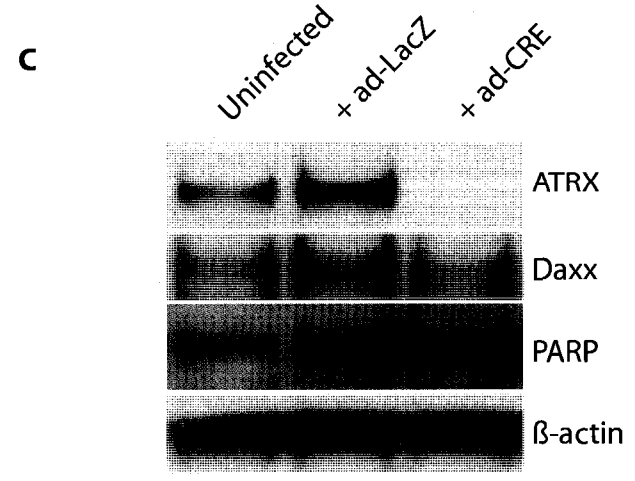
C
Uninfected
+ ad-LacZ
+ ad-CRE
ATRX
Daxx
PARP
ß-actin

Figure 22. The Atrx^{null} MEFs show a reduced growth and a small increase in cell death

Atrx$^{flox/Y}$ MEFs were infected with ad-LacZ and ad-Cre and incubated for 48 hours. (A) Cell proliferation was measured by WST-1 colorimetric assay from day 0 to day 4. Each time point represents the average of 12 replicates (n=12) and the error bars represents the SEM. We observed a significant decrease in the growth rate at day 2, 3 and 4 in the ad-Cre infected MEFs (green) compared to the uninfected (blue) and the ad-LacZ (red) controls. Statistical difference (indicated by *) between the ad-Cre infected MEFs and the 2 controls was determined using the Student's T-test, $p<0.00005$.
(B) The *Atrx*$^{flox/Y}$ MEF infected cells were fixed, analysed by TUNEL assay 48h post-infection, DAPI counterstained, and viewed by microscopy. The percentage of cell death was calculated as the number of TUNEL positive cells over the total number of cells (DAPI positive). Three sections from three slide were counted for the calculations (n=3). The error bars represents the SEM. We observed a significant increase in TUNEL positive cells (designated by *) in the ad-Cre infected MEFs when compared to the uninfected cells and the ad-LacZ control. The p-value (from Student's T-test) for this comparison was found to be $p<0.005$.

A

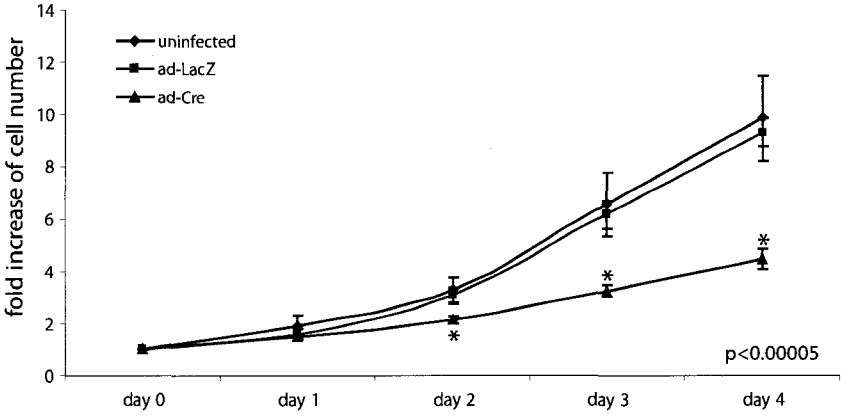
14
12
10
8
6
4
2
0
fold increase of cell number
uninfected
ad-LacZ
ad-Cre
*
*
*
p<0.00005
day 0
day 1
day 2
day 3
day 4

B

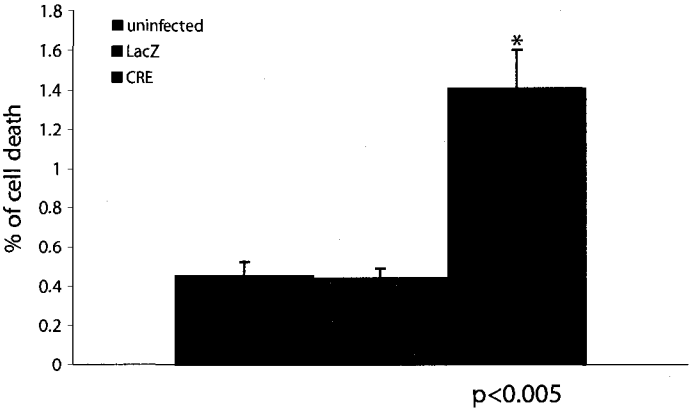
1.8
1.6
1.4
1.2
1
0.8
0.6
0.4
0.2
0
% of cell death
uninfected
LacZ
CRE
*
p<0.005

slower than the controls. By the second day after the infection there already is a significantly smaller increase in cell number that increases with time (figure 22 A; n=12, $p<0.00005$). These results, are consistent with the earlier observations made in the HeLa cell model. Again, the increase in apoptosis may not entirely explain the proliferation delay of the $Atrx^{null}$ MEFs and thus, cell cycle deregulation was also investigated.

3.9 Changes in S to G2-M phase in Atrx KO MEFs

Initially, we used flowcytometry to sort the cells to determine the fraction of the cell population within each phase. We observed that the general cell cycle profile generated by the MEFs is very different from the HeLa cells. The MEFs only have a small amount of replicating cells (S phase) and the rest are divided between the G2-M and G1 phase (figure 23 A). Nonetheless, $Atrx^{null}$ MEFs still showed a small decrease in the number of cells in S phase compared to WT MEFs 48h post-infection (figure 23 A; n=6, $p<0.003$)which was of similar magnitude to the changes observed in the psiRNA ATRX3 C5 clone. Furthermore, a small increase in the G2-M population was also seen in the ad-CRE infected MEFs but no increase in the proportion of cells in the G1 phase was detected (figure 23 A; n=6, $p<0.002$). In addition to the cell cycle profile by flowcytometry, an independent experiment where infected MEFs were BrdU pulse and stained for BrdU by immunohistochemistry was performed. The numbers of BrdU+ and DAPI positive cells were counted under the microscope to calculate the % of BrdU+ cells in the infected MEFs. This experiment confirmed the significant decrease number of cells in S phase previously seen by flowcytometry (figure 23 B; n=4, $p<0.03$).

Figure 23. Cell cycle profile and proliferation changes in the $Atrx^{null}$ MEFs

$Atrx^{flox/Y}$ MEFs were infected with ad-LacZ and ad-Cre and incubated for 48 hours. (A) the BrdU pulsed cells were fixed and immunostained for BrdU and counterstained with PI. Then, 6 independent infections for each sample were analysed by flowcytometry for BrdU incorporation and DNA content. Cell cycle distribution of the cell population was quantified with the FCS Express 2 software. The graphs represent the percentage of cell found in S phase (blue), G1 phase (green) and G2-M phase (red). We observed that the ad-Cre infected MEFs showed an increase number of cells in the G2-M phase ($p<0.002$) and a decrease number of cells in S phase ($p<0.003$) when compareted to the number of cells in thoses phases in the uninfected and the ad-LacZ controls. The error bars represent the SEM. Statistical difference (indicated by *) between the ad-Cre infected MEFs and the controls for each phase was determined using the Student's T-test. (B) The $Atrx^{flox/Y}$ infected MEFs were BrdU pulsed for 1 hour then fixed, immuno stained for BrdU, DAPI counterstained and viewed by microscope. The percentage of cells in S phase was determined as the number of BrdU positive cells over the total cell population (DAPI positive). Four sections from 4 slides were counted for the calculations (n=4). We observed that the ad-Cre infected MEFs showed a significant decrease number of cells in the S phase (designated by *) when compared to the uninfected cells and the ad-LacZ control. The Student's T-test for this comparison gave a p-value under 0.003 ($p<0.03$) and the error bars represent the SEM.

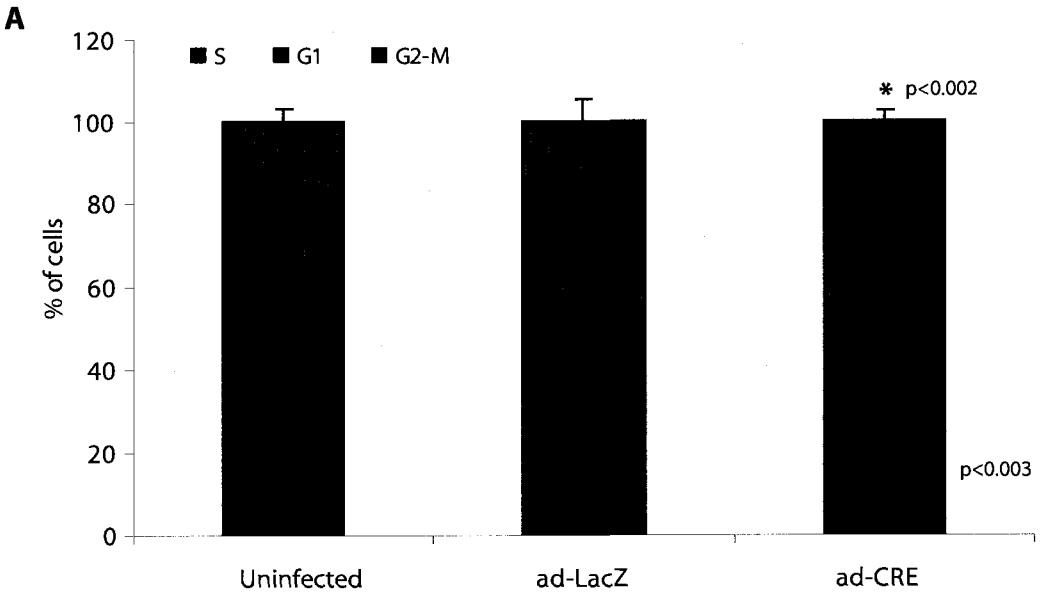
A
120
100
80
60
40
20
0
% of cells
S
G1
G2-M
* p<0.002
p<0.003
Uninfected
ad-LacZ
ad-CRE

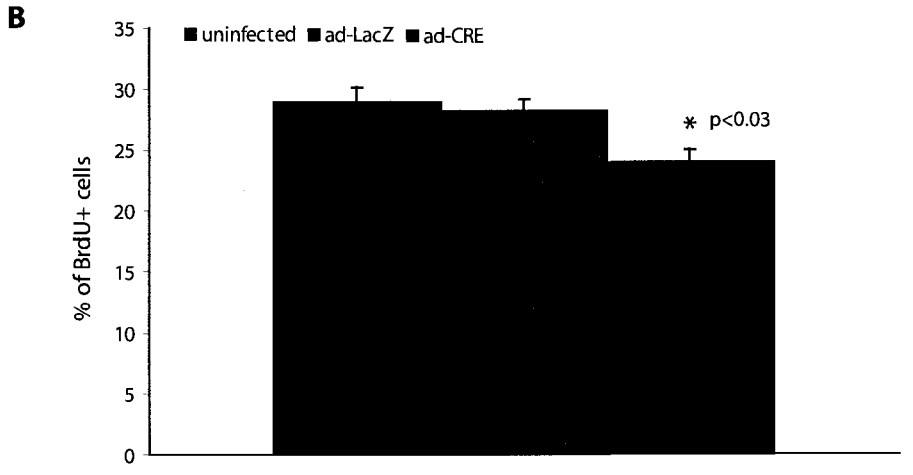
B
35
30
25
20
15
10
5
0
% of BrdU+ cells
uninfected
ad-LacZ
ad-CRE
* p<0.03

The cell cycle profile changes in S and G2-M suggest a potential S to G2-M phase transition defect. A recent study showed prolonged transition from prometaphase to metaphase in siRNA ATRX-depleted HeLa cells (Ritchie, Seah et al. 2008). In that study ATRX depleted cells were shown to have chromosomal segregation problems. There was an increased number of cells with lagging chromosomes and an elevated percentage of intranuclear bridging during late M and G1 phase (Ritchie, Seah et al. 2008). Other studies have suggested that ATRX is important for quick recovery of condensed heterochromatin after replication at late S phase, before progressing into G2 phase (Ishov, Vladimirova et al. 2004; Luciani, Depetris et al. 2006). The passage from S phase to G2-M in the ad-CRE infected MEFs was closely studied using a BrdU pulse chase time course, followed by BrdU and PH3 staining. PH3 is a G2-M phase marker with distinctive staining patterns in G2 and M thereby allowing one to distinguish cells in G2 or M phase (Appendix C). Surprisingly, the amount of cells cycling from S to G2-M within a period of 10 hrs was unaltered in the $Atrx^{null}$ MEFs (figure 24 B). In addition, the PH3 cell staining and counts also failed to confirm the small increase of cells in G2-M phase observed by flowcytometry (figure 24 A). However, DNA bridging and an increase in lobulated nuclei was observed in the $Atrx^{null}$ MEFs (figure 25; $n=4$, $p<0.01$). Taken together, these numbers correspond closely to the number of apoptotic cells previously measured (figure 22 B). The manifestation of these mis-shaped nuclei indicates a mitotic defect in the absence of ATRX and consequently those cells are probably targeted for destruction.

Figure 24. Analysis of the S to G2-M phase progression in the $Atrx^{null}$ MEFs

Atrx$^{flox/Y}$ MEF were infected with ad-LacZ and ad-Cre and incubated for 48 hours. The fixed cells were stained by immunohistochemistry for phospho-histone H3 and DAPI counterstained. The percentage of cells in G2-M phase was determined as the number of PH3 positive cells over the total cell population (DAPI positive). Four sections from 4 slides were counted for the calculations (n=4). The error bars represent the SEM. We observed no difference in the percentage of the G2-M phase cells. (B) The infected cells were BrdU pulsed then chased and fixed after 0, 2, 4, 6, 8 and 10 hrs. Immunohistochemistry for BrdU, PH3 and DAPI counterstaining was performed. The number of single labeled BrdU and double labeled BrdU/PH3 cells were counted. The average of 4 sections in 4 slides for each treatment was used for the calculations (n=4). The error bars represent the SEM. The ratio of BrdU+PH3+/BrdU+ represents the number of G2-M phase cells that were in S phase at 0 hr and illustrate the cell transition from S phase to the G2-M phase. We observed no difference in the percentage of BrdU+PH3+/BrdU+ cell when comparing the uninfected, ad-LacZ and ad-Cre infected cells at each time point.

A


Uninfected
ad-LacZ
ad-CRE
% of cells in G2-M phase
16
14
12
10
8
6
4
2
0

B

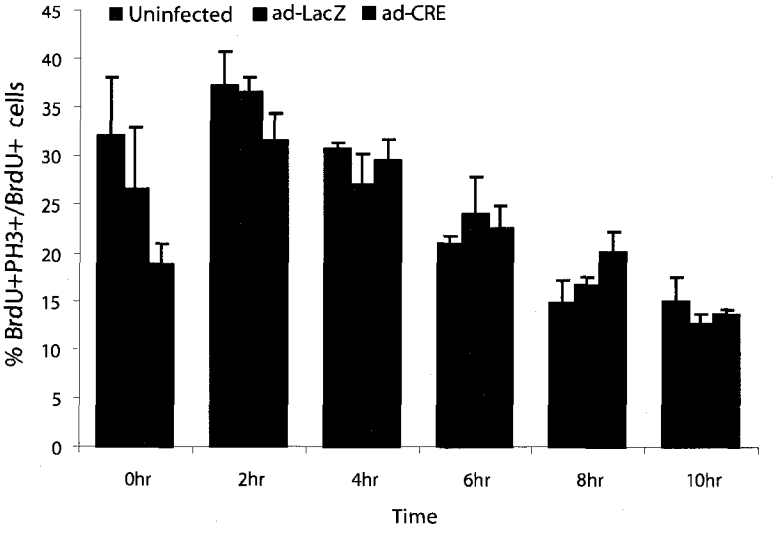
Uninfected
ad-LacZ
ad-CRE
% BrdU+PH3+/BrdU+ cells
45
40
35
30
25
20
15
10
5
0
0hr
2hr
4hr
6hr
8hr
10hr
Time

Figure 25. The Atrx^{null} MEFs show an increase in lobulated and intranucleated cells

Atrx$^{flox/Y}$ MEF were infected with ad-LacZ and ad-Cre and incubated for 48 hours. The percentage of lobulated and intranucleated cells was calculated after counting all the cells. Four fields from 4 slides were counted from each cell treatment for the calculations (n=4). The error bars represent the SEM. We observed an increase in the number of lobulated and intranucleated cells in the Atrx^{null} MEFs (ad-Cre infected) compared to the uninfected cells and the ad-LacZ infected control. Statistical difference (indicated by *) between the ad-Cre infected MEFs and the controls was determined using the Student's T-test, $p<0.01$. The lower portion of the figure shows the morphology of the normal, lobulated and intranucleated cells found in Atrx^{null} MEF culture.

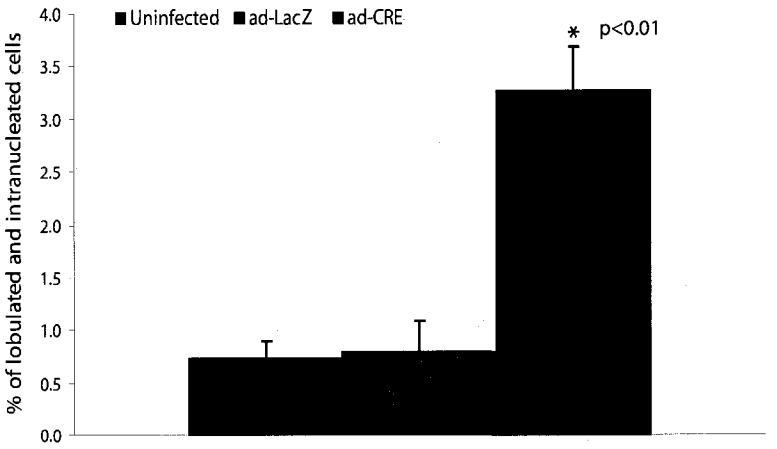
Uninfected
ad-LacZ
ad-CRE
% of lobulated and intranucleated cells
4.0
3.5
3.0
2.5
2.0
1.5
1.0
0.5
0.0
*
p<0.01

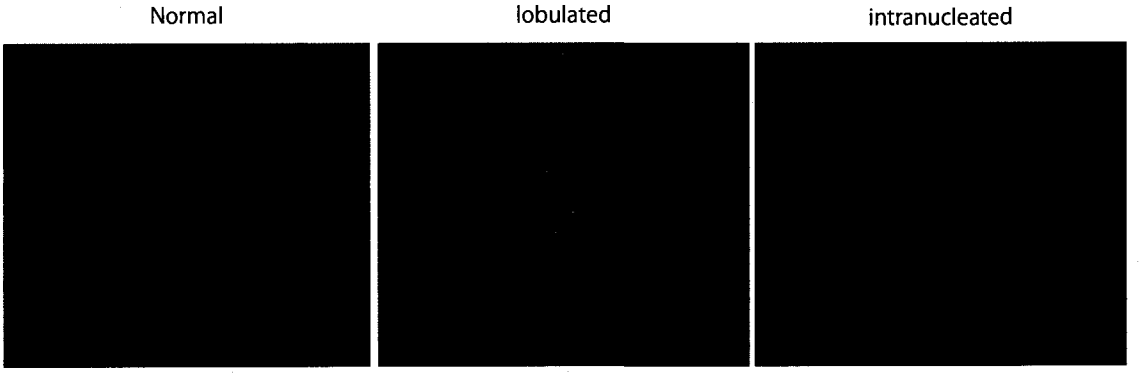
Normal
lobulated
intranucleated

3.10 Atrx KO MEFs have an increased level of pRb and hypophosphorylated Rb.

The HeLa psiRNA ATRX3 C5 clone harboured many proteins that were down-regulated and involved in the G1 cell cycle check point including Rb, E2F-1 and Cyclin A. Even though the cell cycle profile analysis of the MEFs and the clones did not reveal identical defects in the G1 phase these proteins were also examined in the MEFs since Rb's role is not restricted to the G1-S phase progression. Indeed, Rb hypophosphorylation can also occur in S and G2 phases. Similar to the C5 clone, the $Atrx^{null}$ MEFs showed an increase in hypophosphorylated Rb (figure 26). Conversely, hyperphosphorylated Rb expression was not altered from control levels. Unfortunately, E2F-1 and Cyclin A were not assessed. Altogether, the increase in hypophosphorylated Rb could be related to the cell proliferation delay by acting on an alternate phase other than G1, potentially at S or the G2-M phase.

Figure 26. The hypophosphorylated Rb protein expression increases in the Atrx^{null} MEFs

A western blot from 30ug of a RIPA protein extract from *Atrx$^{flox/Y}$* MEFs infected with ad-LacZ and ad-Cre was probed for ATRX, Rb, and β-actin. We observed in the Atrx^{null} MEFs (ad-Cre infected) a important downregulation of the ATRX protein expression whereas the ATRXt protein is faintly present in all samples. The ad-Cre infected MEFs also show an increase in the hypophosphorylated Rb protein level (lower arrow) compared to the controls. The protein expression of the hyperphosphorylated Rb protein (top arrow) is comparable to the control levels. The β-actin loading control is even for all the samples.

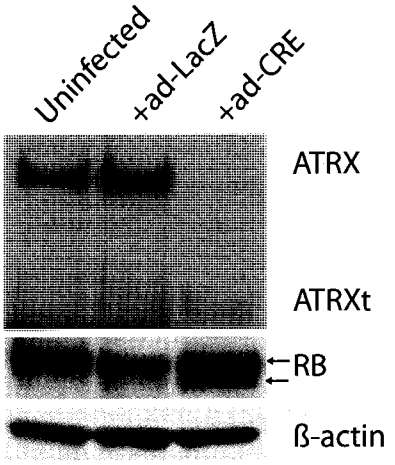
Uninfected
+ad-LacZ
+ad-CRE
ATRX
ATRXt
RB
ß-actin

4 Discussion

The role of ATRX in cell cycle progression was investigated using three complementary models. First, a siRNA transient ATRX downregulation in HeLa cells; second, a shRNA expressing clone and third, an $Atrx^{null}$ MEF cell line. Initially, I will discuss some of the advantages and disadvantages of each model and later will discuss in detail some key results.

4.1 Advantages and disadvantages of the different models

From the 3 models that were used to study ATRX downregulation all had advantages and disadvantages for the purpose of the work performed in this study. The first model consisted of HeLa cells transiently transfected with siRNA targeted for ATRX. One advantage is that siRNA allows for rapid acute decreases in protein levels without the need for clone selection. However, while this model generates significant ATRX downregulation, one of the major drawbacks observed was that this method is transient with respect to gene silencing. The siRNA gene downregulation occurs quickly, will last 3-5 days and normal protein levels are back within 5-7 days post-transfection (Elbashir, Harborth et al. 2002; Holen, Amarzguioui et al. 2002). Therefore this method is not the best to examine the effect of ATRX knockdown on cell cycle changes, hence the generation of the shRNA stable clone for long term effects.

The transfection also induced a lot of cell death in the mock and the siControl transfections. The increased TUNEL staining in the siControl and the mock treatments

suggests that the transfection procedure and/or the reagents affect cell integrity and survival (figure 10 B). The aboundant cell death after the transfection made it harder to assess the significance and amount of death caused by the ATRX downregulation.

Despite the problems with this model, we were able to use it to verify the efficiency of the siRNA oligonucleotides for ATRX downregulation. Both ATRX full-length and truncated isoforms were targeted resulting in an almost complete ATRX downregulation by the siRNAs in 24hrs (figure 9). We determined that the oligonucleotide siATRX3 targeted ATRX expression as efficiently as the manufactured siATRX pool. Indeed, the results from the transient knockdown convinced us to utilize the siATRX3 oligonucleotide for shRNA expression by psiRNA-hH1 neo plasmid in stable cell lines

The second model used was the HeLa stable cell lines, the stably transfected cells expressed an shRNA targeted for ATRX. For this study, multiple psiRNA ATRX 3 clones were created. However, the majority of them regained ATRX expression during the selection process (figure 12). Only the clone C5 maintained a constitutively low level of ATRX throughout selection in G418 media. The mechanism by which the clones revert to expressing ATRX is unknown. One may speculate that the psiRNA-hH1 vector stopped expressing the shRNA for different reasons; possibly the promoter driving the shRNA expression was silenced. Nevertheless, ATRX does seem to confer a survival advantage to the cells since expression is regained. Therefore, in culture when certain cells regain ATRX expression they obtain a growth advantage over the other cells that maintain low levels of ATRX. Eventually because of a competitive selective presure the cells re-expressing ATRX overtake the culture resulting in ATRX expression slowly reappearing in the culture. Even

the psiRNA ATRX3 C5 clone was found to regain ATRX expression if cultured for an extended period of time and the status of ATRX expression had to be verified before using cells for experiments.

The psiRNA ATRX3 C5 clone did harbour efficient ATRX downregulation (figure 13). The amount of ATRX remaining in the cell is so low that ATRX was considered totally ablated. ATRX full length and ATRXt isoforms were both affected as expected since the shRNA sequence targeted exon 1 which is common to both isoforms. The constant production of shRNA facilitates the study of the long term effect of ATRX downregulation on the cell. The creation of the psiRNA ATRX3 C5 clone was essential to make a more thorough study of the cell cycle. This model allowed us to identify cell cycle defects such as slower growth and G1/S phase abnormalities.

Even though the C5 cell line is a great model and resulted in a novel finding on the role of ATRX in the cell cycle it still has limitations. Past analysis of multiple human cervical adenocarcinoma cell lines revealed altered expression of the tumour suppressor genes, p53 and Rb (Scheffner, Munger et al. 1991). The expression of these proteins was found to be reduced because of gene mutations and interactions with transforming viral proteins from the human papilloma virus (HPV). There is evidence that the HPV oncoproteins E6 and E7 can complex with p53 and Rb to alter their expression/activation and confer a selective advantage (Scheffner, Munger et al. 1991). HeLa cervical adenocarcinoma cells are positive for HPV-18 DNA (Schwarz, Freese et al. 1985) and have been shown to have an unaltered expression of Rb but a greatly reduced expression of p53 (Scheffner, Munger et al. 1991). Because of the transformed nature of the HeLa cancer cell line the cells

are more robust and less likely to die. Therefore, the effects of the ATRX downregulation seen in HeLa cells may not perfectly reflect what happens *in vivo*. The use of non-transformed cells such as a primary cell lines will further help in elucidating the role of ATRX in cell cycle progression and could corroborate our finding in the HeLa clones.

The third model, the $Atrx^{null}$ MEF model permitted us to study the effects of Atrx downregulation in primary cells. This model is more physiological (closer to an *in vivo* model) than the psiATRX3 C5 clone. The generation of the $Atrx^{null}$ MEFs was convenient because of the readily available $Atrx^{flox}$ mice and the simplicity of the adenoviral infection. The quick downregulation of Atrx after the CRE recombination was definitely an advantage. Nevertheless, as with the Atrx shRNA clone the MEF model did have some limitations. The primary cells have a limited lifespan; they can be grown for only a short time period, about a week (2-3 passages). After too many passages the MEFs would stop growing and undergo senescence. This time constraint is important since most experiments are performed after a couple of days of expansion and an infection of 48 hrs. Freshly extracted MEFs are more vigorous but not always available when needed. Several experiments carried out with the HeLa shRNA clone could not be performed with the MEFs as they would not survive the length of the experiment. Although the $Atrx^{null}$ MEF line was not the optimal model for longer experiments, it did help to corroborate our previous findings. We did confirm the slower growth rate and the S phase change seen in the psiATRX3 C5 clone.

4.2 Daxx and PARP-1 protein levels in the absence of ATRX

The protein level of Daxx and PARP-1 were investigated because of their known interactions with ATRX (Ishov, Vladimirova et al. 2004; Tang, Wu et al. 2004) or their suspected interactions, namely our unpublished work showing that Daxx is decreased and PARP-1 activity levels are increased in the forebrain of conditional Atrx KO mice. However, similar results could not be obtained in the models we studied. The transiently transfected cells had Daxx and PARP protein levels that were both down including the mock, control and the ATRX siRNA transfection (figure 9). For this reason, the ATRX knockdown by siRNA is thought to have no effect Daxx and PARP expression levels despite the preliminary work. In the psiRNA ATRX3 C5 clone we observed no change in PARP-1 levels (figure 13 B); Daxx protein level showed to be down by immunohistochemistry analysis (figure 13 A) however, was unaffected in the immunoblot (figure 13 B). In addition, we observed in the $Atrx^{null}$ MEFs no changes in Daxx and PARP-1 protein expression (figure 21 B, C). All thoghether, the cell models studied showed no consistent changes in Daxx and PARP-1 protein expression levels. These results suggest that loss of the ATRX-Daxx complex does not affect the Daxx protein levels within the cell. Similarly, PARP-1 expression is unaffected by ATRX protein levels. The inconsistency of these results with the previous unpublished findings from the forebrain of conditional Atrx KO mice may be due to the type of tissues or the cells that were analysed. Daxx protein levels may only be affected by Atrx expression in the forebrain, *in vivo* or during embryonic development and not in our cells line models. Therefore, whether the loss of ATRX impacts on Daxx function remains to be determined.

4.3 Loss of ATRX leads to enhanced cell death

In the three ATRX downregulation models studied, we observed increased cell death. The siRNA transient transfection model had the highest number of TUNEL positive cells compared to the psiATRX3 C5 and the $Atrx^{null}$ MEF lines (compare figure 10, 15 and 22). This result can be partially attributed to the method and the transfection process since significant cell death was found in the mock and the siControl. The TUNEL assay was performed 24 hrs post-transfection; at that time, the cell viability is still affected by the transfection treatment. In the future, cells should be left to recover from the transfection more then 24 hrs before assessing the apoptosis induced by the lower level of ATRX. Allowing for a longer cell recovery period before performing the TUNEL analysis would result in lower levels of apoptotic cells observed in the controls and emphasize the ATRX siRNA induced death in the treated cells. Although some cell death was found in the controls, the ATRX siRNA still induced a greater level of apoptosis.

The increased level of apoptosis observed in the three models suggests that ATRX downregulation has an effect on cell survival. Additionally, these observations are consistent with what we have observed in the forebrain Atrx KO mice where neuronal survival at the early stages of corticogenesis is compromised (Berube, Mangelsdorf et al. 2005).

The cause of this increased cell death may be linked to the protein Daxx which interacts and is found in the same complex as ATRX (Ishov, Vladimirova et al. 2004; Tang, Wu et al. 2004). Literature on Daxx is conflicting, this protein was first identified as pro-apoptotic factor but more recently, studies describe Daxx as an anti-apoptotic protein

(Salomoni and Khelifi 2006). For example, studies demonstrated that Daxx interacts within the FAS pro-apototic pathway and is responsible for JNK activation (c-Jun-N-terminal kinase) (Yang, Khosravi-Far et al. 1997; Khelifi, D'Alcontres et al. 2005). However, other studies showed that *Daxx*$^{-/-}$ ES cells and cells treated with RNAi for Daxx have increased apoptosis, and that *Daxx*$^{-/-}$ embryos show extensive apoptosis by E7.5 suggesting an anti-apoptotic role (Michaelson, Bader et al. 1999; Michaelson and Leder 2003). These two roles for Daxx can lead us to different explanations resulting in increased cell death in the absence of ATRX. We can speculate that the Daxx protein which is now "free" of the ATRX complex (because ATRX is absent in the cell) can promote apoptosis if pro-apoptotic. However, we can also speculate that the increased cell death may be related to Daxx expression which is downregulated in some of our models and is similar to what we have observed in the forebrain of Atrx KO mice. Therefore, the reduced expression of the anti-apoptotic protein Daxx could also lead to an increase in apoptosis. The only difficulty with this explanation is that we did not see a consistent decrease in Daxx levels in each of our models.

Another cause for the increased cell death may be the increased incidence of lobulated and intranucleated cells that are observed in the absence of ATRX. Dr. Bérubé's group found that ATRX ablation impairs chromosome cohesion, congression and segregation resulting in a longer M phase in cells (Ritchie, Seah et al. 2008). ATRX depletion by siRNA in HeLa cells resulted in unusual nuclear morphology with increased lobulated and intra-nucleated cells (Ritchie, Seah et al. 2008). Abnormal cell morphology was also noted in our ATRX siRNA transient transfection but was not quantified or further studied. Similarly, Atrx downregulation in the MEFs also produced these aberrant cellular morphologies but to

a lesser extent then reported by Dr. Bérubé's group. The proportion of mis-shaped nuclei in the $Atrx^{null}$ MEFs did correlate closely to the level of cell death, and may infer that the abnormal cells are probably targeted for apoptotic destruction because of integrity issues. The DNA intergrity of those cells might be affected by the inability to re-condense properly the heterochromatin during late S phase, a process in which ATRX is thought to be involved (Ishov, Vladimirova et al. 2004; Luciani, Depetris et al. 2006).

Another question that arises is why only a small subset of the population dies in the absence of ATRX. If ATRX was essential for cell survival then removing it would result in complete death within the population, however this was not observed. The reason may be that death only occurs when the cell accumulates a specific amount of multiple apoptotic factors then, when that threshold is reached the cell dies. However, the cell may have a difficult time to reach that threshold. The apoptotic factor expression may be affected because of an altered epigenetic regulation involving the now absent ATRX protein.

4.4 ATRX regulates growth rate and the G1/S checkpoint

ATRX downregulation in both the psiATRX3 C5 clone and the $Atrx^{null}$ MEF model disrupted cell proliferation. In both models the growth reduction was distinguishable after 2-4 days after initial cell seeding (figures 14 and 22). The growth delay was suggested to be partially caused by the small increase of apoptosis but other factors are thought to be involved. No effect on BrdU incorporation was found in the ATRX siRNA treated cells (figure 10 A), even though ATRX downregulation did affect incorporation in our other models. The lack of change in the replication rate may be attributable to the poor

experimental design with that model. Replication was assayed by BrdU incorporation 24hrs post siRNA transfection. We know that ATRX protein expression is downregulated by 24hrs but it is probably too early to observe a replication defect resulting from a lack of ATRX. In the $Atrx^{null}$ MEF model, a slight growth reduction is seen 48 hrs post CRE infection but no change was observed at 24 hrs (figure 22 A). The percentage of BrdU+ cells in the siATRX3 and siATRX pool do look slightly lower at 24hrs but it was not statistically significant, a later time point at 72 or 96hrs might have shown a significant difference.

Futher investigation of the cell cycle profile in the C5 clone and the $Atrx^{null}$ MEFs revealed a shorter S phase. The percentage of cells in S phase in both models was very different because of the cell type but altogether the magnitude of the decrease (% of decrease) in both models was comparable (figure 17 and 23). During S phase ATRX localizes to PML-NBs and interacts with the proteins HP1α, Daxx and PML (Ishov, Vladimirova et al. 2004). At that same time period, ATRX is thought to be involved in the recovery of condensed heterochromatin after DNA synthesis and before mitosis (Ishov, Vladimirova et al. 2004; Luciani, Depetris et al. 2006). In the absence of ATRX, the cell may not reconstitute the heterochromatin properly but still proceed to the G2-M phase. We can speculate that the decondensed heterochromatin may promote faster replication of the DNA therefore accelerating the progression of the cells through the S phase. However, the quicker S phase does not explain the overall slower growth rate of these cells.

In the psiRNA ATRX3 C5 clone, in addition to the faster S phase change, we observed that the cell cycle was disregulated at other points as well. A prolonged G1 phase was observed by the flowcytometry analysis and is dicussed in more detail below. While the

G2 phase length seemed unchanged there was a little lag in G2-M phase exit suggested in the data. This lag could correspond to a subset of dying cells in G2-M phase, specifically those with intranucleated bridges and lobulated nuclei. The G2 phase cells unfit for mitosis because of DNA damage will remain in G2 until they get repaired or die (Maity, McKenna et al. 1994). Even though the S phase was more rapid, the overall length of the cell cycle in the clone was prolonged because of the longer G1 phase. From the flowcytometry results, the cell cycle was estimated to take an extra 4 hours to be completed in the absence of ATRX.

In the $Atrx^{null}$ MEFs, we also observed other cell cycle changes in addition to the faster S phase. Some, but not all, of the experiments revealed a slightly longer G2-M phase. According to the cell cycle profile by flowcytometry, the G2-M phase was found to be longer (figure 23 A). However, cells stained for phospho-histone H3, a G2-M marker (figure 24 A), did not corroborate the increase in the G2-M phase cells in the $Atrx^{null}$ MEFs. It is believed that the cell staining method is not as sensitive as the flowcytometry, because only a smaller number of cells can be analyzed per experiment and it has to be counted manually. Consequently, the small increase in cells found at the G2-M phase by flowcytometry may not actually be detected with the staining and count method. The study of the S to G2 phase progression using a BrdU pulse chase in combination with staining for the G2-M phase marker PH3 did not reveal an overall change in transition time (figure 24 B). The subtle difference in the percentage of BrdU+PH3+/BrdU+ cells that occur at each time point is not significant. These results are puzzling. In fact, we have proven by BrdU staining and flowcytometry that the S phase is shorter. Therefore, there must be an increase in the G2-M phase to explain why the time for the cells to progress from S phase to the G2-M phase is the same. As previously stated the difference in the G2-M phase is probably very subtle and

could not be detected by the stain and count method. With the shorter S phase and a longer G2-M phase the overall time to go from S to G2-M phase could possibly remain unchanged. Since the analysis of the S to G2-M phase progression was unclear, a more sensitive method such as the BrdU pulse chase experiment performed with the C5 clone combined with flowcytometry analysis could have increased the resolution of this experiment.

Similarly, the results found with the psiRNA ATRX3 C5 clone were not all corroborated by the $Atrx^{null}$ MEFs. Discrepancies at the G1 and G2-M phase between the models could be explained by the fact that one of the models is still expressing the truncated ATRX isoform (ATRXt). Both ATRX isoforms are downregulated in the psiRNA ATRX3 C5 clones whereas only the full length Atrx protein is ablated in the MEFs. The Cre mediated excision of exon 18 only affects the expression of the full length Atrx protein (Berube, Mangelsdorf et al. 2005; Garrick, Sharpe et al. 2006). ATRXt lacks the ATPase/helicase domain of the ATRX full length protein but it still contains the PHD-like domain and it localises at PCH but not at the PML-NBs. ATRXt is thought to have important biological functions because it is highly conserved and tightly regulated. Moreover, it was suggested to act as a dominant negative like seen in other SWI/SNF members; the ATPase/helicase activity of ATRX could be regulated by ATRXt by taking the place of ATRX in the chromatin remodelling complex (Garrick, Samara et al. 2004). Therefore, ATRXt could still be part of a chromatin remodelling complex and have a role at PCH which could influence the outcome of cell cycle progression in the absence of ATRX. The origin of the cells is another important aspect that could generate divergent results from the cell cycle analysis in the two models. The importance of ATRX and its role might be different depending on the cell type or tissue examined. Fibroblast and epithelial cervical

adenocarcinoma cells might have different ATRX requirements for cell cycle progression that could account for the differences observed between our two model systems.

The expression of G1/S checkpoint proteins like Rb, cyclin A and E2F-1 were altered in the absence of ATRX suggesting they may be regulated by ATRX during the cell cycle. Furthermore, the change in expression of these proteins corresponds with the cell cycle changes that were observed in our ATRX downregulated models. In the psiRNA ATRX3 C5 clone, the cell cycle profile analysis revealed an overall slower growth; this defect was found to be caused by an extension of the G1 phase. The study of proteins known to regulate the G1 checkpoint does corroborate the profile analysis. For the cells to proceed from G1 to S phase, Rb needs to be hyperphosphorylated by the cyclin/cdk complex (cylcinD/cdk4-6) (Schafer 1998). Phosphorylated Rb releases the transcription factor E2F which in turn activates its own transcription and the transcription of essential genes for S phase progression (Arroyo and Raychaudhuri 1992; Mudrak, Ogris et al. 1994). Cyclin A is expressed during S phase and is an E2F transcriptional target (Schulze, Zerfass et al. 1995; Lavia and Jansen-Durr 1999).

In the psiRNA ATRX3 C5 clone the level of hypophosphorylated Rb protein was found to be increased, which is a land mark of G1 arrest (Weinberg 1995). Furthermore, the more abundant hypophosphorylated Rb means less free E2F and reduced expression of E2F target genes, which was confirmed. E2F-1 and cyclin A protein levels were both lower in the psiRNA ATRX3 C5 clone (figure 20). Cyclin A-cdk2 is suggested to maintain phosphorylation of Rb during S phase (Sherr 1996) therefore cyclin A protein reduction could also influence the levels of phosphorylated Rb. The $Atrx^{null}$ MEFs did not show any

difference in the G1 phase length. However, our analysis of Rb protein levels also revealed an increase in the level of hypophosphorylated Rb in this system. Thaken together, the presence of more hypophosphorylated Rb in both models reinforced the implication that ATRX regulates the G1/S checkpoint.

The involvement of Rb with chromatin remodelling proteins is not a novel observation. Multiple groups have suggested that SWI/SNF proteins and Rb could be part of the same protein complex. One group found that Rb binds the SWI/SNF protein BRM and E2F simultaneously which led them to suggest that these proteins can form a complex at promoters with E2F binding sites (Trouche, Le Chalony et al. 1997). Another group found that Rb recruits HDAC and SWI/SNF together in the same complex (Zhang, Gavin et al. 2000). From these studies, we could suggest that ATRX might form a complex with Rb since ATRX is also a member of the SWI/SNF protein family. Indeed, it has been stated as an unpublished observation that ATRX interacts with the Rb protein by co-immunoprecipitation in human lyphoblastoid cells (Cardoso, Couillault et al. 2005). Therefore, a direct interaction between ATRX and the Rb protein in a complex is a real possibility.

Many studies on the SWI/SNF chromatin remodelling proteins BRG1 and BRM found that they were implicated in the G1/S checkpoint and Rb mediated cell cycle arrest. Initially, chromatin remodelling complexes containing the ATPase BRG1 and BRM were found to negatively regulate cell cycle progression by binding to Rb (Dunaief, Strober et al. 1994; Trouche, Le Chalony et al. 1997; Zhang, Gavin et al. 2000). Other experiments overexpressing BRG1 in BRG1 and BRM deficient cells induced the Rb-mediated inhibition

of E2F-1 transcriptional activity and subsequently arrested the cell cycle (Dunaief, Strober et al. 1994; Trouche, Le Chalony et al. 1997; Zhang, Gavin et al. 2000). This phenomenon was also associated with downregulation of Cyclin E and A (Zhang, Gavin et al. 2000). In addition, the expression of a dominant-negative BRG1 and BRM containing a non-functional ATPase domain blocked the Rb dependent growth arrest (Dunaief, Strober et al. 1994; Strobeck, Knudsen et al. 2000). From these studies, it was suggested that the BRG1/BRM complex is important at the G1/S checkpoint and also to regulate cyclin A, cyclin E and cdk expression during the cell cycle. Furthermore, BRG1 and BRM are characterised as tumour suppressors and are downregulated in human tumour cell lines (Reisman, Strobeck et al. 2002). The study of those tumor cell lines suggested that BRG1 and BRM were transcriptional repressors more than activators.

Taken from our study, the effect of ATRX on the cell cycle appears to be opposite to the one just described for the BRG1 and BRM proteins. ATRX downregulation induced an Rb mediated cell cycle prolongation at the G1 phase, a reduction of cyclin A expression and ATRX is not considered a tumour suppressor. Our results suggest that ATRX could have a role opposite to BRG1 and BRM at the G1/S checkpoint and act as a transcriptional activator. Therefore ATRX and Rb could be part of a complex involved in transcriptional activation whereas BRG1 and BRM are part of a transcriptional repression complex when in complex with Rb. One would predict if ATRX promotes cell cycle progression that overexpression would lead to increased proliferation. Indeed, this was shown in a transgenic mouse line where overexpression of ATRX led to an increased number of neuroprogenitor cells in the developing telencephalon (Berube, Jagla et al. 2002).

Overall, this study suggests that ATRX may have different key functions at different periods of the cell cycle. Previous work suggested a role for ATRX in late S phase where ATRX associated with HP1α, Daxx and PML-NBs to re-establish the heterochromatin state after replication (Ishov, Vladimirova et al. 2004; Luciani, Depetris et al. 2006). Our work suggests a role for ATRX at the G1 phase where ATRX associates with Rb to act as a transcriptional activator. The chromatin remodelling activity of ATRX may be important for access to promoters by transcription factors such as E2F-1 in the G1 phase. Finally, the study by Richie *et al.* suggested that ATRX as an important role at the G2-M phase in regulating chromosome congression at mitosis. Taken together, ATRX may form a complex with different proteins throughout the cell cycle to perform multiple phase-specific tasks.

4.5 Future work

Future work related to the findings made in this thesis would be to reconfirm certain observations made in our ATRX downregulated models. A more rigorous analysis of the cell cycle from the G1/S to the G2-M phase should be performed in both the C5 clone and the $Atrx^{null}$ MEFs. To carry out this analysis, cells arrested in the G1 phase (by serum starvation) are subsequently released (by serum re-introduction) and then pulsed with BrdU at various time points after the G1 phase release. Cell cycle profiles are then analyzed by staining for BrdU and DNA content (PI) prior to flowcytometry. A similar experiment was made in this study but now with the cell synchronisation and shorter time point intervals (shorter then 6 hrs) we would hope to see a more specific effect on cell cycle progression. In addition, the altered protein levels observed for the G1/S checkpoint proteins Rb, E2F-1 and cyclin A found by immunoblot should be confirmed by another method. In this regard, the

protein levels could be reconfirmed in both our models by cell staining and flowcytometry cell sorting.

Future work should also focus on confirming that the cell cycle defects seen in our cell lines are truly due to the downregulation of ATRX. The ATRX protein can be re-introduced into the cell lines to see if the cell cycle phenotype can be rescued. ATRX expression can be re-introduced in the cell by an ATRX expressing adenovirus infection; our laboratory already possesses an adenovirus expressing ATRX. After adenoviral infection, ATRX expression can be assessed by immunoblot. ATRX expression by the adenovirus will have to overcome the ATRX shRNA present in the C5 clone. Therefore, the MOI optimisation to obtain a sufficient ATRX expression in the C5 clone is important. The cell lines now re-expressing ATRX can be studied to see if the slow growth phenotype and the cell cycle changes previously observed are rescued. The growth rate and cell cycle profile analysis can be performed as described in this study. The protein levels of Rb, cyclin A and E2F-1 should also be assessed by immunoblot and flowcytometry to see if their expression returned to the control levels.

The direct interaction of Rb and ATRX was indicated in human lymphoblastoid cells by co-immunoprecipitation but this work is still unpublished (Cardoso, Couillault et al. 2005). To further prove that ATRX and Rb interact and are part of the same complex co-immunoprecipitation of these proteins should be performed with the HeLa and the MEF cell lines.

4.6 Conclusions

Based on this study we found that ATRX can be downregulated by transient siRNA transfection and shRNA expression in stable clones. We also created two ATRX downregulated cell models in HeLa cells and in MEFs to study the effects of ATRX level on the cell cycle. The ATRX downregulated cell models showed a slower growth rate, a faster S phase in addition to an increase in hypophosphorylated Rb protein. The psiRNA ATRX3 C5 clone was shown to have a longer G1 phase coupled with an increased level of Rb hypophosphorylation and reduced expression of E2F-1 and cyclin A. All together, we suggest that ATRX plays a role in Rb-mediated cell cycle arrest at the G1 phase and may also be involved in chromatin remodelling at specific target genes for promoter access by the E2F transcription factor.

5 References

Current Protocols in Stem Cell Biology.

A, E. M. (2007). "Isolation and propagation of mouse embryonic fibroblasts and preparation of mouse embryonic feeder layer cells." Curr Protoc Stem Cell Biol **Chapter 1**: Unit1C 3.

Abidi, F., C. E. Schwartz, et al. (1999). "Carpenter-Waziri syndrome results from a mutation in XNP." Am J Med Genet **85**(3): 249-51.

Alberts, B. (1999). L'Essentiel de la biologie cellulaire : introduction * la biologie mol*culaire de la cellule. Paris, Flammarion m*decine-sciences.

Arroyo, M. and P. Raychaudhuri (1992). "Retinoblastoma-repression of E2F-dependent transcription depends on the ability of the retinoblastoma protein to interact with E2F and is abrogated by the adenovirus E1A oncoprotein." Nucleic Acids Res **20**(22): 5947-54.

Ausubel, F. M. (2001). "Current protocols in molecular biology." from https://login.proxy.bib.uottawa.ca/login?url=http://www.mrw.interscience.wiley.com/cp/cpmb Current protocols in molecular biology (Restricted to University of Ottawa)

Bachoo, S. and R. J. Gibbons (1999). "Germline and gonosomal mosaicism in the ATR-X syndrome." Eur J Hum Genet **7**(8): 933-6.

Berube, N. G., M. Jagla, et al. (2002). "Neurodevelopmental defects resulting from ATRX overexpression in transgenic mice." Hum Mol Genet **11**(3): 253-61.

Berube, N. G., M. Mangelsdorf, et al. (2005). "The chromatin-remodeling protein ATRX is critical for neuronal survival during corticogenesis." J Clin Invest **115**(2): 258-67.

Berube, N. G., C. A. Smeenk, et al. (2000). "Cell cycle-dependent phosphorylation of the ATRX protein correlates with changes in nuclear matrix and chromatin association." Hum Mol Genet **9**(4): 539-47.

Bezhani, S., C. Winter, et al. (2007). "Unique, shared, and redundant roles for the Arabidopsis SWI/SNF chromatin remodeling ATPases BRAHMA and SPLAYED." Plant Cell **19**(2): 403-16.

Borden, K. L. (2002). "Pondering the promyelocytic leukemia protein (PML) puzzle: possible functions for PML nuclear bodies." Mol Cell Biol **22**(15): 5259-69.

Bradford, M. M. (1976). "A rapid and sensitive method for the quantitation of microgram quantities of protein utilizing the principle of protein-dye binding." Anal Biochem **72**: 248-54.

Brown, C. E., T. Lechner, et al. (2000). "The many HATs of transcription coactivators." Trends Biochem Sci **25**(1): 15-9.

Brummelkamp, T. R., R. Bernards, et al. (2002). "A system for stable expression of short interfering RNAs in mammalian cells." Science **296**(5567): 550-3.

Cardoso, C., C. Couillault, et al. (2005). "XNP-1/ATR-X acts with RB, HP1 and the NuRD complex during larval development in C. elegans." Dev Biol **278**(1): 49-59.

Cardoso, C., S. Timsit, et al. (1998). "Specific interaction between the XNP/ATR-X gene product and the SET domain of the human EZH2 protein." Hum Mol Genet **7**(4): 679-84.

Carlson, M. and B. C. Laurent (1994). "The SNF/SWI family of global transcriptional activators." Curr Opin Cell Biol **6**(3): 396-402.

Carpenter, N. J., Y. Qu, et al. (1999). "X-linked mental retardation syndrome with characteristic "coarse" facial appearance, brachydactyly, and short stature maps to proximal Xq." Am J Med Genet **85**(3): 230-5.
Chellappan, S. P., S. Hiebert, et al. (1991). "The E2F transcription factor is a cellular target for the RB protein." Cell **65**(6): 1053-61.
Chen, P. L., P. Scully, et al. (1989). "Phosphorylation of the retinoblastoma gene product is modulated during the cell cycle and cellular differentiation." Cell **58**(6): 1193-8.
Cook, J. A. and J. B. Mitchell (1989). "Viability measurements in mammalian cell systems." Anal Biochem **179**(1): 1-7.
Dalby, B., S. Cates, et al. (2004). "Advanced transfection with Lipofectamine 2000 reagent: primary neurons, siRNA, and high-throughput applications." Methods **33**(2): 95-103.
Darzynkiewicz, Z., J. Gong, et al. (1996). "Cytometry of cyclin proteins." Cytometry **25**(1): 1-13.
De La Fuente, R., M. M. Viveiros, et al. (2004). "ATRX, a member of the SNF2 family of helicase/ATPases, is required for chromosome alignment and meiotic spindle organization in metaphase II stage mouse oocytes." Dev Biol **272**(1): 1-14.
de Murcia, J. M., C. Niedergang, et al. (1997). "Requirement of poly(ADP-ribose) polymerase in recovery from DNA damage in mice and in cells." Proc Natl Acad Sci U S A **94**(14): 7303-7.
Dimitri, P., N. Corradini, et al. (2005). "The paradox of functional heterochromatin." Bioessays **27**(1): 29-41.
Dunaief, J. L., B. E. Strober, et al. (1994). "The retinoblastoma protein and BRG1 form a complex and cooperate to induce cell cycle arrest." Cell **79**(1): 119-30.
Dyson, N. (1998). "The regulation of E2F by pRB-family proteins." Genes Dev **12**(15): 2245-62.
Elbashir, S. M., J. Harborth, et al. (2001). "Duplexes of 21-nucleotide RNAs mediate RNA interference in cultured mammalian cells." Nature **411**(6836): 494-8.
Elbashir, S. M., J. Harborth, et al. (2002). "Analysis of gene function in somatic mammalian cells using small interfering RNAs." Methods **26**(2): 199-213.
Elbashir, S. M., W. Lendeckel, et al. (2001). "RNA interference is mediated by 21- and 22-nucleotide RNAs." Genes Dev **15**(2): 188-200.
Flaus, A., D. M. Martin, et al. (2006). "Identification of multiple distinct Snf2 subfamilies with conserved structural motifs." Nucleic Acids Res **34**(10): 2887-905.
Garrick, D., V. Samara, et al. (2004). "A conserved truncated isoform of the ATR-X syndrome protein lacking the SWI/SNF-homology domain." Gene **326**: 23-34.
Garrick, D., J. A. Sharpe, et al. (2006). "Loss of Atrx affects trophoblast development and the pattern of X-inactivation in extraembryonic tissues." PLoS Genet **2**(4): e58.
Gibbons, R. (2006). "Alpha thalassaemia-mental retardation, X linked." Orphanet J Rare Dis **1**: 15.
Gibbons, R. J., S. Bachoo, et al. (1997). "Mutations in transcriptional regulator ATRX establish the functional significance of a PHD-like domain." Nat Genet **17**(2): 146-8.
Gibbons, R. J., L. Brueton, et al. (1995). "Clinical and hematologic aspects of the X-linked alpha-thalassemia/mental retardation syndrome (ATR-X)." Am J Med Genet **55**(3): 288-99.
Gibbons, R. J. and D. R. Higgs (2000). "Molecular-clinical spectrum of the ATR-X syndrome." Am J Med Genet **97**(3): 204-12.

Gibbons, R. J., T. L. McDowell, et al. (2000). "Mutations in ATRX, encoding a SWI/SNF-like protein, cause diverse changes in the pattern of DNA methylation." Nat Genet **24**(4): 368-71.
Gibbons, R. J., D. J. Picketts, et al. (1995). "Mutations in a putative global transcriptional regulator cause X-linked mental retardation with alpha-thalassemia (ATR-X syndrome)." Cell **80**(6): 837-45.
Gibbons, R. J., G. K. Suthers, et al. (1992). "X-linked alpha-thalassemia/mental retardation (ATR-X) syndrome: localization to Xq12-q21.31 by X inactivation and linkage analysis." Am J Hum Genet **51**(5): 1136-49.
Gibbons, R. J., T. Wada, et al. (2008). "Mutations in the chromatin-associated protein ATRX." Hum Mutat.
Guerrini, R., J. L. Shanahan, et al. (2000). "A nonsense mutation of the ATRX gene causing mild mental retardation and epilepsy." Ann Neurol **47**(1): 117-21.
Higgs, D. R., M. A. Vickers, et al. (1989). "A review of the molecular genetics of the human alpha-globin gene cluster." Blood **73**(5): 1081-104.
Holen, T., M. Amarzguioui, et al. (2002). "Positional effects of short interfering RNAs targeting the human coagulation trigger Tissue Factor." Nucleic Acids Res **30**(8): 1757-66.
Huang, J., J. M. Hsu, et al. (2004). "The RSC nucleosome-remodeling complex is required for Cohesin's association with chromosome arms." Mol Cell **13**(5): 739-50.
Ishov, A. M., A. G. Sotnikov, et al. (1999). "PML is critical for ND10 formation and recruits the PML-interacting protein daxx to this nuclear structure when modified by SUMO-1." J Cell Biol **147**(2): 221-34.
Ishov, A. M., O. V. Vladimirova, et al. (2004). "Heterochromatin and ND10 are cell-cycle regulated and phosphorylation-dependent alternate nuclear sites of the transcription repressor Daxx and SWI/SNF protein ATRX." J Cell Sci **117**(Pt 17): 3807-20.
Khelifi, A. F., M. S. D'Alcontres, et al. (2005). "Daxx is required for stress-induced cell death and JNK activation." Cell Death Differ **12**(7): 724-33.
Kraus, W. L. and J. T. Lis (2003). "PARP goes transcription." Cell **113**(6): 677-83.
Krebs, J. E., C. J. Fry, et al. (2000). "Global role for chromatin remodeling enzymes in mitotic gene expression." Cell **102**(5): 587-98.
Lavia, P. and P. Jansen-Durr (1999). "E2F target genes and cell-cycle checkpoint control." Bioessays **21**(3): 221-30.
Le Douarin, B., A. L. Nielsen, et al. (1996). "A possible involvement of TIF1 alpha and TIF1 beta in the epigenetic control of transcription by nuclear receptors." Embo J **15**(23): 6701-15.
Lossi, A. M., J. M. Millan, et al. (1999). "Mutation of the XNP/ATR-X gene in a family with severe mental retardation, spastic paraplegia and skewed pattern of X inactivation: demonstration that the mutation is involved in the inactivation bias." Am J Hum Genet **65**(2): 558-62.
Luciani, J. J., D. Depetris, et al. (2006). "PML nuclear bodies are highly organised DNA-protein structures with a function in heterochromatin remodelling at the G2 phase." J Cell Sci **119**(Pt 12): 2518-31.
Luger, K., A. W. Mader, et al. (1997). "Crystal structure of the nucleosome core particle at 2.8 A resolution." Nature **389**(6648): 251-60.
Maity, A., W. G. McKenna, et al. (1994). "The molecular basis for cell cycle delays following ionizing radiation: a review." Radiother Oncol **31**(1): 1-13.

Martens, J. A. and F. Winston (2003). "Recent advances in understanding chromatin remodeling by Swi/Snf complexes." Curr Opin Genet Dev **13**(2): 136-42.
Matson, S. W., D. W. Bean, et al. (1994). "DNA helicases: enzymes with essential roles in all aspects of DNA metabolism." Bioessays **16**(1): 13-22.
McDowell, T. L., R. J. Gibbons, et al. (1999). "Localization of a putative transcriptional regulator (ATRX) at pericentromeric heterochromatin and the short arms of acrocentric chromosomes." Proc Natl Acad Sci U S A **96**(24): 13983-8.
Michaelson, J. S., D. Bader, et al. (1999). "Loss of Daxx, a promiscuously interacting protein, results in extensive apoptosis in early mouse development." Genes Dev **13**(15): 1918-23.
Michaelson, J. S. and P. Leder (2003). "RNAi reveals anti-apoptotic and transcriptionally repressive activities of DAXX." J Cell Sci **116**(Pt 2): 345-52.
Mohrmann, L., K. Langenberg, et al. (2004). "Differential targeting of two distinct SWI/SNF-related Drosophila chromatin-remodeling complexes." Mol Cell Biol **24**(8): 3077-88.
Mohrmann, L. and C. P. Verrijzer (2005). "Composition and functional specificity of SWI2/SNF2 class chromatin remodeling complexes." Biochim Biophys Acta **1681**(2-3): 59-73.
Mudrak, I., E. Ogris, et al. (1994). "Coordinated trans activation of DNA synthesis- and precursor-producing enzymes by polyomavirus large T antigen through interaction with the retinoblastoma protein." Mol Cell Biol **14**(3): 1886-92.
Narlikar, G. J., H. Y. Fan, et al. (2002). "Cooperation between complexes that regulate chromatin structure and transcription." Cell **108**(4): 475-87.
Neely, K. E. and J. L. Workman (2002). "The complexity of chromatin remodeling and its links to cancer." Biochim Biophys Acta **1603**(1): 19-29.
Negoescu, A., C. Guillermet, et al. (1998). "Importance of DNA fragmentation in apoptosis with regard to TUNEL specificity." Biomed Pharmacother **52**(6): 252-8.
Nevins, J. R. (1998). "Toward an understanding of the functional complexity of the E2F and retinoblastoma families." Cell Growth Differ **9**(8): 585-93.
Ng, P., R. J. Parks, et al. (2002). "Preparation of helper-dependent adenoviral vectors." Methods Mol Med **69**: 371-88.
Novina, C. D. and P. A. Sharp (2004). "The RNAi revolution." Nature **430**(6996): 161-4.
Okano, M., D. W. Bell, et al. (1999). "DNA methyltransferases Dnmt3a and Dnmt3b are essential for de novo methylation and mammalian development." Cell **99**(3): 247-57.
Picketts, D. J., D. R. Higgs, et al. (1996). "ATRX encodes a novel member of the SNF2 family of proteins: mutations point to a common mechanism underlying the ATR-X syndrome." Hum Mol Genet **5**(12): 1899-907.
Picketts, D. J., A. O. Tastan, et al. (1998). "Comparison of the human and murine ATRX gene identifies highly conserved, functionally important domains." Mamm Genome **9**(5): 400-3.
Plasterk, R. H. (2002). "RNA silencing: the genome's immune system." Science **296**(5571): 1263-5.
Poirier, G. G., G. de Murcia, et al. (1982). "Poly(ADP-ribosyl)ation of polynucleosomes causes relaxation of chromatin structure." Proc Natl Acad Sci U S A **79**(11): 3423-7.
Realini, C. A. and F. R. Althaus (1992). "Histone shuttling by poly(ADP-ribosylation)." J Biol Chem **267**(26): 18858-65.

Rechsteiner, M. and S. W. Rogers (1996). "PEST sequences and regulation by proteolysis." Trends Biochem Sci **21**(7): 267-71.
Regad, T. and M. K. Chelbi-Alix (2001). "Role and fate of PML nuclear bodies in response to interferon and viral infections." Oncogene **20**(49): 7274-86.
Reisman, D. N., M. W. Strobeck, et al. (2002). "Concomitant down-regulation of BRM and BRG1 in human tumor cell lines: differential effects on RB-mediated growth arrest vs CD44 expression." Oncogene **21**(8): 1196-207.
Ritchie, K., C. Seah, et al. (2008). "Loss of ATRX leads to chromosome cohesion and congression defects." J Cell Biol **180**(2): 315-24.
Rutz, S. and A. Scheffold (2004). "Towards in vivo application of RNA interference - new toys, old problems." Arthritis Res Ther **6**(2): 78-85.
Saha, A., J. Wittmeyer, et al. (2006). "Chromatin remodelling: the industrial revolution of DNA around histones." Nat Rev Mol Cell Biol **7**(6): 437-47.
Salomoni, P. and A. F. Khelifi (2006). "Daxx: death or survival protein?" Trends Cell Biol **16**(2): 97-104.
Schafer, K. A. (1998). "The cell cycle: a review." Vet Pathol **35**(6): 461-78.
Scheffner, M., K. Munger, et al. (1991). "The state of the p53 and retinoblastoma genes in human cervical carcinoma cell lines." Proc Natl Acad Sci U S A **88**(13): 5523-7.
Schulze, A., K. Zerfass, et al. (1995). "Cell cycle regulation of the cyclin A gene promoter is mediated by a variant E2F site." Proc Natl Acad Sci U S A **92**(24): 11264-8.
Schulze, S. R. and L. L. Wallrath (2007). "Gene regulation by chromatin structure: paradigms established in Drosophila melanogaster." Annu Rev Entomol **52**: 171-92.
Schwarz, E., U. K. Freese, et al. (1985). "Structure and transcription of human papillomavirus sequences in cervical carcinoma cells." Nature **314**(6006): 111-4.
Sherr, C. J. (1996). "Cancer cell cycles." Science **274**(5293): 1672-7.
Simone, C. (2006). "SWI/SNF: the crossroads where extracellular signaling pathways meet chromatin." J Cell Physiol **207**(2): 309-14.
Strahl, B. D. and C. D. Allis (2000). "The language of covalent histone modifications." Nature **403**(6765): 41-5.
Strobeck, M. W., K. E. Knudsen, et al. (2000). "BRG-1 is required for RB-mediated cell cycle arrest." Proc Natl Acad Sci U S A **97**(14): 7748-53.
Stubbert, L. J., J. D. Hamill, et al. (2007). "DDB2-independent role for p53 in the recovery from ultraviolet light-induced replication arrest." Cell Cycle **6**(14): 1730-40.
Sudarsanam, P. and F. Winston (2000). "The Swi/Snf family nucleosome-remodeling complexes and transcriptional control." Trends Genet **16**(8): 345-51.
Tang, J., S. Wu, et al. (2004). "A novel transcription regulatory complex containing death domain-associated protein and the ATR-X syndrome protein." J Biol Chem **279**(19): 20369-77.
Trouche, D., C. Le Chalony, et al. (1997). "RB and hbrm cooperate to repress the activation functions of E2F1." Proc Natl Acad Sci U S A **94**(21): 11268-73.
Truett, G. E., P. Heeger, et al. (2000). "Preparation of PCR-quality mouse genomic DNA with hot sodium hydroxide and tris (HotSHOT)." Biotechniques **29**(1): 52, 54.
Vance, V. and H. Vaucheret (2001). "RNA silencing in plants--defense and counterdefense." Science **292**(5525): 2277-80.
Villard, L., M. Fontes, et al. (2000). "Identification of a mutation in the XNP/ATR-X gene in a family reported as Smith-Fineman-Myers syndrome." Am J Med Genet **91**(1): 83-5.

Villard, L., J. Gecz, et al. (1996). "XNP mutation in a large family with Juberg-Marsidi syndrome." Nat Genet **12**(4): 359-60.
Villard, L., D. Lacombe, et al. (1996). "A point mutation in the XNP gene, associated with an ATR-X phenotype without alpha-thalassemia." Eur J Hum Genet **4**(6): 316-20.
Villard, L., A. M. Lossi, et al. (1997). "Determination of the genomic structure of the XNP/ATRX gene encoding a potential zinc finger helicase." Genomics **43**(2): 149-55.
Villard, L., A. Toutain, et al. (1996). "Splicing mutation in the ATR-X gene can lead to a dysmorphic mental retardation phenotype without alpha-thalassemia." Am J Hum Genet **58**(3): 499-505.
Wada, T., H. Sugie, et al. (2005). "Non-skewed X-inactivation may cause mental retardation in a female carrier of X-linked alpha-thalassemia/mental retardation syndrome (ATR-X): X-inactivation study of nine female carriers of ATR-X." Am J Med Genet A **138**(1): 18-20.
Wang, Z. Q., L. Stingl, et al. (1997). "PARP is important for genomic stability but dispensable in apoptosis." Genes Dev **11**(18): 2347-58.
Weatherall, D. J., D. R. Higgs, et al. (1981). "Hemoglobin H disease and mental retardation: a new syndrome or a remarkable coincidence?" N Engl J Med **305**(11): 607-12.
Weinberg, R. A. (1995). "The retinoblastoma protein and cell cycle control." Cell **81**(3): 323-30.
Westphal, T. and G. Reuter (2002). "Recombinogenic effects of suppressors of position-effect variegation in Drosophila." Genetics **160**(2): 609-21.
Wu, J. and M. Grunstein (2000). "25 years after the nucleosome model: chromatin modifications." Trends Biochem Sci **25**(12): 619-23.
Xie, S., Z. Wang, et al. (1999). "Cloning, expression and chromosome locations of the human DNMT3 gene family." Gene **236**(1): 87-95.
Xue, Y., R. Gibbons, et al. (2003). "The ATRX syndrome protein forms a chromatin-remodeling complex with Daxx and localizes in promyelocytic leukemia nuclear bodies." Proc Natl Acad Sci U S A **100**(19): 10635-40.
Yang, X., R. Khosravi-Far, et al. (1997). "Daxx, a novel Fas-binding protein that activates JNK and apoptosis." Cell **89**(7): 1067-76.
Zhang, H. S., M. Gavin, et al. (2000). "Exit from G1 and S phase of the cell cycle is regulated by repressor complexes containing HDAC-Rb-hSWI/SNF and Rb-hSWI/SNF." Cell **101**(1): 79-89.
Zhang, Y., H. H. Ng, et al. (1999). "Analysis of the NuRD subunits reveals a histone deacetylase core complex and a connection with DNA methylation." Genes Dev **13**(15): 1924-35.

Appendix A

Sequence of the shRNA oligonucleotides inserts cloned in the psiRNA-hH1 neo expression vector. The oligonucleotides were design to form a hairpin loop when expressed by psiRNA-hH1 neo and target *ATRX* mRNA degradation through the RNAi pathway.

Oligonucleotide	Sequence (5'- 3')
ATRX psiRNA 1- sense	ACC TAA TTG GTG CAG AAG CTT CAT GAC CAC CTC ATG AAG CTT CTG CAC CAA TTT
ATRX psiRNA 1- antisense	CAA AAA ATT GGT GCA GAA GCT TCA TCA GGT GGA CAT GAA GCT TCT GCA CCA ATT
ATRX psiRNA 2 - sense	ACC TAA GTT CTC CTC CAC GAC TTG CAC CAC CTG CAA GTC GTG GAG GAG AAC TTT
ATRX psiRNA 2 - antisense	CAA AAA AGT TCT CCT CCA CGA CTT GCA GGT GGT GCA AGT CGT GGA GGA GAA CAT
ATRX psiRNA 3 - sense	ACC TAA CAC TCA TCA GAA GAA TCT GAC CAC CTC AGA TTC TTC TGA TGA GTG TTT
ATRX psiRNA 3 - antisense	CAA AAA ACA CTC ATC AGA AGA ATC TGA GGT GGT CAG ATT CTT CTG ATG AGT GTT

Appendix B

Sequence of the primers use for PCR amplification

Primer	Sequence (5'- 3')
OL381 (reverse)	CCC TAA CTG ACA CAC ATT CC
psiRNA-hH1-neo fwd	AGG TAT GTA GGC GCT AC
pTet-on rtTA fwd #2	TCG ACG CCT TAG CCA TTG AG
pTet-on rtTA rev	TAG CTT GTC GTA ATA ATG GCG G
SRY-F	TTG TCT AGA GAG CAT GGA GGG CCA TGT CAA
SRY-R	CCA CTC CTC TGT GAC ACT TTA GCC CTC CGA
fabp1-F	TGG ACA GGA CTG GAC CTC TGC TTT CCT AGA
fabp1-R	TAG AGC TTT GCC ACA TCA CAG GTC ATT CAG
Seq 36.2	TTT GAA GTG GTG TTC CTG TT
pps1.15	GGT TTT AGA TGA AAA TGA AGA G
B-actin rev	CCG TCA GGC AGC TCA TAG CTC TTC
B-actin fwd	CTG AAC CCT AAG GCC AAC CGT

Appendix C

The G2-M phase marker PH3 generates differential staining for cells in G2 or M phase. Cells were fixed and stained by immunohistochemistry for PH3 (green) and counterstained for DAPI (blue). The M phase cells were characterized by intense PH3 staining and well defined mitotic chromosomes (top panel). The G2 phase cell were characterized by a speckled PH3 staining (bottom right picture). The G2 and M phase staining patterns of PH3 are both present in the bottom left picture.

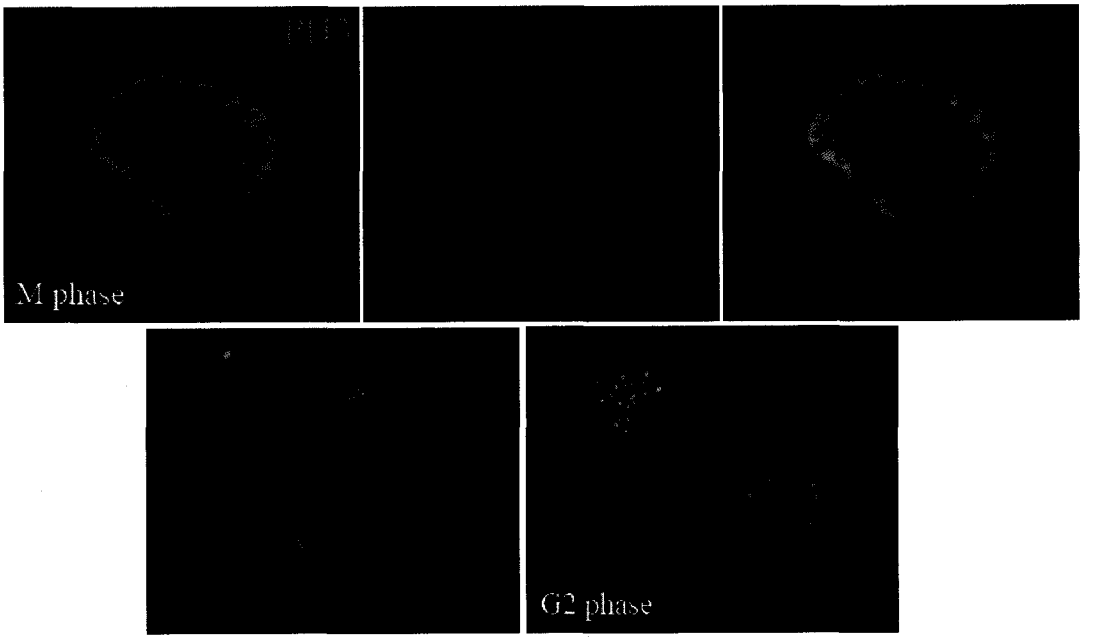
M phase
G2 phase